Understanding DNA repair in Aspergillus nidulans - paving the way for efficient gene targeting

Hoof, Jakob Blæsbjerg; Nielsen, Michael Lynge; Mortensen, Uffe Hasbro

Publication date:
2009

Document Version
Publisher's PDF, also known as Version of record

Understanding DNA repair in *Aspergillus nidulans* – paving the way for efficient gene targeting

Jakob Blæsbjerg Nielsen

PhD thesis, May 2008

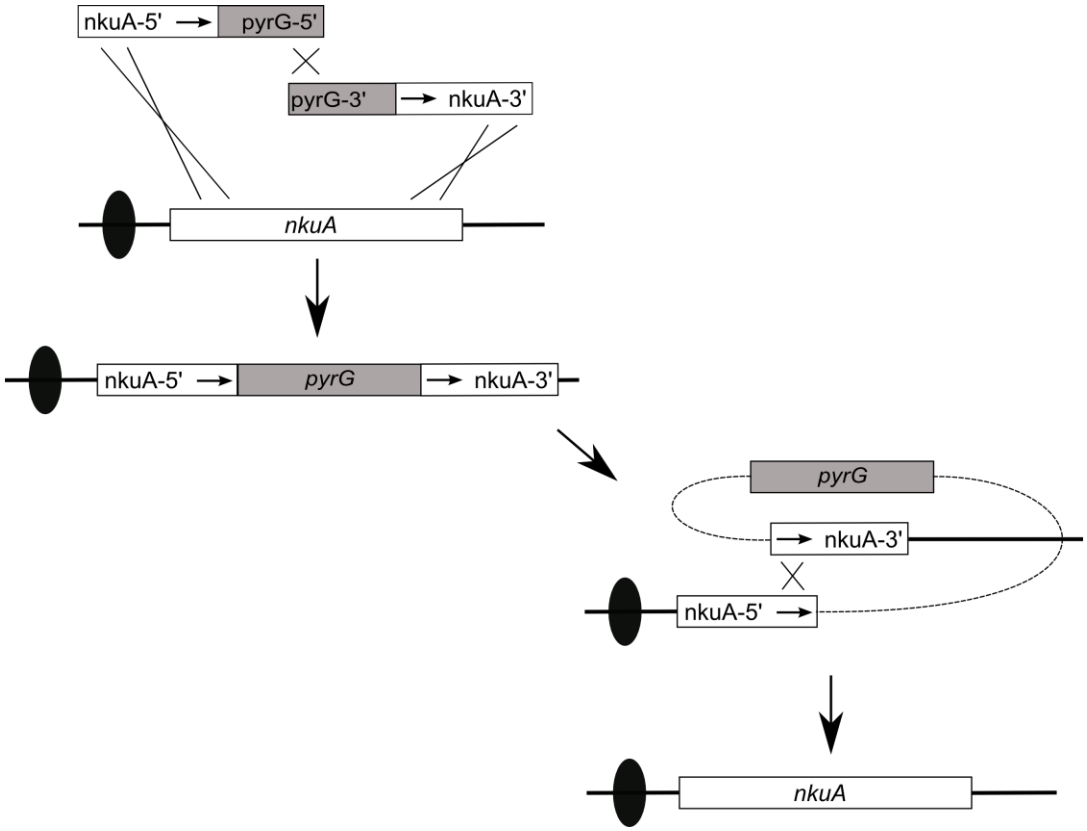

Center for Microbial Biotechnology
Department of Systems Biology

Summary

Aspergillus nidulans is a ubiquitous filamentous fungus and has a long history of use in research. Particularly the work by Guido Pontecorvo in classical genetics paved the way for *A. nidulans* as an attractive fungal model system. However, research in *A. nidulans* is not limited to fungal issues, but also encompasses topics generally relevant for eukaryotic organisms. The close relation to ecologically and industrially important species of aspergilli as well as several prominent pathogens has given *A. nidulans* a strong advantage as a model system. *A. nidulans* has unlike most of the abovementioned fungi the ability to reproduce sexually, which facilitates combination of genetic traits. Moreover, due to the long tradition as a model system many techniques and molecular tools are available for *A. nidulans*, which other species have benefited from.

The first part of the experimental work presented in this thesis is devoted to creating efficient tools and host strains for manipulating *A. nidulans* by gene targeting. This technology has traditionally been cumbersome to conduct in filamentous fungi, which has restricted many research areas. However, in this thesis I have demonstrated that the application of the bipartite gene-targeting technology, which employs 5'- and 3'-truncated genetic markers, flanked by target sequences, that assembled constitute a functional marker, improved targeting compared to the continuous substrates with a reduction in false positive transformants. These transformants could practically be eliminated by blocking one of the two main pathways in double-strand break repair, non-homologous end-joining (NHEJ), responsible for random integrations. In these mutants, the gene-targeting substrates are integrated through error-free repair in homologous recombination (HR). Temporarily disrupted NHEJ strains were constructed with a NHEJ deficiency corresponding to permanent deletion of the corresponding gene.

However, the disruptions were constructed to allow rapid regeneration of NHEJ activity when needed without having to cross strains. The two advances in gene-targeting described were applied in my first attempts to start dissecting double-strand break repair in *A. nidulans*, which is important for numerous processes.

It was demonstrated that RadC, a homolog of Rad52, an important HR protein in yeast, is also a key repair DNA protein in *A. nidulans*. Deletion mutants of RadC, displayed sensitivity to the selection of genotoxins applied in this study, as described for yeast *rad52*Δ, apart from being resistant to γ-irradiation. However this resistance depended on which phase of the cell cycle the treated cells were in, since germlings of *radC*Δ were sensitive to γ-rays. Moreover, *radC*Δ strains were still able to perform gene targeting, albeit at lower rates than wild-type cells, thereby resembling the situation in mammals. This indicates an intermediate function for RadC between yeast and human Rad52. Further, RadC was also observed to be around 100 aa longer than the homologs mentioned, which could indicate that RadC in *A. nidulans* has additional roles compared the shorter versions known from other species. Mutants lacking the UvsC protein, a homolog to Rad51, were not as impaired as strains with RadC deficiency genotoxin tests, which indicates that this protein do not have the equivalent profound roles as in mammals.

Several genes involved in NHEJ were investigated during the thesis work. Strains deleted in the NHEJ genes, *nkuA* and *ligD*, were more sensitive than wt towards γ-irradiation. *nkuA*Δ*ligD*Δ was in a gene-targeting assay more impaired in end-joining activity than the *nkuA*Δ, however there were still some residual end-joining activity in the double mutant. Thus, at least three distinct end-joining type pathways appear to exist in *A. nidulans*. Deletion of *nkuA* gave the most significant phenotype when it was combined to Rad52 or Rad51 displaying an extreme sensitivity to γ-rays. Moreover the *nkuA*Δ*radC*Δ did not produce a single transformant by gene targeting, even though the

respective single mutant both had NHEJ and HR activity. Future experiments will aim at uncovering these relations.

Sammenfatning

Aspergillus nidulans, der tilhører gruppen af skimmelsvampe, forekommer hyppigt i naturen, men har også en lang historie i forskning. Det var Guido Pontecorvos banebrydende arbejde i den klassiske genetik, der lagde grundlaget for at *A. nidulans* kunne udvikle sig til det attraktive svampemodelsystem, som den er den dag i dag. Det er ikke kun temaer, der er relevante for svampe, *A. nidulans* bruges til, men også områder, der er generelt vigtige for eukaryote organismer. Slægtskabet til vigtige industrielle og patogene arter, samt arternes enorme betydning for økosystemet, giver *A. nidulans* indlysende fordele i anvendelsen som modelorganisme. En af disse er, at den, i modsætning til mange af de vigtige beslægtede arter, kan reproducere sig seksuelt, og derved kan genetiske udtryk let kombineres og studeres. Derudover har mange års forskning i denne svamp, resulteret i meget biologisk viden, molekylære værktøjer samt teknikker, hvilket har været til gavn for mange andre arter.

De præsenterede resultater i afhandlingen vil delvist omhandle udviklingen af effektive værktøjer til at lave genetiske modificeringer i skimmelsvampe via den Nobel pris vindende "gene targeting" teknologi. Denne teknologi har traditionelt været svær at udøve i skimmelsvampe, hvilket har hæmmet arbejdet i adskillige forskningsområder. Dette er dog markant forbedret gennem arbejdet præsenteret her i afhandlingen. Den todelte "gene targeting" metode er blevet modificeret til anvendelse i *A. nidulans*. Metoden bruger afkortede genetiske markørsekvenser, flankeret af specifikke kromosomale sekvenskopier, og kun ved sammensmeltning af de to markørdele gennem rekombination giver det et funktionel markørgen. Dette har vist sig at reducere antallet af falske positive kolonier efter transformations eksperimenter. Ydermere vises det at disse falske positive mutanter helt kan elimineres ved at blokere aktiviteten af et

enzym i en af de to hovedsynteseveje, der reparerer dobbeltstrengsbrud i DNA. Denne syntesevej kaldes illegitim rekombination (IR) og står for de tilfældige integrationer af det tilsatte DNA i cellerne. I stedet vil den anden syntesevej, homolog rekombination (HR), sørge for at DNA fejlfrit integreres på den tiltænkte plads i kromosomet. Dette resultat har vist at være gældende for et permanent manglende, såvel som afbrudt IR gen. Derfor kan der fordel anvendes en værtsstamme med et midlertidigt afbrudt IR gen til at lave "gene targeting" i, hvorefter IR aktiviteten, hvis ønsket, let kan gendannes ved en simpel selektion i stedet for et tidskrævende kryds af stammer. De nye tiltag er blevet brugt til at skabe de resterende resultater i afhandlingen. Her tilstræbes det at starte på en dissekering af de ovennævnte synteseveje in *A. nidulans*, da denne viden vil komme til gavn i mange henseender grundet deres store betydning for mange processer.

Det blev vist at RadC, en homolog til et vigtigt HR protein i gær, også er en nøglefaktor i reparation af DNA skader i *A. nidulans*. "Knock-out" mutanter i *radC* viste, ligesom rapporteret for gær homologen, følsomhed overfor en række mutagener undtagen γ-stråling. Denne resistens var dog betinget af, hvilket fase af cellecyklus kernerne befandt sig i, da spirende *radC*Δ sporer var sensitive overfor strålingen. Derudover var *radC*Δ i stand til at udføre "gene targeting", dog i lav frekvens sammenlignet med vildtype, hvilket minder om situationen i mammale celler. Dette indikerer en rolle for RadC i *A. nidulans*, der ligger mellem gærs og menneskers Rad52. Derudover blev det i dette studiet vist, at RadC er ca. 100 aminosyrer længere end de andre homologe nævnt, hvilket kunne tyde på en tilegnelse af flere funktioner for RadC gennem evolutionen. Rad51 homologen, UvsC, viste sig ikke at være så påvirket som RadC af mutagerne. Ved behandling af *uvs*CΔ med hydroxyurea, der medfører replikations stress, var cellerne ikke sensitive, hvilket ikke minder om de mammale systemer.

To gener fra IR, *nkuA* og *ligD* fra Ku og DNA ligase IV komplekserne, blev også undersøgt for eventuel følsomhed over mutagener. Mangel på disse to gener medførte kun følsomhed over γ-stråling, ellers var de upåvirkede i forhold til vildtypen. Til

gengæld var dobbeltmutanten mere effektiv i udførelsen af "gene targeting" end *nkuA*Δ mutanten, men der var stadig IR aktivitet. Derfor er der med al sandsynlighed mindst tre IR former i *A. nidulans*. Til sidst skal det nævnes at sammenkoblingen af de vigtige IR og HR proteiner ikke er blevet studeret i skimmelsvampe og der derfor aldrig er demonstreret specifikke interaktioner mellem de to mekanismer. I dette studie vises der dog, at dobbeltmutanter af *nkuA*Δ og både *radC*Δ og *uvsC*Δ er ekstremt følsomme overfor γ-stråling. Derudover har *nkuA*Δ *radC*Δ ikke givet en eneste transformant ved "gene targeting", selv om begge de respektive enkeltmutanter både har IR og HR aktivitet. Den igangværende generation af mutanter og udvikling af genetiske metoder vil bidrage væsentligt til forståelsen af DNA reparation i *A. nidulans*.

Preface

The PhD thesis describes the primary results generated during my graduate program running from April 2004 to December 2007. The work was conducted at Center for Microbial Biotechnology (CMB) at Department of Systems Biology, DTU Biosys (the former BioCentrum-DTU), Technical University of Denmark. The core of the project was to create tools for efficient genetic manipulation in the filamentous fungus *Aspergillus nidulans* as well as to gain understanding of the underlying biochemical pathways.

Acknowledgements

The last four years have been fascinating, developing and has given me the greatest job I could imagine. The people and atmosphere at CMB have a large share in this. At CMB there are always social activities, friendly atmosphere and skilled people from all parts of the world. Therefore many thanks to the employees and students of CMB with whom I have been so fortunate to work or amuse myself with over the years. I would like to give my highest appreciation to my two Supervisors, who have been there for me throughout the project, Uffe Hasbro Mortensen and Michael Lynge Nielsen. They have always supported me, and have always tried to take all ideas seriously. Both are sincere, generous and extremely competent in their research fields, and I recommend everyone, who gets the opportunity, to work with them. I cannot count the laughs we have shared. In this context, I would like to address special thanks to the rest of the members of my research group, DSBR and MutLib, for fruitful discussions and relevant critique. Moreover, thanks to my office mates during the years, Peter Meincke, Kiran R. Patil, Line Albertsen, Gaëlle Lettier, Iben Plate, Steen L. Westergaard and Melanie Z. Khodaie. Further, I have been fortunate to supervise talented students at different levels carrying out different projects related to my thesis, and for this I am grateful. I have learned

many things from things, and hopefully they have too: Katrine Husted Brogaard (M.Sc.), Jimmy Hoffmann (B.Sc.), Stig Rattleff (B.Sc.), Louise Slot Høegh (B.Sc.), Dorte Koefoed Pedersen (B.Sc.), Thomas Durhuus (special project (Sp)), Xiaole Wang (Sps), and lab-technician trainee Maya Appreleva Pedersen. Also a special thanks to the greatly skilled lab-technician trainees Simo Abdessamad Jakobsen and Martin Engelhard Kornholt, who has helped keeping our laboratories at high standards and order.

I was fortunate to spend an educational and great month with Professor Axel Brakhage at Department of Molecular and Applied Microbiology, Leibniz Institute for Natural Product Research and Infection Biology at Hans-Knoell-Institute Jena, see Chapter 5 - extra materials. I would like to thank, all the people there for their eagerness to help and spend their time with me after working hours with a special thanking to Dr. Thorsten Heinekampp, who spend time and made all arrangements for me to be there.

My PhD was interrupted by a 15 months halftime Chairman Position in PR and Recruitment at DTU Biosys, as well as the BiC-Day symposium arrangement committee. This implied a lot of contact to students, fellow researchers, DTU Communication, and other institutions. But most of all, I have in this period done a lot of teaching, which personally has taught me much about communicating Science. Many thanks to all who have been involved in the two committee groups for all the ideas that came up, the things we have initiated and pulled together. Here I will point out Professor Lisbeth Olsson and Institute Director Ole Filtenborg, as well as the cooperation with webmaster Kasper Antonsen.

The thesis could never have been completed, if I did not have the financial funding. Therefore, thanks to “Statens Forskningsråd” (IVC) and DTU for financing my work. Also, the “Otto Mønsted Fond” funded my conference stay at the 24th conference on Fungal Genetics, Asilomar California, USA, where I was fortunate to receive the

honorable Dick Weiss award for outstanding service to the fungal community. This work is represented in Chapter 5.

And last, but not least, super-thanks to all my family and friends for their support and for believing in me - and to Melanie Khodaie for being there and putting up with my absence.

Jakob Blæsbjerg Nielsen, Kgs. Lyngby - May 2008.

PhD defence

Date & time: September 11, 2008, 13:30-16:30

Venue: Auditorium 32, building 306 - Technical University of Denmark

Chairman of the defence

Associate Professor, Dr. Timothy J. Hobley

DTU Systems Biology, Denmark.

Examiners

Professor, Dr. Jens C. Frisvad

DTU Systems Biology, Denmark

Associate Professor, Dr. Michael Lisby

Institute of Molecular Biology, University of Copenhagen, Denmark

Senior Research Scientist II, Dr. Scott E. Baker

Chemical and Biological Process Development Group, Pacific Northwest National Laboratory, USA

Thesis outline

The thesis entitled "Understanding DNA repair in *Aspergillus nidulans* – paving the way for efficient gene targeting" is divided into 7 chapters where Chapters 1-3 serve as background chapters leading up to the results achieved in Chapters 4-7 presented as manuscripts. After the introduction to filamentous fungi in Chapter 1, Chapter 2 is devoted to the biology of *A. nidulans*, and the standard tools available for manipulating the fungus. The success of genetic engineering relies on the activity of DNA repair systems in the cell, thus understanding how these pathways function is important and is the topic of Chapter 3. In Chapter 4 and 5, the work on improving gene-targeting in *A. nidulans* is described and presented as original papers. An extra section in both Chapter 4 and 5 describes further developments of the work published. Chapter 6 and 7 give the latest reports on my initial contributions to the dissection of DNA repair pathways and are presented as manuscripts. Chapter 6 has been submitted for publication.

Contents

Summary **I**

Sammenfatning **II**

Preface **III**

Acknowledgements

Thesis outline **IV**

Contents **V**

List of figures **VI**

List of tables **VII**

Nomenclature **VIII**

1. Introduction to filamentous fungi **1**

Mycotechnology 2

Spoilage of feedstock and materials 3

Disease caused by *Aspergillus* 4

References 5

2. *Aspergillus nidulans* - a model organism **7**

Life of *A. nidulans* **9**

Asexual cycle 9

Heterokaryon 12

Sexual reproduction 13

Parasexual proliferation 14

Transformation of *A. nidulans* **15**

Genetic markers in *A. nidulans* 15
Vectors for transformation 16
References 18

3. DNA damage & repair 21

Spontaneous DNA damage 21
Induced DNA damage - endogenous factors 22
Induced DNA damage - exogenous factors 23

General DNA repair 25

Photoreactivation 25
Nucleotide-excision repair 25
Base-excision repair 26
Mismatch repair 26
Postreplication repair and mutagenesis 27

Double-strand break repair 28

Non-homologous end-joining 29

Mechanism of non-homologous end-joining 29
End protection and bridging 30
Gap filling and ligation 32
NHEJ in mammals 33
NHEJ proteins at telomeric ends 33

Homologous recombination 34

Models of recombination 35
Double-strand break repair model 35
Synthesis-dependent strand annealing 37
Single-strand annealing 38
Enzymatic core in HR 38
Double-strand break formation & resection 39
Recruitment of the recombinase to processed ends 40

Rad51 filament formation and strand invasion 42
Regulation of crossovers by the Srs2 and Sgs1 43
Mammalian HR 44
DNA replication fork rescue by HR 45
Gene targeting 46
References 50

4. Efficient PCR-based gene targeting with a recyclable marker for *Aspergillus nidulans* 60

Spore-PCR on *Aspergillus* conidia 74
Procedure 74
References 75

5. Transient disruption of non-homologous end-joining facilitates targeted genome manipulations in the filamentous fungus *Aspergillus nidulans* 76

Transient NHEJ disruption in *Aspergillus* 85
References 86

6. The role of *radC* in homologous recombination and DNA repair in *Aspergillus nidulans* 87

Summary 89
Introduction 90
Materials and methods 91
Strains, media and plasmids 91
cDNA analysis 91

Sensitivity to DNA damaging agents 92
Gene targeting assay 92
Analysis of meiosis in *radC*Δ strains 92
Growth rate determination 93
Results **93**
cDNA sequence analysis of the *radC* gene 93
Growth and spore formation of the *radC*Δ strain 94
The response of the *radC*Δ strain to genotoxins 95
Efficiency of gene targeting in the *radC*Δ strains 96
Analysis of meiosis in the *radC*Δ mutant 96
Discussion **97**
Acknowledgements 100
Figure legends 100
References 103

7. Repair of double-strand breaks in recombination and end-joining deficient mutants of *Aspergillus nidulans* 116
Abstract **117**
Introduction **118**
Results **120**
*nkuA*Δ*radC*Δ displays synergistic sensitivity to γ-rays 120
uvsCΔ strains were not sensitive to replication stress by HU 122
*ligD*Δ is not more sensitive than *nkuA*Δ to the genotoxins tested 122
Random integration can occur without NkuA and LigD 123
No targeting in the *radC*Δ*nkuA*Δ and *uvsC*Δ strains 123
Discussion **124**
Materials and methods **128**
Figure legends 130

References 131

Conclusions & Perspectives **138**

List of figures

2.1	Vegetative growth of *A. nidulans*	9
2.2	Spore germination and cellular compartmentalization	10
2.3	The life of *A. nidulans*	11
2.4	Deletion of *yA* in *A. nidulans*	17
3.1	DNA damage	22
3.2	Overview of DNA damaging agents, types of DNA damage and the corresponding repair processes	24
3.3	The postreplication repair and mutagenesis pathway	27
3.4	The rejoining of ends in non-homologous end-joining	29
3.5	The mechanism and core proteins of NHEJ in yeast	31
3.6	The main purposes of HR in mitosis and meiosis	34
3.7	Repair mechanisms of double-strand breaks	35
3.8	Double-strand break repair model	36
3.9	Synthesis-dependent strand annealing model	37
3.10	Single-strand annealing model	38
3.11	Strand invasion	41
3.12	Regulation of crossovers by Sgs1-Top3 with hemicatenane formation	43
3.13	Recombination and translesion synthesis in replication fork restart	45
3.14	Two scenarios for gene targeting	47
3.15	Two models for ends-out gene targeting	48
4.1	Spore-PCR	74
4.2	*Taq* polymerase spore-PCR	75
5.1	Replacement of *pyrG* in *nkuA* with either *TK* or *sacB*	86
6.1	The position of the start codon in *radC*	112

6.2	Conidiospore formation, but not colony growth, is impaired in *radC*Δ	112
6.3	Sensitivity of *radC*Δ strains to γ-irradiation and bleomycin	113
6.4	Sensitivity of *radC*Δ strains to MMS, HU and UV-irradiation	113
6.5	RadC is required for development cleistothecia	113
6.S1	RACE analysis of RadC	115
6.S2	Nuclear localization signal (NLS) in the C-terminal of RadC	115
7.1	Sensitivity of wt, *nkuA*Δ, *radC*Δ and *nkuA*Δ*radC*Δ strains to γ-irradiation and bleomycin at the concentrations indicated	134
7.2	Sensitivity of wt, *nkuA*Δ, *radC*Δ and *nkuA*Δ*radC*Δ strains to MMS, HU and UV	134
7.3	Sensitivity of wt, *nkuA*Δ, *uvsC*Δ and *nkuA*Δ*uvsC*Δ strains to γ-irradiation and bleomycin	135
7.4	Sensitivity of wt, *nkuA*Δ, *uvsC*Δ and *nkuA*Δ*uvsC*Δ strains to MMS, HU and UV	135
7.5	Sensitivity of wt, *nkuA*Δ, *ligD*Δ and *nkuA*Δ*ligD*Δ strains to γ-irradiation and bleomycin	136
7.6	Sensitivity of wt, *nkuA*Δ, *radC*Δ, *nkuA*Δ*radC*Δ, *uvsC*Δ and *nkuA*Δ*uvsC*Δ to cisplatin	136

List of tables

Table 2.1	A selection of genome data for six selected aspergilli	8
Table 2.2	A collection of common genetic selection markers for *A. nidulans*	15
Table 5.s1	Oligonucleotides used in this study	84
Table 5.s2	PCR fragments for bipartite gene-targeting substrate construction	84
Table 6.1	Spore density of colonies resulting from 4 days incubation	114
Table 6.2	Gene targeting in *radC* and *radC*Δ strains	114
Table 7.1	Gene targeting in DNA repair mutants	137

Nomenclature

AMA1	autonomous maintenance in *Aspergillus*
An	*Aspergillus nidulans*
AP	apurinic/apyrimidinic
BER	base-excision repair
CPD	cyclobutane-pyrimidine dimer
DSB	double-strand break
DSBR	double-strand break repair
DNA	deoxyribonucleic acid
dsDNA	double-stranded DNA
gDNA	genomic DNA
G1	growth phase 1
G2	growth phase 2
GRAS	generally regarded as safe
HJ	Holliday junction
HR	homologous recombination
Hs	*Homo sapiens*
HU	hydroxy urea
IR	ionizing radiation
M	mitosis
MMR	mismatch repair
MMS	methyl-methan sulfonate
NHEJ	non-homologous end-joining
NER	nucleotide excision repair
PCR	polymerase chain reaction

PRR	postreplication repair
RNA	ribonuclei acid
RNS	reactive nitrogen species
ROS	reactive oxygen species
S	DNA synthesis
Sc	*Saccharomyces cerevisiae*
SDSA	synthesis-dependent strand annealing
SSA	single-strand annealing
SSB	single-strand break
ssDNA	single-stranded DNA
TCR	transcription coupled repair
TLS	translesion synthesis
UVR	ultraviolet radiation

Chapter 1

Introduction to filamentous fungi

What are fungi? Fungi constitute an exciting and very heterogenous group of eukaryotes, and a common definition is difficult to give. Fungi are widespread in nature, and many species have more than one preferred habitat. Mistakenly, fungi were once believed to belong to the kingdom of plants, due to their obvious lack of mobility, but ironically they have more in common with animals (Dissing *et al*., 1985). Fungi have cell wall defined cells containing nuclei, no chloroplast, and nutrient uptake can take place by diffusion (Dissing *et al*., 1985). Some species are filamentous as well as multicellular, whereas others grow as unicellular yeast. Several species even have the ability to attain both forms (i.e. dimorphic). Today, fungi have been assigned to their own kingdom, which is believed to count at least 1.6 million species, an estimate based on plant to fungal ratios observed from independent species counts at different habitats (Carlile & Watkinson, 1994).

The most encountered fungi in everyday life are subdivided in three of four classes within the division of true fungi (Eumycota); the basidiomycetes, zygomycetes, and ascomycetes, which all are characterized by having a defined sexual cycle (perfect state). However within these classes there are a large number of imperfect fungi (non-sexual). Therefore, an artificial group named the deuteromycetes that constitutes a broad group of fungi has been formed to account for this. A substantial part of the basidiomycetes and some ascomycetes are found as mushrooms. Many mushrooms have an extremely important role in our ecosystem as they share an essential symbiotic relationship with trees as mycorrhizae. Here the fungus extends the limited root net of the trees providing

minerals and water in return of sugars from the trees (Dissing *et al*., 1985). Many of the zygomycetes, ascomycetes and deuteromycetes are common saprotrophs, also known as molds, and they are essential for recycling of organic matter. This utilization of complex substrates illustrates the ability of fungi to produce and secrete high quantities of different enzymes that enables growth. In addition, released sugars initiate a competition for nutrients from bacterial and fungal competitors forcing the fungus to produce antibiotics to secure the substrate for own use. These compounds now comprise a billion dollar natural-product industry and have strengthened the importance of filamentous fungi in biotechnology, which have brought new life to the term mycotechnology.

Mycotechnology

There is a large versatility in natural products from fungi, and the commercially available compounds are only the tip of the iceberg (recently reviewed in Hoffmeister & Keller, 2007; Meyer, 2008). In addition to the treasury of natural compounds, many fungi are well-suited for industrial processes that can attain GRAS[1] status. They can be cultivated in batch, fed-batch and continuous fermentation, where large-scale fermentation typically is run as fed-batch (reviewed by Papagianni, 2004). Further, growth is often supported by both complex and defined media. The majority of the mycotechnological products produced by molds are within three fields; primary and secondary metabolites, and enzymes.

The citric acid production with *Aspergillus niger* is the most successful case of primary metabolite production, and it annually exceeds 1 million tons (Soccol *et al*., 2003). The secondary metabolites are highly diversified compounds ranging from pharmaceuticals to mycotoxins. Within the pharmaceuticals many types of compounds are already in production. The most famous example originated in 1929, when Alexander Fleming

[1] Generally Regarded As Safe (GRAS) is a FDA concept, which denotes that the products resulting from a given process are safe as consumable ingredients

discovered the invasion of a *Staphylococcus* culture by a *Penicillium notatum* that resulted in inhibited bacterial growth. This led to the discovery of penicillin, the first wonder drug from fungi (Dissing *et al*., 1985). A group of secondary metabolites with great potential is the diverse polyketides. Biosynthesis of polyketides may involve very large gene clusters, such as the cholesterol-lowering drug lovastatin produced from a cluster of 17 genes within a 64 kb region in *A. terreus* (Hoffmeister & Keller, 2007). Protein production by molds, especially by *Trichoderma* and *Aspergillus*, is another large and growing marked, not only for enzymes of fungal origin, but also heterologous proteins (Punt *et al*., 2002; MacKenzie *et al*., 2004; Papagianni, 2004). Aside from these defined singular products, filamentous fungi also deliver world-wide consumables, such as mushrooms, soy sauce and ripened cheeses (Dissing *et al*., 1985; Bennett, 1998).

Some of the properties and benefits that justify the utilization of filamentous fungi in industry are ironically also features that enable some of these fungi to cause problems for humans in daily life. Thus, the presence of filamentous fungi is often far from positive and imposes massive crisis in some parts of the world.

Spoilage of feedstock and materials

Filamentous fungi are major spoilers of crops and fodder, destroying for billions of dollars worldwide, and can thus indirectly be a cause of social displacements in developing countries (Timberlake & Marshall, 1989; Williams *et al*., 2004). Most of the invading fungi produce mycotoxins that have significant impact on human and animal health. Carcinogenic mycotoxins such as aflatoxin and ochratoxin A, e.g. from *A. flavus* and *A. orchrateus*, respectively, are particularly hazardous, especially where there is a lack of fodder control and inefficient detection techniques. Aside from individual toxic effect, these two toxins have even shown to act synergistically (Huff & Doerr, 1981).

A world-wide health issue is the potential fungal influence on the indoor climate in buildings. Exposure to spores from molds such as *Alternaria*, *Aspergillus*, *Penicillium* and

Stachybotrys can cause from mild to severe allergies and mycotoxicosis (Bardana, 2003; Chang & Gershwin, 2004; Fung & Clark, 2004). In addition to allergies, certain species of *Aspergillus* have the unpleasant capability to cause invasive diseases in mammals.

Disease caused by *Aspergillus*

Most aspergilli are opportunistic pathogens and cause the aspergillosis disease in mammals. Aspergillosis ranges from allergies and skin infections to severe and often fatal invasive growth of the fungus inside the host, typically in the lungs[2] (Latgé, 1999). In healthy individuals inhaled spores are normally combated by the innate and acquired immune system. Immuno-compromised patients lack this defense and are extremely vulnerable to fungal attack. *A. fumigatus* is the most encountered species in aspergillosis followed by *A. flavus* and in fewer cases *A. niger*, *A. clavatus*, *A. nidulans*, *A. terreus*, and *A. versicolor* (Haines, 1995; Latgé, 1999). Treatment is hampered by the fact that some of the few drugs available also target the host cells (Denning *et al*., 2002). Therefore it is of interest to find efficient targets that for example attack wall epitopes of the fungus or block essential enzyme activities.

Thus, as described in the previous sections, *Aspergillus* stands out as a significant positive and negative influence in our society and much can be gained by understanding their biology. In line of this, *A. nidulans* has for more than 60 years shown to be an ideal biological model system for other fungi (Roper, 1994). Moreover, the possibility for combining traits by crossing strains and the many molecular tools available for numerous applications offers a solid research platform (Pontecorvo, 1953; Krappmann, 2006; Meyer, 2008). Importantly, the production of unicellular spores makes *A. nidulans* easy to distribute and handle, and growth requirements are simple and inexpensive. Moreover, recent years has opened new dimensions into *A. nidulans* research due to the genome sequence release and new attractive tools such as an *A. nidulans* DNA

[2] The three stages of the lung infection are allergic bronchopulmonary aspergillosis, pulmonary aspergilloma and invasive aspergillosis (Latgé, 1999).

microarray and metabolic model (Galagan *et al*., 2005; Andersen *et al*., 2008; David *et al*., 2008).

References

Andersen, M.R., Vongsangnak, W., Panagiotou, G., Salazar, M.P., Lehmann, L., and Nielsen, J. A trispecies *Aspergillus* microarray: comparative transcriptomics of three *Aspergillus* species. *PNAS* 105(11): 4387-4392.

Bardana, E.J., 2003. Indoor air quality and health does fungal contamination play a significant role? *Immunol. Allergy Clin. North. Am.***23(2)**: 291-309.

Bennett, J.W., 1998. Mycotechnology: the role of fungi in biotechnology. *J. Biotechnol*. **66**: 101–107.

Carlile, M.J. and Watkinson, S.C., 1994. The fungi. Academic press, London.

Chang, C. and Gershwin, M.E., 2004. Indoor air quality and human health - truth vs. mass hysteria. *Clin. Rev. Allergy Immunol*. **27(3)**: 219-239.

David, H., Ozçelik, I.S., Hofmann, G., Nielsen, J., 2008. Analysis of *Aspergillus nidulans* metabolism at the genome-scale. *BMC Genomics* **9**: 163.

Denning, D.W., Anderson, M.J., Turner, G., Latgé, J.P., Bennett, J.W., 2002. Sequencing the *Aspergillus fumigatus* genome. *Lancet Infect Dis.* **2(4)**: 251-253.

Dissing, H., Hansen, L., and Søchting, U., 1985. Introduktion til svampe. 2nd ed., Nucleus, Århus.

Fung, F. and Clark, R.F., 2004. Health effects of mycotoxins: a toxicological overview. *J. Toxicol. Clin. Toxicol*. **42(2)**: 217-234.

Galagan, J.E., Calvo, S.E., Cuomo, C., Ma, L.J., Wortman, J.R., Batzoglou, S., Lee, S.I. *et al*., 2005. Sequencing of *Aspergillus nidulans* and comparative analysis with *A. fumigatus* and *A. oryzae*. *Nature* **438(7071)**: 1105-1115.

Haines, J., 1995. *Aspergillus* in compost: Straw man or fatal flaw? *Biocycle* **36 (4)**: 32-35.

Hoffmeister, D. and Keller, N.P., 2007. Natural products of filamentous fungi: enzymes, genes, and their regulation. *Nat. Prod. Rep.* **24(2)**: 393-416.

Huff, W.E. and Doerr, J.A., 1981. Synergism between aflatoxin and ochratoxin A in broiler chickens. *Poult. Sci.* **60(3)**: 550-555.

Krappmann, S., 2006. Tools to study molecular mechanisms of *Aspergillus* pathogenicity. *Trends Microbiol*. **14(8)**: 356-364.

Latgé, J.P., 1999. *Aspergillus fumigatus* and aspergillosis. *Clin. Microbiol. Rev.* **12(2)**: 310-350.

Mackenzie, D.A, Jeenes, D.J., and Archer, D.B., 2004. Filamentous fungi as expression systems for heterologous proteins. Chapter 15 in The Mycota II, 2nd edition, Springer-Verlag, Berlin-Heidelberg.

Meyer, V., 2008. Genetic engineering of filamentous fungi – progress, obstacles and future trends. *Biotechnol. Adv.* **26**: 177-185.

Papagianni, M., 2004, Fungal morphology and metabolite production in submerged mycelial processes. *Biotech. Adv.* **22**: 189-259.

Pontecorvo, G., 1953. The genetics of *Aspergillus nidulans*. *Adv. Genet. Incorp. Mol. Genet. Med*. **5**: 141-238.

Punt, P.J., van Biezen, N., Conesa, A., Albers, A., Mangnus, J., and van den Hondel, C.A., 2002. Filamentous fungi as cell factories for heterologous protein production. *Trends. Biotechnol*. **20**: 200–206.

Roper, A., 1994. The early history. Chapter 1 in *Aspergillus*: 50 years on. Progress in industrial microbiology vol. 29, Elsevier, Amsterdam-London-New York-Tokyo.

Soccol, C.R., Prado, F.C., Vandenberghe, L.P.S., and Pandey, A., 2003. General aspects in citric acid production by submerged and solid-state fermentation. In: Concise Encyclopedia of Bioresource Technology. The Haworth Press, New York. pp. 652-664.

Timberlake, W.E. and Marshall, M.A., 1989. Genetic engineering of filamentous fungi. *Science* **244**: 1313-1317.

Williams, J.H., Phillips, T.D., Jolly, P.E., Stiles, J.K., Jolly, C.M., and Aggarwal, D., 2004. Human aflatoxicosis in developing countries: a review of toxicology, exposure, potential health consequences, and interventions. *Am. J. Clin. Nutr.* **80(5)**: 1106-1122.

Chapter 2

Aspergillus nidulans as a model system

The name *Aspergillus* was given in 1729 by Pietro Antonio Micheli after he inspected a mold microscopically, and observed the resemblance to the aspergillum[3] (Thom & Raper, 1945). So far, 250 species are all having an aspergillum shape that depicts its asexual (anamorphic) state (Geiser *et al*., 2007). However, at least 81 species can also propagate sexually (Frisvad, J.C., personal communication). Thus, some members of *Aspergillus* can have an alternative grouping within 11 genera characterizing the sexual state (teleomorph)[4] and placing them within the ascomycetes. Most of these are homothallic (self-fertile), since only 5 of the 81 species are heterothallic (Frisvad, J.C., personal communication).

The best characterized *Aspergillus* is the cosmopolitan *A. nidulans*, which also is named *Emericella nidulans*. However due to traditional and wide use of the name *A. nidulans* as well as to avoid confusion, the fungus will be addressed as *A. nidulans* throughout this work regardless of the context. The popularity of *A. nidulans* is mainly due to the pioneering work of Guido Pontecorvo back in the 1940s and 50s that in light of the defined sexual state has established *A. nidulans* as a strong model for classical genetics (Pontecorvo, 1953). The model status has been expanded later on by topics such as fungal morphology, mitosis, invasive growth and general cell biology, expanding the model system status to apply for eukaryotes in general (Fiddy & Trinci, 1976; Holden *et al*., 1994; Timberlake & Marshall, 1998). Here are reasons of a more practical character

[3] A device used in the Catholic Church to sprinkle holy water

[4] The 11 genera comprise *Hemicarpenteles, Neocarpenteles, Petromyces, Neopetromyces, Eurotium, Neosartorya, Emericella, Chaetosartorya, Fennellia, Sclerocleista,* and *Warcupiella*.

such as the fact that *A. nidulans* is rapidly cultivated on inexpensive defined media. Moreover, research has greatly been facilitated by the publicly available genome sequence in 2003 (Galagan *et al*., 2005). This sequence project was followed by seven other aspergilli projects[5]. Inspired by the successful *Saccharomyces* Genome Database (SGD), the sequences have been compiled in the *Aspergillus* Comparative Database[6] (ACD) in 2007. This highly facilitates genome comparisons. A selection of genome data for *A. nidulans* and three other aspergilli are shown in Table 2.1 to portray the diversity between these related fungi.

Table 2.1 A selection of genome data for six selected aspergilli

Species	Grouping[a]	Genome	# Genes	Gene Length	Exons
		Mb	Number	bp (mean)	Number
A. nidulans	Ascomycete	30.07	10.701	1.868	3.6
A. oryzae	Deuteromycete	37.12	12.336	1.414	2.9
A. fumigatus	Deuteromycete	29.38	9.887	1.644	2.8
A. niger	Deuteromycete	34.85	11.200	1.696[b]	3.1[b]
N. fischeri	Ascomycete	32.55	10.406	n.a.	n.a.
A. flavus	Deuteromycete	36.79	12.604	1.384 [c]	n.a.

Refs: see [6] and Galagan *et al*., 2005; [a] all the fungi represented in the table are ascomycetous fungi, but some can be grouped within the imperfect fungi; [b] Andersen, M.R., pers. comm.; [c] http://www.aspergillusflavus.org/genomics/

For all aspergilli, both perfect and imperfect, the vegetative life phase is dominating, see **Figure 2.1**, and they usually grow as haploid homokaryotic organisms. Moreover, *A. nidulans* and many aspergilli can exchange genetic information in a life phase termed the parasexual cycle (Pontecorvo, 1956). The different life styles of *A. nidulans* will be described in the following sections, where at least nine different cell types are displayed during the asexual and sexual stages.

[5] *A. fumigatus*, *A. niger*, *A. oryzae*, *A. clavatus*, *A. terreus*, *A. flavus*, and *A. fischeri* (*Neosartorya fischeri*)
[6] http://www.broad.mit.edu/annotation/genome/aspergillus_group/MultiHome.html

Life of *A. nidulans*

Asexual cycle

In the vegetative phase, the life of a colony begins with the germination of an *A. nidulans* asexual spore (conidium) when the right conditions are present. These include water, oxygen, CO_2, sugars, amino acids and salts (Carlile & Watkinson, 1994). Conidia then start to take up water and begin swelling in isotropic growth. In this very early phase of breaking dormancy, RNA and protein synthesis is observed after the shut-down in dormant conidia. Shortly after, DNA replication and nuclear division occurs. In fact cell cycle in *A. nidulans* is better termed duplication cycle, since there is no cell separation. Nevertheless, the nuclear division still contains the four general phases and the duration is for wild-type strains under optimal growth conditions, 28-37 °C and rich media, as follows; G1 takes 10-15 min. S and G2 are longer and last up to 30-40 min. Finally mitosis is around 5 min (Morris & Enos, 1992).

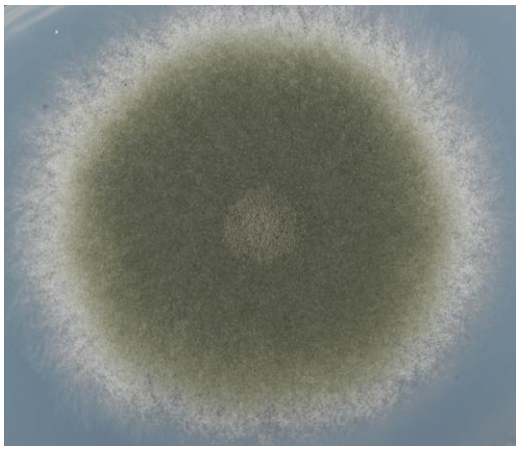

Figure 2.1 Vegetative growth of *A. nidulans*. The colony was grown on minimal medium at 37 °C. Note the white mycelium and that the density of the green conidia increases towards the middle, see text for details.

Upon the finishing of the first round of mitosis, isotropic growth switches to polarized growth via the formation of a germtube as illustrated in **Figure 2.2** (Harris, 1999). This is the beginning of a multinuclear tubular filamentous (hyphae) state. Two types of hyphae are defined in the initial phase of growth; pre- and postdivisional hyphal cells

(Harris, 1997). Within the first 4 to 6 hours the germlings, or predivisional hyphal cells, have been formed. These germlings are characterized by more than a 10-fold increase in size from the conidia and are having around eight nuclei in a shared compartment (Harris *et al.*, 1994). But after the third nuclear division, the transition from germlings to postdivisional hyphal cells takes place. These cells are distinguished by a regular doubling in the number of nuclei and formation of septa that serve to partition the hyphae into compartments (Robinow & Caten, 1969; Harris, 1997). Thus, a cell will be considered as the cellular compartments confined by septa, even though it seems ambiguous to define a cell in multinucleate hyphae. Septa are not closed passages as communication between cells is achieved through pores in the septa that allow passage of nutrients, proteins and even nuclei (Carlile & Watkinson, 1994; Walther & Wendland, 2003).

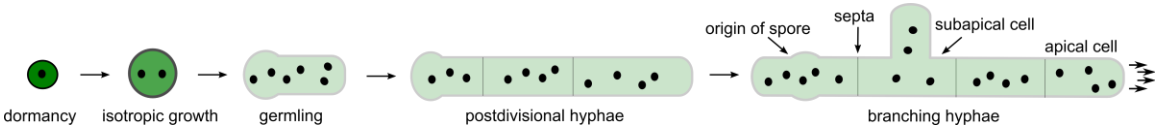

Figure 2.2 Spore germination and cellular compartmentalization. The process of spore germination and duplication cycle in *A. nidulans* is shown from dormant spore to the branching of hyphae. Besides the branching in subapical cells, the conidium will in the end germinate in more directions. Arrows indicate growth direction.

Mature cells usually have ca. three or four nuclei (Trinci and Morris, 1979), however the number can vary with nuclear migration within hyphae. This migration is presumably assisted by microtubules and tends to be in the same direction as the hyphal extension. In fact, hyphal cell-wall synthesis and extension is one of the most extreme examples of polarized growth in nature. To coordinate this, septation as well as several other structures are necessary. The actin cytoskeleton localizes both at the sites of cell-wall deposition and at the septation site (Harris & Momany, 2004). In the tip of the apical cells, small unique granules called spitzenkörpers are mediating the extension and direction of the hyphae, since they act as a docking station for vesicles, brought there by microtubules, carrying materials for cell wall synthesis (Riquelme *et al.*, 1998).

The exact coordination and timing of the events in hyphal growth is not entirely clear. For example, the duplication cycles in hyphal cells are not synchronized, since only the apical cells in the hyphae are actively dividing. Thus, the majority of cells consist of the subapical cells where hyphal extension has stopped. These cells can if needed form a germ tube and launch a new axis of hyphal growth. The result is formation of branches from the established hyphae. Branches can branch themselves and thus make a massive network of hyphae, the mycelium (Carlile & Watkinson, 1994; Harris, 1997). The vegetative mycelium has the capacity to spread over a large area effectively until growth is limited for example by lack of nutrients or physical barriers.

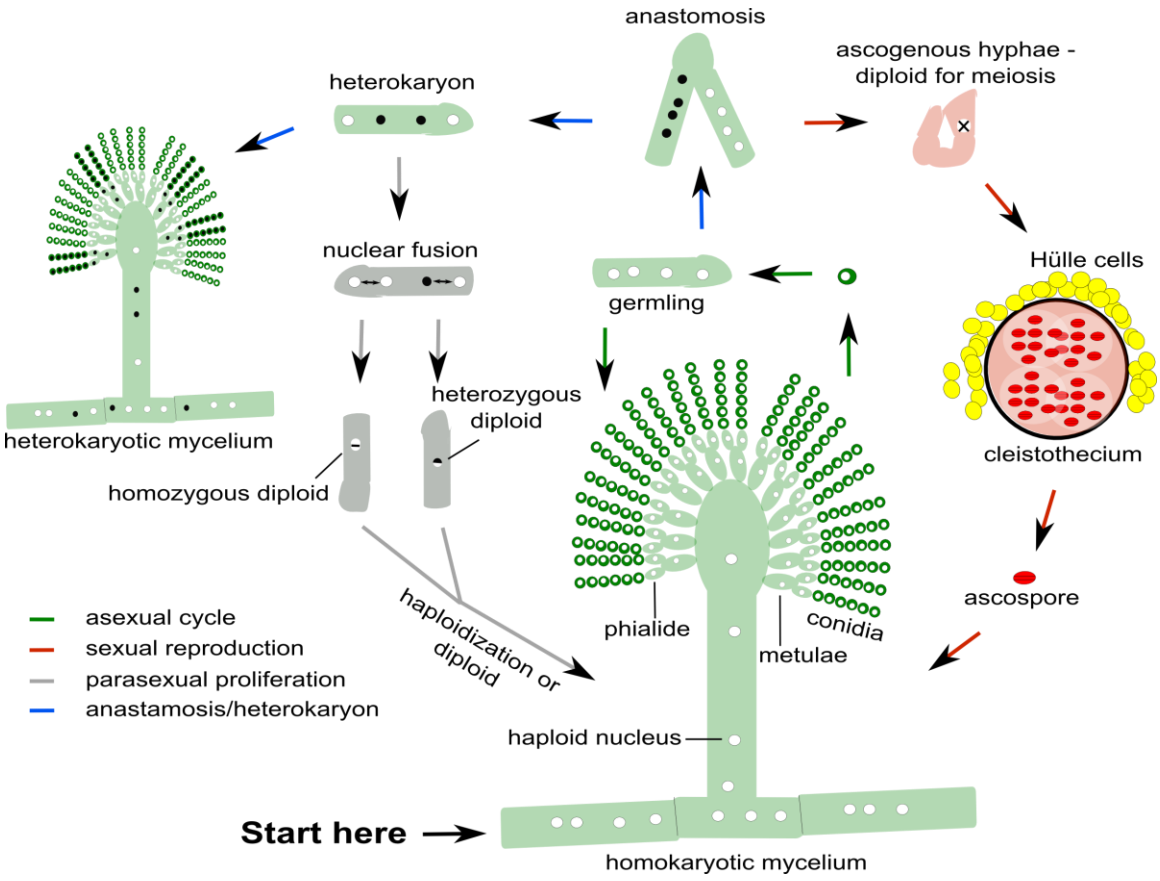

Figure 2.3. The life of *A. nidulans*. The starting point can be the mycelium as indicated, but also the single conidium above the conidiophore. Note that after parasexual proliferation there is a possibility for diploid conidia. See text for details.

The rapid and forceful extension of hyphae penetrates substrates to secure nutrients (Carlile & Watkinson, 1994). On a homogenous substrate a differentiated growth pattern is firstly seen in the center of the colony. When a certain and low nutrient level is reached, spore formation will take place. Stalks rise from hyphal foot-stem cells and the tips swell to form a vesicle on top of the stalk (Adams *et al*., 1998) as illustrated in **Figure 2.3**. From each vesicle three specialized structures are developed. Firstly, approximately 60 metulae are formed, and from each of these two phialides bud out resulting in a conidiophore. Every phialide is extended by long chains of up to 100 spherical green conidiospores. A single conidiophore can thus bear more than 10.000 conidia, which can be distributed to the environment (Adams *et al*., 1998). The metulae, phialides and conidia are all uninucleate, however the stalk and vesicles are multinucleate. However, during growth hyphae often collide and fuse with each other in a process called anastomosis. The protoplasm is hence shared in a common mycelium that contains nuclei from both of the fused hyphae (Reviewed in Glass *et al*., 2000).

Heterokaryon

Three scenarios will be the outcome from anastomosed hyphae. Firstly, if nuclei originate from different colonies and a common protoplasm is maintained a heterokaryotic mycelium is established. To keep the heterokaryon state, it requires selective pressure on both types of nuclei to ensure that one type of nuclei is not lost from the mycelium (Pontecorvo, 1953). When phialides are formed in a heterokaryon, one type of nuclei will enter and through mitosis serve as genetic template for the whole conidial chain that emerges from that particular phialides. Therefore, a conidiophore can display neighbor chains of conidia harboring different nuclei, since the genotype depends on the original nucleus in the metulae (Thom & Raper, 1945; Adams *et al*., 1998). The two alternative scenarios involve generation of diploids through nuclear fusion. Sexual propagation is in nature the far most common of the two, as the parasexual exchange of genetic information mainly is considered to be an event controlled in the laboratory.

Sexual reproduction

Sexual proliferation starts after the vegetative growth phase, and begins with formation of a network of ascogenous dikaryotic mycelium, as illustrated by red arrows in **Figure 2.3**. Exactly how the sexual development initiates is unknown. However, the mycelial network is believed to originate from fused hyphae, where the original dikaryotic cell arises. The part of the mycelial network surrounding the initial cell is called cleistothecial primordium and it is here that the specialized Hülle cells will be formed. From this nest of hyphae and Hülle cells, spherical fruiting bodies (cleistothecia) will form. These structures are 100-200 μm large when mature and are packed with thousands of sacs (asci) that all have eight sexual spores, the ascospores (Champe *et al*., 1994; Meilus & Castro-Prado, 1998). The development of progeny begins with multiple synchronous divisions of the dikaryotic cell. At one point, diploid meiocytes (zygotes) will briefly form from the two haploid nuclei within the dikaryotic cells and they enter meiosis (Pontecorvo, 1953; Champe *et al*., 1994; Hoffmann *et al*., 2001). After meiosis, one round of duplication takes place and the final outcome is the eight recombinant products in the form of bright red ascospores. In comparison, ascospores usually take from 7-10 days to develop, whereas the conidiospores use less then 20 hours to form (Brown & Salvo, 1994). This course of sexual reproduction can be followed macroscopically as cleistothecia go from deep red to black when they mature, though cleistothecia are partly covered by the bright yellow Hülle cells (Pontecorvo, 1953; Adams *et al*., 1998). The sexual offspring can give rise to new recombinant colonies, or result in homokaryotic reproduction, if diploids merge from genetically identical nuclei.

Ascospores are more stable in storage than the vegetative counterpart and can survive many years of dormancy in soil. Hence the course of ascospore germination is similar to the one described for conidia, however it is slower in the initiation phase[7]. Further, the development of both asexual and sexual structures relies to some extent on some of the same genes, like *stuA*, *medA* and *veA* as well as the availability of light, but the

[7] http://www.fgsc.net/fgn48/Kaminskyj.htm

regulation of sexual development displays large complexity (Adams *et al.*, 1998). This degree of complexity is absent when genetic information is exchanged in the parasexual proliferation.

Parasexual proliferation

Within a mycelium, two nuclei can occasionally fuse to generate a diploid nucleus, which is homo- or heterozygous depending on the genotypes of the nuclei that were fused, as indicated by grey arrows in **Figure 2.3**. The diploid nucleus can exist without undergoing meiosis, as it can propagate through the duplication cycle. These nuclei can be identified by DNA content as well as having a larger size, hence making conidia 1/4 larger, to ~4 μm in total, than the haploid conidia (Upshall, 1981). However, the homologous chromosomes can at some point undergo mitotic recombination and if the parents were genetically different they can generate recombinant progeny (see Chapter 3). Additionally, mitotic recombination can be erroneous and create aneuploid strains. These phenomena are accompanied with poor growth, but loss of chromosomes during the next mitotic divisions can result in a complete haploidization of the strain. This can thus lead to a genetically new haploid strain (Carlile & Watkinson, 1994). This mode of genetic exchange is not limited to *A. nidulans*, but has also been found in other aspergilli, *Penicillium* and *Fusarium* (Pontecorvo, 1956).

The life modes of *A. nidulans* underline the ease of handling and the great opportunities for combining genetic traits. It is also possible to alter the phenotype imprint of *A. nidulans* strains by random mutagenesis of spores or by introducing DNA to the fungus. The latter will briefly be introduced in the remaining part of the Chapter.

Transformation of *A. nidulans*

The introduction of DNA can be mediated by different transformation strategies, where each method has advantages and drawbacks (recently reviewed in Meyer, 2008). The most widely used method for *A. nidulans* is the protoplast based transformation. Here the fungal cell wall is degraded by enzymes liberating spherical structures representing bits of hyphal compartments. DNA carrying a marker gene for selection is added to these protoplasts that vary in size as well as in nuclear contents (Fincham, 1989), and transformants can be retrieved by selection.

Genetic markers in *A. nidulans*

The outcome of genetic transformation experiments relies partially on a strong and stable genetic marker system for selection of mutant strains. Here *A. nidulans* has due to the extensive use as a model system relatively many markers available and a selection of the most popular markers is listed in **Table 2.2**. Moreover, equivalent marker systems can usually be developed for other aspergilli and filamentous fungi. The direct selection of mutants by ability to grow on defined media is often provided by two classes of genetic markers; auxotrophic markers of both endogenous or heterologous origin, and genes conferring resistance to various antibiotics (Turner, 1994).

Table 2.2 A collection of common genetic selection markers for *A. nidulans*

Gene	Gene product	Selection	Reference
trpC	Trifuctional enzyme	Tryptophane aux$^{+?}$	Yelton *et al*., 1984
argB	Ornithine carbamoyl transferase	L-arginine aux	John & Peberby, 1984
pyrG	Orotine-5´-phosphate decarboxylase	Uracil/uridine aux^{+}	Oakley *et al*., 1987
niaD	Nitrate reductase	Nitrate util^{+}	Whitehead *et al*., 1989
hph	Hygromycin B phosphotransferase	Hygromycin res	Punt *et al*., 1987
ble	Phleomycin-binding protein	Phleomycin res	Drocourt *et al.*, 1990

Aux. = auxotrophy, util.= utilization, res = resistance. $^{+}$Two-way selection marker, $^{+?}$counter selection not validated yet.

Both system types usually provide an easy and reliable screening procedure. However, the following considerations are important when choosing markers:

- Growth (or production) cost of selection
- Toxicity, dosage, and action of the antibiotics
- Influence of auxotrophy on growth of mutants
- Gene expression varies with the position of marker in the genome

Some of the marker genes can also be used for counter selection (see **Table 2.2**). Here the presence of the marker gene and of a synthetic antimetabolite, or a normally harmless substrate for wild-type cells, result in suppression of growth. The antimetabolites are typically analogs to metabolites normally present in the cell with a single modification. Chapter 4 and 5 are presenting counter-selectable marker systems, where the markers are recycled in sequential *Aspergillus* transformations. The markers described so far are characterized by the monitoring absent growth. Another class of markers is the "color marker genes" that enables screening of individual strains based on color difference, see **Figure 2.4**. Hence, *Aspergillus* and many other fungi produce pigmented structures such as spores, and mutations in the biosynthetic pathway leading to pigment production can change the colors. In *A. nidulans*, two genes, the *wA* and *yA*, encode laccases responsible for the pigmentation of conidia. Deficiencies in one of the two genes give white and yellow conidia, respectively (Kurtz and Champe, 1982), and wA^- will mask yA^- due to epistasis (Pontecorvo, 1953). The marker genes are thus included in the DNA introduced in two different ways, either as self-replicating plasmids or as a substrate that aims at integration into the genome.

Vectors for transformation

The evenly distribution of plasmids to all nuclei within a mycelium require a selection marker as well as an AMA1 element for autonomous maintenance in *Aspergillus* (Gems *et al*., 1991). However, cross-feeding between nuclei usually result in a gradual loss of plasmids from the mycelium. This uneven propagation of plasmids will thus affect the overall expression level of the genes located on the plasmid.

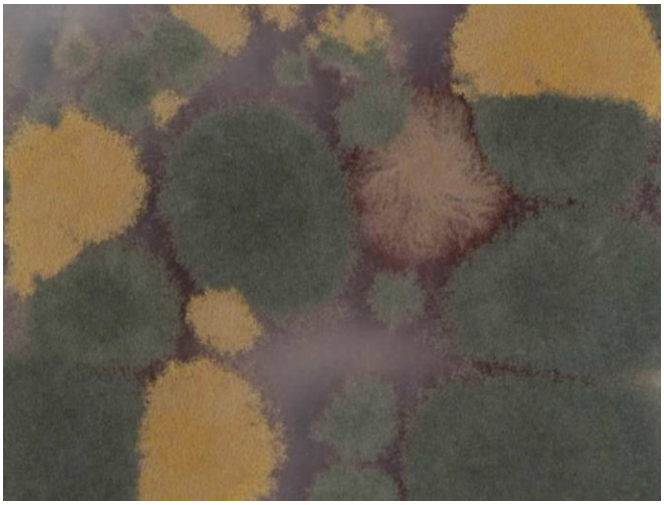

Figure 2.4 Deletion of *yA* in *A. nidulans*. *yA*$^{+}$ strains are green, whereas *yA*$^{-}$ results in yellow colonies.

An alternative is the integration of the exogenous DNA into the chromosome, which can occur randomly in the genome or at a defined locus. The permanent insertion of DNA can thus offer a stable expression level of the introduced gene depending on the chromosomal locus of integration and the regulation of expression. Gene targeting is the most important technique to conduct site-specific integrations in fungi as well as in several other eukaryotes, albeit with varying efficiency. In line of this, gene targeting is believed to be the favored strategy for human gene-therapy in the near future, if the efficiency can be increased. In order to fully utilize the potential of this technology, it is necessary to understand the fundamental processes behind gene targeting. These processes are DNA repair, which preserves the integrity of DNA against damage. Therefore, the following chapter describes DNA damage and repair before it closes with a section on gene targeting.

References

Adams, T.H, Wieser, J.K, and Yu, J.H., 1998. Asexual sporulation in *Aspergillus nidulans*. Microbiol. *Mol. Biol. Rev.* **62(1)**: 35-54.

Brown, D.W. and Salvo, J.J., 1994. Isolation and characterization of sexual spore pigments from *Aspergillus nidulans*. *Appl. Environ. Microbiol.* **60(3)**: 979-983.

Carlile, M.J. and Watkinson, S.C., 1994. The fungi. Academic press, London.

Champe, S.P., Nagle, D.L., and Yager, LN., 1994. Sexual sporulation. Chapter 17 in *Aspergillus*: 50 years on. *Progress in industrial microbiology* **29:** 429-54, Elsevier, Amsterdam-London-New York-Tokyo.

Drocourt, D., Calmels, T., Reynes, J.P., Baron, M., and Tiraby, G., 1990. Cassettes of the *Streptoalloteichus hindustanus ble* gene for transformation of lower and higher eukaryotes to phleomycin resistance. *Nucleic Acids Res*. **18(13)**: 4009.

Fiddy, C. and Trinci, A.P., 1976. Mitosis, septation, branching and the duplication cycle in *Aspergillus nidulans*. *J. Gen. Microbiol.* **97(2)**: 169-84.

Fincham, J.R., 1989. Transformation in fungi. *Microbiol Rev.* **53(1)**: 148-170.

Galagan, J.E., Calvo, S.E., Cuomo, C., Ma, L.J., Wortman, J.R., Batzoglou, S., Lee, S.I. *et al*., 2005. Sequencing of *Aspergillus nidulans* and comparative analysis with *A. fumigatus* and *A. oryzae*. *Nature* **438(7071)**: 1105-1115.

Geiser, D.M., Klich, M.A., Frisvad, J.C., Peterson, S.W., Varga, J., and Samson, R.A., 2007. The current status of species recognition and identification in *Aspergillus*. *Stud. Mycol.* **59(1)**: 1-10.

Gems, D., Johnstone, I.L., Clutterbuck, A.J., 1991. An autonomously replicating plasmid transforms *Aspergillus nidulans* at high frequency. *Gene* **98(1)**: 61-67.

Glass, N.L., Jacobson D.J., and Shiu, P.K., 2000. The genetics of hyphal fusion and vegetative incompatibility in filamentous ascomycete fungi. *Annu. Rev. Genet*. **34**: 165-186.

Harris, S.D., Morrell, J.L., and Hamer J.E., 1994. Identification and characterization of *Aspergillus nidulans* mutants defective in cytokinesis. *Genet*. **136(2)**:517-32.

Harris, S.D., 1997. The duplication cycle in *Aspergillus nidulans*. *Fungal Genet. Biol*. **22(1)**: 1-12.

Harris, S.D., 1999. Morphogenesis is coordinated with nuclear division in germinating *Aspergillus nidulans* conidiospores. *Microbiol*. **145**: 2747-56.

Harris, S.D. and Momany, M., 2004. Polarity in filamentous fungi: moving beyond the yeast paradigm. *Fungal Genet. Biol*. **41(4)**: 391-400.

Holden, D.W., Tang, C.M., Smith, J.M., 1994. Molecular genetics of *Aspergillus* pathogenicity. *Antonie Van Leeuwenhoek*. **65(3)**: 251-255.

Hoffmann, B., Eckert, S.E., Krappmann, S., Braus, G.H., 2001. Sexual diploids of *Aspergillus nidulans* do not form by random fusion of nuclei in the heterokaryon. *Genetics* **157(1)**: 141-147.

John, M.A. and Peberdy, J.F., 1984. Transformation of *Aspergillus nidulans* using the *argB* gene. *Enzyme Microbial Techn*. **6**: 386-389.

Kurtz, M.B. and Champe, S.P., 1982. Purification and characterization of the conidial laccase of *Aspergillus nidulans*. *J Bacteriol*. **151(3)**: 1338-1345.

Meilus, M. and Castr-Prado, M.A.A., 1998. Gene inactivation system extension into a unique sequence outside of the II to I insertional duplication in *Aspergillus nidulans*. *Can. J. Microbiol.* **44**: 1037-1044.

Meyer, V., 2008. Genetic engineering of filamentous fungi – progress, obstacles and future trends. *Biotechnol. Adv.* **26**: 177-185.

Morris, N.R. and Enos, A.P., 1992. Mitotic gold in a mold: *Aspergillus* genetics and the biology of mitosis. *Trends Genet.* **8(1)**: 32-37.

Oakley, B.R., Rinehart, J.E., Mitchell, B.L., Oakley, C.E., Carmona, C., Gray, G.L., May, G.S., 1987. *Gene* **61(3)**: 385-399. Cloning, mapping and molecular analysis of the *pyrG* (orotidine-5'-phosphate decarboxylase) gene of *Aspergillus nidulans*.

Pontecorvo, G., 1953. The genetics of *Aspergillus nidulans*. *Adv. Genet. Incorp. Mol. Genet. Med*. **5**: 141-238.

Pontecorvo, G., 1956. The parasexual cycle in fungi. *Annu. Rev. Microbiol*. **10**: 393-400.

Punt, P.J., Oliver, R.P., Dingemanse, M.A., Pouwels, P.H., and van den Hondel, C.A., 1987. Transformation of *Aspergillus* based on the hygromycin B resistance marker from *Escherichia coli*. *Gene* **56(1)**: 117-124.

Riquelme, M., Reynaga-Pena, C.G., Gierz, G., and Bartnicki-Garcia, S., 1998. What determines growth direction in fungal hyphae? *FungalGenet. Biol*. **24**, 101–109.

Robinow, C.F. and Caten, C.E., 1969. Mitosis in *Aspergillus nidulans*. *J. Cell. Sci*. **5**: 403-431.
Thom, C. and Raper, K.B., 1945. Manual of the aspergilli. Waverly Press Inc., Baltimore.

Timberlake, W.E. and Marshall, M.A., 1998. Genetic regulation of development in *Aspergillus nidulans*. *Trends Genet*. **4(6)**: 162-169.

Trinci, A.P.J. and Morris, N.R., 1979. Morphology and growth of a temperature-sensitive mutant of *Aspergillus nidulans* which forms aseptate mycelia at non-permissive temperatures. *J. Gen. Microbiol*. **114**: 53-59.

Turner, G., 1994. Vectors for genetic manipulation. Chapter 24 in *Aspergillus*: 50 years on. *Progress in industrial microbiology* **29**, Elsevier, Amsterdam-London-New York-Tokyo.

Upshall, A., 1981. Naturally occurring diploid isolates of *Aspergillus nidulans*. *J. Gen. Microbiol.* **122(1)**: 7-10.

Walther, A. and Wendland, J., 2003. Septation and cytokinesis in fungi. *Fungal Genet Biol*. **40(3)**: 187-196.

Whitehead, M.P., Gurr, S.J., Grieve, C., Unkles, S.E., Spence, D., Ramsden, M., and Kinghorn, J.R., 1990. Homologous transformation of *Cephalosporium acremonium* with the nitrate reductase-encoding gene (*niaD*). *Gene* **90(2)**: 193-198.

Yelton, M.M., Hamer, J.E., and Timberlake, W.E., 1984 Transformation of *Aspergillus nidulans* by using a *trpC* plasmid. *PNAS* **81(5)**: 1470-1474.

Chapter 3

DNA damage & repair

The fitness and viability of living organisms depends on the preservation of DNA, since the DNA within cells is under constant attack. The DNA damage can manifest in various lesions that are detrimental to the cell if left unrepaired because they lead to mutations, chromosomal aberrations, and even cell death. Fortunately, an array of elegant DNA repair mechanisms acts as caretakers to ensure fitness. Repair of DNA damage often leads to an accurate sequence restoration, however in some cases repair can be error-prone and mutations are unavoidable. The individual DNA repair pathways have preferences for the repair of specific lesions, and appear to be separated in function. However as it will be presented in this chapter, a picture will emerge of pathways that are interconnected and that share features to cope with the serious threats the damage imposes. Thus, the overall picture of the individual DNA lesions and how they can be repaired has to be drawn to comprehend to subtleness of these systems. Regarding the descriptions of the repair mechanisms and proteins, it will generally represent yeast unless otherwise stated. Firstly, the lesions and how they can be created will be introduced. There are two main categories of DNA damages, see **Figure 3.1**, the spontaneously occurring and the induced lesions.

Spontaneous DNA Damage

The most common mutation is the loss of DNA bases from the duplex. Generally, the *N*-glycosyl bond between the DNA base and deoxyribose is relatively stable, however it can react with water in a spontaneous hydrolysis process yielding a free base and an abasic site (Lindahl, 1993). These abasic sites, apurinic or apyrimidinic (AP) sites can

block both essential processes such as replication and transcription. In addition DNA bases can also undergo deamination, where ammonia is lost from the base leading to miscoding base analogs (Lindahl, 1993). DNA polymerases can make errors during replication causing a mutation at the locus. The induced DNA damage produces other lesions, either via endo- and exogenous factors.

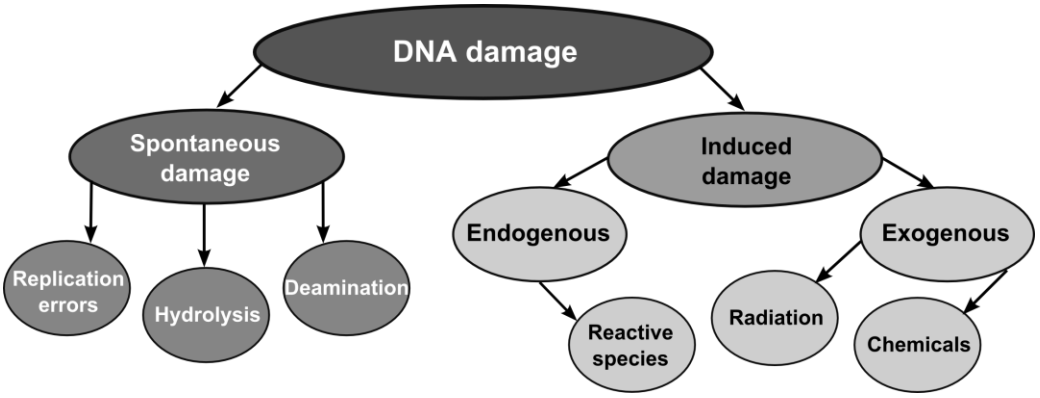

Figure 3.1 DNA damage. The respective types of spontaneous and induced damages.

Induced DNA Damage – endogenous factors

Products or byproducts from metabolism or other cellular processes can be highly reactive. The reactive oxygen species (ROS, e.g. O_2^-, H_2O_2, and OH^-) and the equivalent reactive nitrogen species (RNS, e.g. NO^- and NO_2^-) are the most frequently produced byproducts (Wiseman & Halliwell, 1996; De Bont & van Larebeke, 2004). The hydroxyl ions are the most reactive, since they react with almost everything, whereas the other species are more specific. The consequence of a ROS or RNS attack is typically materialized in DNA base oxidization, as in the conversion of guanine to 8-oxo-deoxyguanosine (8-oxo-dG), see **Figure 3.2**. Adenine prefers to pair with 8-oxo-dG rather than cytosine, generating GC→TA transversion mutations (Powell et al., 2005). ROS and RNS are also generated when high-energy waves and particles, or genotoxic chemicals enter cells.

Induced DNA damage – exogenous factors

Ultraviolet radiation (UVR) from the sun is the most common type of radiation and it covers a broad wavelength spectrum ranging from 10-400 nm. The UV-A (320-400 nm) and the UV-B (280-320 nm) are ecologically significant, while UV-C (<280 nm) is absorbed by ozone and oxygen before reaching Earth (Sinha & Häder, 2002; Godar, 2005). The UV-A creates secondary photoproducts such as free radicals, see **Figure 3.2**. In contrast, UV-B causes cyclobutane-pyrimidine dimers (CPDs) and 6-4 photoproducts (6-4 PPs). Both these lesions distort the DNA double helix via kinks and bends, thus blocking transcription and replication. More than 10^5 of CPDs are created in a human cell after one minute's exposure to the sun (Ward, 2000). Ionizing radiation (IR), e.g. γ-rays/X-rays, is a type of radiation that arises from decay of certain isotopes, and though UVR normally is more frequently encountered by human cells than IR, IR will deposit more energy in the matter than UVR. γ-rays creates a variety of lesions, such as single-strand breaks (SSBs) and double-strand breaks (DSBs). Further, in reactions with water ROS are formed (Kupiec, 2000; Ward, 2000; Hoeijmakers, 2001). Thus, IR often makes clustered damage on DNA and at double-strand breaks (DSBs) the ends will be frayed (Elkind & Redpath, 1977; Ward, 2000; Rothkamm & Löbrich, 2003). In addition to the environmentally based radiation, a wide array of synthetic chemicals is very effective at generating DNA damage (i.e. genotoxins), see **Figure 3.2**. Some of the most commonly used will be given in the following section to reflect their broad actions.

The radiomimetic drug bleomycin causes oxidization of the deoxyribose in DNA with an estimate of 10 % of the lesions being bi-stranded occurring at opposite bases creating chemically identical breaks at each strand, mainly GC or GT, resulting in a DSB (Povirk, 1996). 4-Nitroquinoline 1-oxide (4-NQO) is UV-mimetic drug that forms a bulky adduct mainly at guanine and to some extent adenine (Ikenaga et al., 1975). The alkylating agents, e.g. ethyl-methane sulfonate (EMS) and methyl-methane sulfonate (MMS) are adding an alkyl group to the nucleobase, for example through methylation of the nucleobases to 7-deoxyguanine and 3-methyladenine (3MeA). The presence of 3MeA in

the helix can lead to a block of replication. Cross-linking agents such as cisplatin and mitomycin induce reactions between two DNA bases forming an intra- or interstrand crosslink preventing strand separation and replication (Dolling *et al.*, 1999). Hydroxyurea is a drug that depletes the pool of ribonucleotides by inhibiting the enzyme ribonuleotide reductase, which eventually turns into replication stress. The multifaceted lesions from the damaging agents, requires an equally flexible and broad-acting DNA-repair system as described below. As seen from the sections above DNA lesions can be divided into lesions occurring on single-strand level and DSBs. The focus in this chapter will be on DSB repair (DSBR). However, the general DNA repair pathways deserve a brief introduction since DNA repair pathways to some extent are entangled into each other, and thus collaborations or crosstalk between the different pathways when handling DNA damage cannot be ruled out.

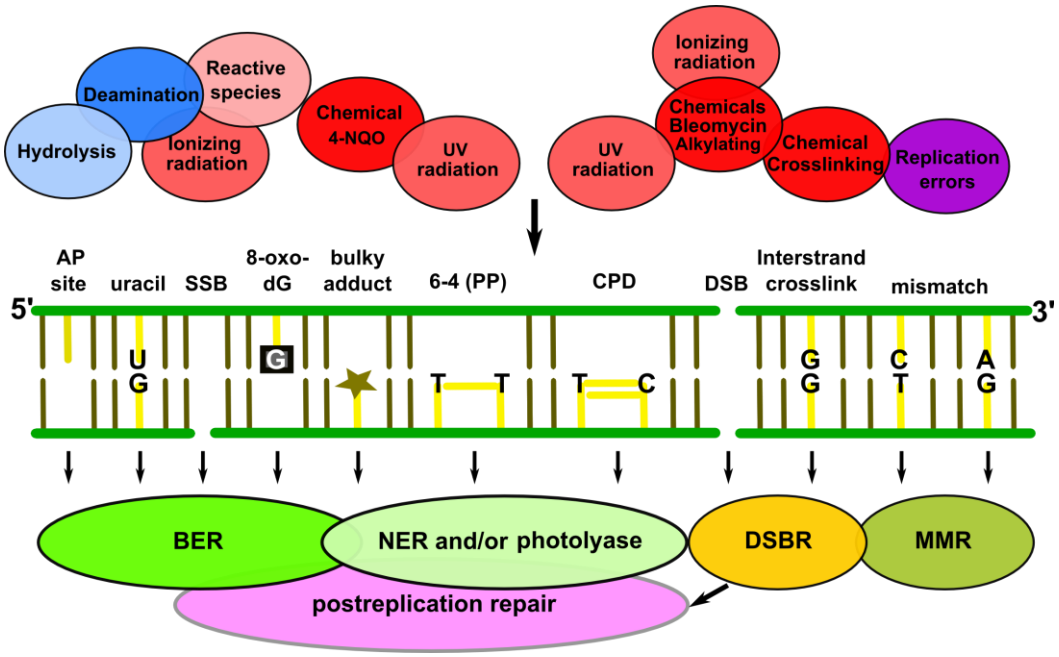

Figure 3.2 Overview of DNA damaging agents, types of DNA damage and the corresponding repair processes. The brownish connection in the DNA illustrates correct pairing whereas the yellow or lack of connectors symbolizes DNA abnormalities, please see text for details. Double-strand break repair (DSBR) proteins can be recruited in postreplication repair, hence the arrow. BER=base-excision repair, NER=nucleotide-excision repair and MMR=mismatch repair.

General DNA repair

Mutations, base modifications, AP sites and single-strand breaks are frequently occurring lesions. They all interfere with basic cellular functions such as replication and transcription. Several repair pathways are coping with these damage types.

Photoreactivation

The simplest form of repair is by the enzyme photolyase, which single-handed binds to UV-induced lesions, i.e. CPD and 6-4 PPs, and corrects them by using the energy of light. It has been demonstrated to be an important repair pathway in archaea, bacteria, and yeast, but the system has not been documented in mammals (Kato *et al*., 1994). The photolyase seems particularly active when lesions are occurring in the promoter regions and at the non-transcribed strands (Sancar, 2000). However in the transcribed strands, the RNA polymerase appears to block access for photolyase. Instead photolyase is believed to stimulate nucleotide-excision repair (NER) to repair the equivalent lesions as well as bulky adducts on the transcribed strand.

Nucleotide-excision repair

NER was discovered during investigations of the photoreactivation pathway. The initial phase of NER is divided into two separate pathways, global-genome NER (GG-NER) and transcription coupled repair (TCR). GG-NER is commenced when disrupted base pairing is detected as a bubble structure on the DNA (Sugasawa *et al*., 2001), whereas a blocked RNA polymerase II at the transcribed strand initiates TCR. After the initial processing, GG-NER and TCR pathways are believed to follow the same pathway in the remaining steps from the excision of ~24-32 nucleotides around the site of damage by Rad2 and Rad1-Rad10. Replication protein A (RPA) stabilizes the undamaged strand while excision occurs and gap filling is made by polymerases Polδ/ε and DNA ligase 1 or 3 (Hanawalt, 1994). Lesions that escape the NER surveillance can be repaired by base-excision repair (BER).

Base-excision repair

There are two modes of BER repair; short- and long-patch BER, here the human BER is stated. Lesions such as deamination are damages that are channeled through the short-patch BER (Wilson & Thompson, 1997). Glycosylases initiate BER by flipping out the damaged base creating an AP site after the excision and removal of the base. One base is inserted and the nick in the DNA is sealed. The long-patch BER can be employed for repairing SSBs. The SSB ends are trimmed, and proliferating cell nuclear antigen (PCNA) and Polδ/ε drives synthesis of a 2-10 nt stretch (Hoeijmarkers, 2001). Flaps are removed by the FEN1 endonuclease before DNA ligase 1 seals the gap. If BER is activated due to a block of transcription, TCR can be utilized for repair. The three repair modes described above deal with chemical abnormalities in the helix. Bases can also be paired incorrectly, and this can be fixed by mismatch repair (MMR).

Mismatch Repair

Errors from DNA polymerases as well as insertions and deletions resulting in heteroduplex DNA are all subjected to repair by MMR. The course of the MMR process can be divided in four parts; mismatch recognition, recruitment of additional MMR factors, signaling for error identification with degradation of sequence flanking the mismatch, and lastly the filling of excised sequence. In MMR, two distinct and conserved complexes distinguish between the types of mismatches; the Msh2-Msh6 complex acts on single-base mismatches, whereas larger mismatches in the DNA such as insertion or deletion loops are recognized by Msh2-Msh3. This complex is also required for processing of non-homologous ends in recombination (Sugawara *et al*., 1997). Recombination as well as mismatch correction is also associated with the postreplication repair and mutagenesis (PRRM) pathway.

Postreplication repair and mutagenesis

DNA polymerases δ to ε are easily blocked by many obstacles in the DNA helix, leading to stalling of replication forks. However, flexible DNA polymerases (ζ to κ) called translesion polymerases have evolved to permit the DNA synthesis passing distortions in the template by less stringent base pairing ensuring the continued replication. This translesion synthesis (TLS) can be error-prone and is thus responsible for substantial proportion of point mutations occurring in the genome (Lawrence, 1994; Hoeijmakers, 2001; Prakash *et al*., 2005).

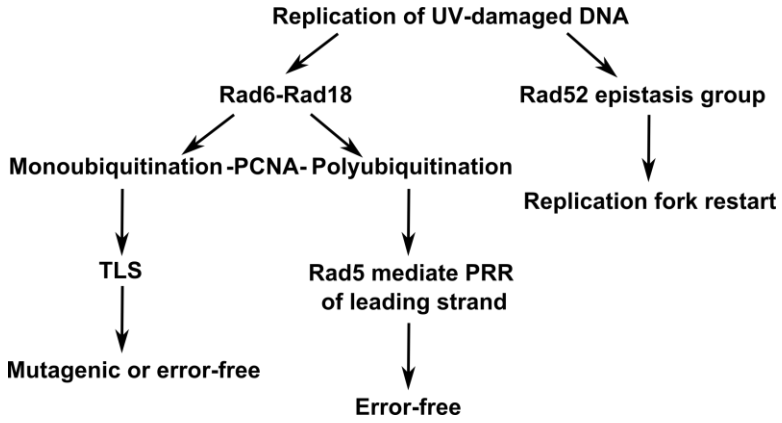

Figure 3.3 The postreplication repair and mutagenesis pathway. The central events are the regulation of ubiquitination of PCNA by Rad6-Rad18. PRR denotes the Rad5 mediated error-free branch. Recombination is also an option, but will be described in the 'Replication fork restart' section (Modified from Gangavarapu *et al*., 2007).

The TLS genome-protection system is governed by Rad6-Rad18 from the *RAD6* epistasis group, which through ubiquitination of PCNA also controls an error-free Rad5 conducted repair of lesions in the leading strand, see **Figure 3.3** (Gangavarapu *et al*., 2007). Some proteins of the recombination process are involved in rescuing the stalled replication forks especially when the lesion is located on the lagging strand (Gangavarapu *et al*., 2007), which is described in the section on 'Replication fork restart'. The recombination process is an integrated part of DSBR, and deals with the most severe lesions, the DSBs, also being programmed intermediates in meiosis essential for

chromosome segregation and genetic diversity (e.g. reviewed in Pâques & Haber, 1999 and Helleday *et al*., 2007).

Double-strand break repair

Failure to repair DSBs can lead to chromosomal rearrangements, cell cycle arrest or cell death, and the DSBR is thus of utmost importance. DSBR is accomplished by two distinct pathways; non-homologous end-joining (NHEJ) and homologous recombination (HR). The NHEJ pathway assembles two broken ends of DNA and seals the break, and the process needs very little or no homology at all. NHEJ is capable of performing error-free repair, but often the repair is error-prone, see **Figure 3.4**. HR is more complex as it requires a homologous DNA template to retrieve sequence information from, a repair that is mostly error-free (Pâques & Haber, 1999). The two pathways could in principle be competing for the same DNA substrates to make repair, and are tightly regulated.

During the cell cycle activity of HR and NHEJ are regulated for optimal caretaking of the genome by cyclin-dependent kinase Cdc28 activity, which is under control of the kinase Mec1. A cell-cycle delay will be necessary for sufficient time to repair DSBs (Ira *et al*., 2004). NHEJ is dominant when no homologous template is available for repair. This situation occurs in haploid cells in G1 and early S phase where there is no sister chromatid to repair from. In the end of the S phase and in G2/M the sister has been synthesized and here HR is a much more attractive alternative for repair and is therefore active. In diploid organisms there are always homologous chromosomes available for repair. However, this is not always beneficial due to the possible loss of heterozygosity (LOH). Moreover, higher eukaryotes typically accumulate a high amount of repetitive elements in the genome compared to species such as *S. cerevisiae* (Kidwell, 2002). Repeated sequences in the genome can recombine and contribute to genetic instability. Hence, HR seems more prominent and to have fewer restrictions in *S. cerevisiae* than in multicellular organisms, which have to limit the level of HR by employing NHEJ to comply the risk of instability.

Non-homologous end-joining

All organisms from bacteria to humans are capable of simple curing of breaks via NHEJ (Hefferin & Tomkinson, 2005; Shuman & Glickman, 2007). This repair can, as mentioned above, occur as a simple religation without any errors in base pairing and loss of sequence (Daley *et al.*, 2005).

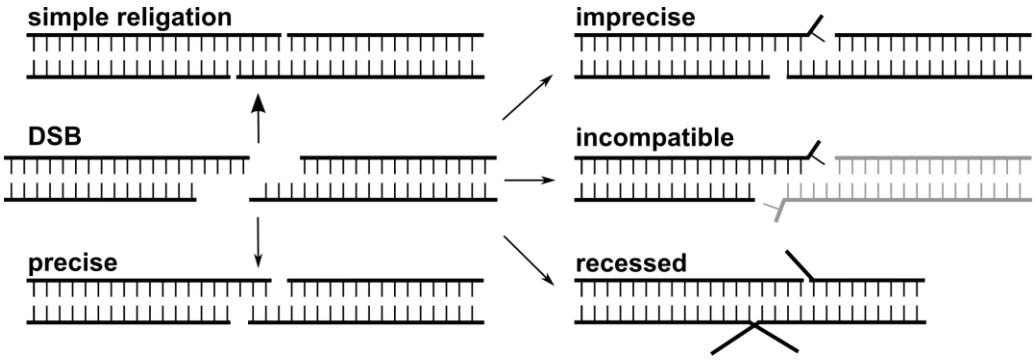

Figure 3.4 The rejoining of ends in non-homologous end-joining. The arrow with the large head is simple relegation and illustrates non-processed and error-free repair, whereas the arrows with small heads depict processed ends. The long flaps in the recessed repair are non-homologous tails (Modified from Daley *et al.*, 2005).

Often a few bases are lost in the processing of the ends prior to reconnection of the two strands. Furthermore, if there are multiple breaks, the ends can be joined incorrectly, i.e. new pairs of ends are joined, leading to rearrangements or insertions of DNA. Thus, sequence alterations by inappropriate NHEJ can lead to mutation or rearrangements ending in loss of gene function. Moreover, the integration of exogenous DNA into the chromosome by NHEJ can be as polymerized DNA (Würtele *et al.*, 2003). The mechanism on DNA level will be outlined briefly, which will be followed by a description of the mechanisms at protein level assigning the involved proteins to functions.

Mechanism of non-homologous end-joining in yeast

The NHEJ process is composed of a few key steps. After the DSB has been formed, the damaged ends are protected from degradation and extensive end processing. Since the

broken ends have to be joined, the two parts of the chromosome are kept in proximity to through a bridged connection. The ends are assembled and gaps are filled and the break is ligated completing the repair (for reviews Lewis & Resnick, 2000; Daley *et al*., 2005; Hefferin & Tomkinson, 2005). The steps described are completed by the core NHEJ protein machinery, which is conserved throughout eukaryotes with few exceptions.

End protection and bridging

Two protein complexes, Ku and MRX, are the first on the spot in NHEJ mediated repair of DSBs though in which order the complexes arrive is not entirely clear (Daley *et al*., 2005). One scenario could be as illustrated in **Figure 3.5** showing one of the current consensus models for yeast NHEJ, where Ku binds at the extreme positions of the DNA ends. This is possible due to Ku being a heterodimer of yKu70 and yKu80 and the assembled dimer is composed of a hole in the core of the dimer wherein the DNA duplex fits (Walker *et al*., 2001). Ku moves away from the break site to make room for the MRX complex. This is possible due to the positive charge of the Ku core that enables Ku to slide in a sequence independent manner along the negative charges of the sugar phosphate backbone (Dynan & Yoo, 1998; Walker *et al*., 2001). The MRX constitutes the bridge over the broken DNA due its structural properties, though early studies also have claimed a bridging activity by Ku alone (Paillard & Strauss, 1991).

The symmetrical topology of the MRX complex, with Rad50 and Mre11 dimers and a Xrs2 monomer, is the foundation for the role and functionality of the complex. The interaction, and potentially the recruitment, between Ku and MRX have been demonstrated to occur between the extreme C-terminal of Ku80 and the FHA domain of Xrs2 (Palmbos *et al*., 2005). Hence, two Rad50 monomers connected to each other provides the physical link between two pieces of DNA (Usui *et al*., 1998; D'amours & Jackson, 2002). This is accomplished by the binding of Rad50 to DNA. Rad50 uses the active associated form of its distally placed Walker type A and B ATPase domains, which are separated by a heptad-repeat region and a CXXC hinge motif. This association

takes form after the whole protein has folded back on itself, creating a coiled-coil arm formed from the repeats extending in the hinge. The DNA binding is likely assisted by the Mre11 dimer that interacts with the globular region containing the ATPase domain of Rad50 (de Jager et al., 2001).

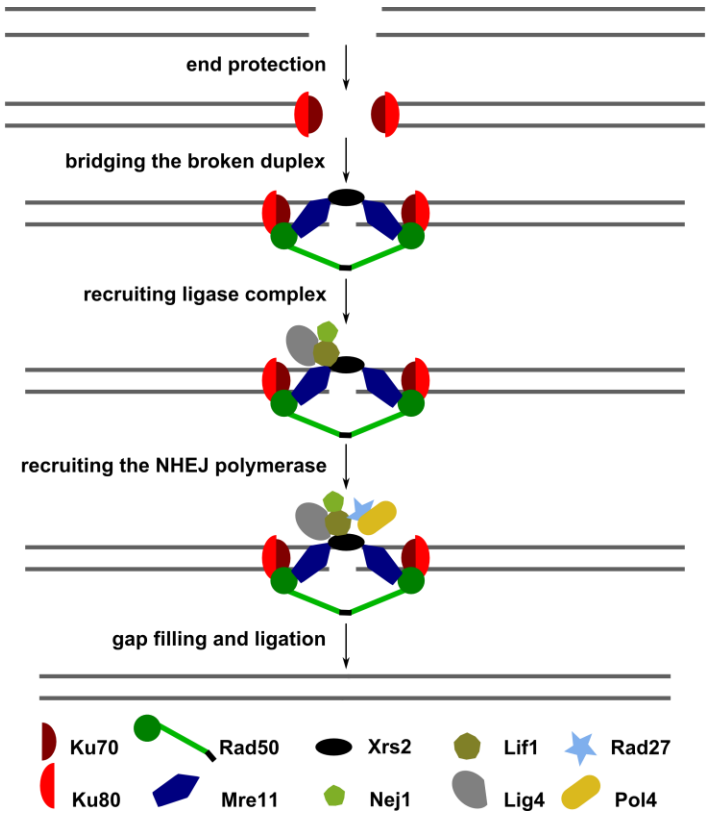

Figure 3.5 The mechanism and core proteins of non-homologous end-joining in yeast. There are several complex formations. Two different Ku units join in a heterodimer, and the MRX is formed from two Rad50 and Mre11 and one Xrs2. The ligase complex is made between Lig4 and Lif1 with a potential role of the regulator Nej1, see text for details.

However, the key activities of Mre11 probably lie in the processing of the DNA, due to the nucleolytic activity mediated by five phosphoesterase domains and two DNA binding domains (Symington, 2002). The exact cleavage activity of Mre11 in NHEJ is not understood, as some NHEJ repair is carried out without end processing. Nevertheless, Mre11 is involved in the actual end processing observed due to the demonstrated 3′ to 5′dsDNA exonuclease activity as well as endonuclease activity (Trujillo & Sung, 2001).

This dual role supports the model where Ku binds prior to MRX, since this would limit the degradation of ends. Still, more pathways can exist, since absence of either Ku or MRX has shown differentiated repair in a plasmid religation assay reported (Boulton and Jackson, 1996a). When Ku was absent, the plasmids were mainly repaired by an error-prone end-joining pathway in contrast to MRX deficiency where the outcome was mostly correct restoration of the original sequence (Critchlow & Jackson, 1998). In addition, Ku and MRX are both important for recruiting the remaining enzymes to complete NHEJ by gap filling and ligation.

Gap filling and ligation

Xrs2 interacts with Lif1, which is bound to the DNA ligase 4, Dnl4, see **Figure 3.5**. The recruitment of the DNA ligase 4 complex is essential for NHEJ in yeast, and interactions between Ku and Lif1 as well as Ku80 and Dnl4 has also been suggested (Teo & Jackson, 2000; Palmbos *et al*., 2005). Further, the Nej1 protein was found also to interact with Lif1. In cells ready for meiosis it was demonstrated that Nej1 regulates the distribution of Lif1 hereby controlling the overall NHEJ activity (Valencia *et al*., 2001). The polishing of the repaired break and completion of repair is assisted by Rad27, a 5′ to 3′ exonuclease/5′ flap endonuclease. This protein removes eventual 5′ flaps, but not 3′ flaps, this function has not been assigned for yet, but Mre11 could be a candidate (Trujillo & Sung, 2001). The mechanism described above is the major end-joining pathway, and is dependent on Ku and Lig4. However, at least one minor end-joining pathway also exists. This pathway is named the microhomology-mediated end-joining pathway (MMEJ) and is a Ku-independent pathway that through 8-10 bp homology anneals end-processed DSBs (Ma *et al*., 2003; Daley *et al*., 2005). It is dependent on the MRX complex and Rad1. It is highly error-prone, since large deletions of 302 bp have been reported (Ma *et al*., 2003). MMEJ resembles the single-strand annealing (SSA) pathway, a subpathway of HR, which is described later in the chapter. The majority of the proteins listed here for NHEJ in yeast have orthologs in humans, albeit some differences do exist. A comprehensive

table, which lists homologs of yeast, *A. nidulans* and human, can be found in Goldman & Kafer, 2004.

NHEJ in mammals

The most remarkable difference between yeast and mammalian NHEJ is that instead of MRX, the alternate proteins in mammalian NHEJ are the serine/threonine kinase DNA-PK_{cs} and a 5′ to 3′ single strand exonuclease named Artemis. Two factors which have not found in fungi. Ku is making DNA-PK_{cs} into the catalytically active DNA-PK, which is essential for NHEJ activity (Gottlieb & Jackson, 1993; Hefferin & Tomkinson, 2005). Interestingly, the phenotypic profile (e.g. γ-ray sensitive, retarded growth etc.) for murine $Ku70^{-/-}$, $Ku80^{-/-}$ and DNA-$PK_{cs}^{-/-}$ (SCID mice) differ between these three intimately related parts of DNA-PK (Gu *et al*., 1997). It is thus the DNA-PK that forms complex with DNA ligase IV and the Lif1 homolog XRCC4. An additional protein has recently been discovered in a radiation-sensitive and immune-deficient patient. This protein was found to interact with XRCC4 in two independent studies. This factor was termed XLF (or Cernunnos) and seems to regulate the equilibrium between polymeric states of XRCC4, hereby stabilizing XRCC4 and thus control the activity of the Lig4-XRCC4 complex (Ahnesorg *et al*., 2006). A homolog to XLF is not found in yeast, but XLF is in the same superfamily of proteins as Nej1 (Hentges *et al*., 2006). In mammals, the NHEJ core proteins has an additional and important role in V(D)J recombination. Their contribution is to create antigen diversity of T-cell receptors and immunoglobulin in vertebrates (Hefferin & Tomkinson, 2005). Some of the NHEJ proteins are also involved in processes occurring at the telomeres, which is general for eukaryotes.

NHEJ proteins at telomeric ends

In knock-out mutants of *yku70* and *yku80*, as well as in the equivalent strains in mammals, the telomeres undergo a rapid shortening (Boulton & Jackson, 1996b; d'Adda di Fagagna et al., 2001). Further, abolishing of Ku also has a telomere position effect (TPE), which denotes the silencing of the genes within or near the telomeres by

transcriptional repression. Ku has been observed to interact with Sir4, a component of the SIR complex also counting Sir2 and Sir3 (Aparicio *et al*., 1991). SIR is mediating TPE via induction of a condensed state (i.e. silent chromatin) of telomere DNA and mating type loci through hypoacetylation of N-terminal tails at histones H3 and H4 (Shore, 2000). In addition to the telomere effects, abolishment of SIR4 gives a NHEJ phenotype indistinguishable of those displayed by deleting either of the two Ku subunits, and SIR is required for NHEJ (Boulton & Jackson, 1998). MRX has also shown to have a role in telomere maintenance (Boulton & Jackson, 1998). The significance of MRX is highlighted as this protein has a unique opportunity to channel repair of DSBs through both NHEJ and HR.

Homologous recombination

HR is a vital process occurring in all living organisms, which is underlined by the fact that the mechanistic steps in the process are highly conserved. The principle of HR is the utilization of homologous sequences to reestablish a broken DNA helix to perform a wide range of processes as shown in **Figure 3.6**.

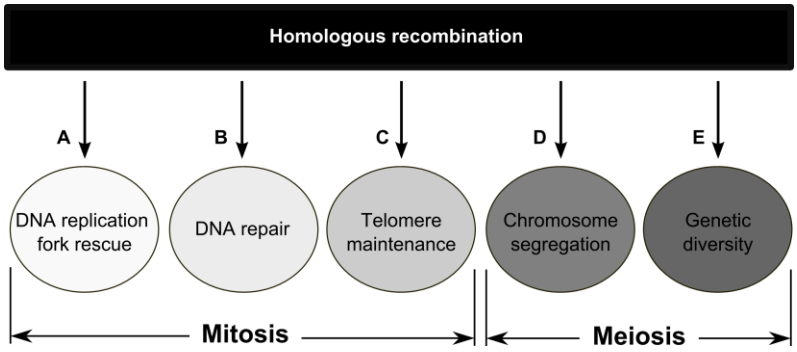

Figure 3.6 The main purposes of HR in mitosis and meiosis. This underlines the importance and versatility of the process. A to C occurs in mitosis and D to E in meiosis.

HR is essential for cellular maintenance and development. Moreover, HR is required for gene targeting, an extremely valuable application in genetic engineering (Scherer & Davis, 1979). The following section will describe the influence of HR and concentrate on

the molecular mechanisms at the level of DNA. Afterwards the key proteins in HR will be presented. This will be concluded by a section on the mechanism and impact of gene targeting.

Models for recombination

During the last three decades, a large amount of data has been collected, especially in *S. cerevisiae*, on meiotic and mitotic recombination (for reviews see e.g. Pâques & Haber, 1999; Symington, 2002). This led to the proposal of hypothetical mechanistic models for recombination. Several diverse models have been proposed for HR, but only the three most normally occurring mechanisms will be presented here; the DSBR model, synthesis-dependent strand-annealing (SDSA), and SSA, see **Figure 3.7**.

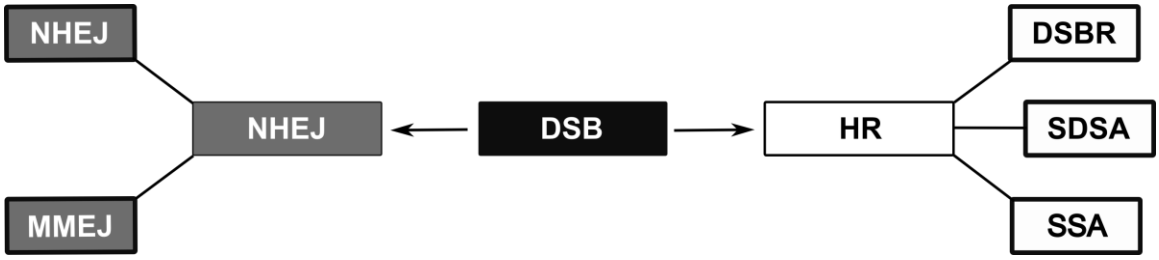

Figure 3.7 Repair mechanisms of DSBs. NHEJ and HR are the two main pathways. The subpathways discussed in this chapter are shown as well. DSBR=double-strand break repair model, SDSA=synthesis-dependent strand annealing, and SSA=single-strand annealing.

Double-strand break repair model

The DSBR model illustrates two scenarios after DSBR. One is gene conversion, a non-reciprocal (one-way) transfer of genetic information from a homologous donor to its recipient, and the reciprocal crossover events by resolution of Holliday junctions (HJ).

The DSBR model begins with the processing of the broken chromosomal ends at the DSB (Szostak *et al.*, 1983; Pâques & Haber, 1999). It will proceed to generate long 3′ single-strand tails, see **Figure 3.8B**. The 3′ ssDNA ends will in turn invade the homologous partner creating a displacement loop (D-loop) that allows DNA synthesis (**Figure 3.8C**). The displaced strand will be complementary to the other end allowing second end capture. This end also permits DNA synthesis after ligation. To maintain this structure,

the two duplexes are kept in connection and in open configuration by a double HJ (dHJ, **Figure 3.8D**). These are intermediate structures that physically link the recombinogenic substrate to the intact DNA duplex. Accordingly, the two HJs need to be resolved in order to liberate the individual DNA duplexes. The endonucleolytic cleavage-pattern of the HJs determines whether a HR event will result in only gene conversion or gene conversion associated with a crossover. HJ can be cleaved in two planes. If the HJs are resolved in a parallel manner, that is by cleavage in the two junctions (arrows 2 and 4 in Figure 3.8D) or in both of the two strands opposite of the HJs (arrows 1 and 3), the outcome will be GC. A crossover will occur when the cleavage pattern is mixed (even or odd arrow numbers, e.g. arrows 2+3 as shown).

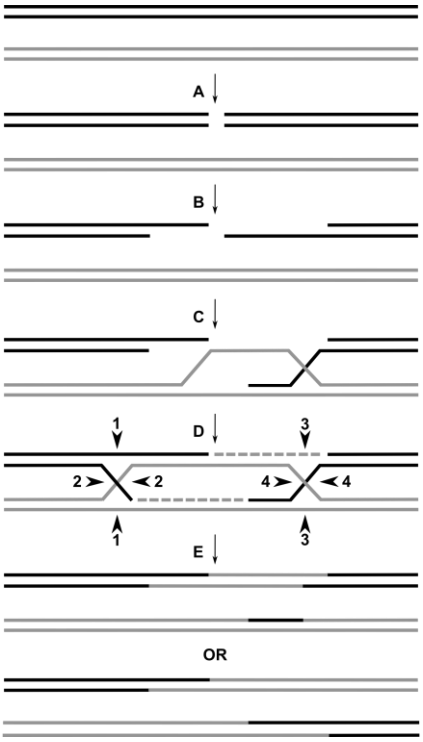

Figure 3.8 Double strand break repair model. A) DSB generation. B) Resection. C) Strand invasion. D) dHJ formation. E) Resolution of HJs. See text for details.

The homology length is an important factor that determines whether gene conversion is associated with crossover. Gene conversion is efficiently taking place in yeast even with less than 500 bp of homology, where crossovers need at least 1.7 kb of homology (Inbar

et al., 2000). In addition, the homologous donor has to share homology to both chromosomal sides of the break to perform cross-over. In meiosis, the majority of GC events are associated with crossovers. In mitosis however, less than 20% of GCs result in crossovers (Pâques & Haber, 1999). The DSBR model cannot explain all experimental observations made, therefore an alternative to the DSBR was put forward in the SDSA model.

Synthesis-dependent strand annealing

The SDSA model describes how to accomplish GC without employing the dHJ structures. SDSA accounts for the high number of GCs without crossovers in mitosis and potentially a substantial proportion of the GC events without crossover encountered in meiosis (Allers & Lichten, 2001). In SDSA, the ends at the break are processed as described in the DSBR model and the strand invasion creates a D-loop that expands with DNA synthesis, see **Figure 3.9C/D**.

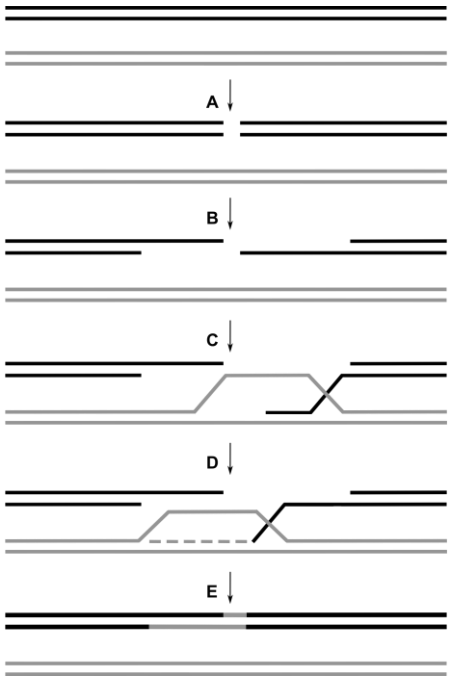

Figure 3.9 Synthesis-dependent strand annealing model. A) DSB generation. B) Resection. C) Strand invasion. D) Synthesis of DNA. E) Displacement of synthesized strand followed by gap-filling and ligation, see detail in text.

The newly synthesized strand, now complementary to the non-invading strand, is displaced and then annealed to the non-invading end of the DSB. Remaining gaps are filled by DNA synthesis and ligation.

Single-strand annealing

A DSB located between two repeated sequences can lead to recombination between the repeat and a subsequent loss of one sequence, either by SSA or by gene conversion with crossover (Sugawara & Haber, 1992). At the break, 3′ ends of the broken duplex are resected extensively, and the single-strand repeat sequence present on both duplexes can anneal to each other, as illustrated in **Figure 3.10**. The extensive resection in SSA is underlined by the fact that SSA will proceed efficiently even with 15 kb of separation between the repeat (Pâques & Haber, 1999). Repeat lengths of more than 2 kb even promote spontaneous annealing. Non-homologous sequences flanking the repeats are not included in the duplex, and will be removed before the nicks in the DNA are sealed (Sugawara & Haber, 1992). The molecular mechanisms behind the three HR models have now been described at DNA level. The following will section will concentrate on assigning the most significant proteins to the different steps.

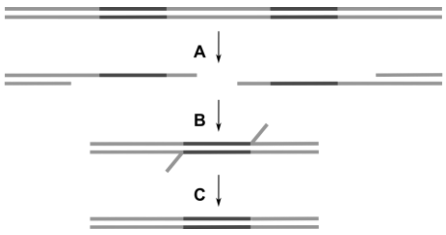

Figure 3.10 Single-strand annealing A) Creation of DSB between two repeats (in black) and extensive processing of ends at the DSB to generate 3′ ssDNA tails. B) Annealing of strands. C) Flanking non-homologous sequences (flaps in B) will be removed before the nicks in the DNA are sealed.

Enzymatic core of HR

The protein core of HR is composed of the classic *RAD52* epistasis group, which was originally defined by their hypersensitivity to IR in *S. cerevisiae*. The group counts the following genes: *RAD50*, *RAD51*, *RAD52*, *RAD54*, *RAD55*, *RAD57*, *RAD59*, *RFA1*,

MRE11, XRS2, and *RDH54*/*TID1* (Game & Mortimer, 1974; Symington, 2002). Rad52 is the most significant protein in yeast HR as it is involved in all HR pathways and Rad52-null mutants display the most severe phenotype of all HR proteins. Despite the prominent role in yeast, Rad52 has not been found in plants and invertebrates, and apparently the significance of Rad52 is not of the same magnitude in filamentous fungi and mammals (Yamaguchi-Iwai, 1998; Chapter 6). Therefore, some differences in HR do exist across evolution and mapping the protein functions will help unraveling the process and provide a fascinating insight into the essential HR that begins with the lethal break of the DNA duplex.

DSB formation & resection

As mentioned earlier in this chapter DSBs can occur in mitosis, albeit at low frequencies, either as a result of collapsed replication forks or induced lesions by genotoxic treatment. In fact DSBs are the rarest occurring lesions in mitotic cells (Fabre *et al*., 2002). In meiosis, DSBs are programmed events taking place through out the genome at DSB hotspots, which are DNase I or micrococcal nuclease hypersensitivity sites located in gene promoter regions (Fan & Petes, 1996). Approximately, 100 DSBs are generated throughout the yeast genome during meiosis. A fundamental feature of meiosis is the meiotic DSB formation by Spo11, a variant of type II topoisomerases (Keeney *et al*., 1997; Dernburg *et al*., 1998; Keeney, 2001). Additionally, the MRX complex which was introduced earlier in NHEJ has a central role for both DSB formation and resection. When the MRX formation is abolished in MRX deletion mutants, no programmed DSBs occur. If the deletions are reduced to certain point mutations in the genes encoding MRX components, such as the *rad50S* strain, it will allow DSB generation, but not resection of ends (Keeney *et al*., 1997; Pâques & Haber, 1999). In this strain, Spo11 remained bound at all 5′ DSB tails, hence the presence of MRX is believed to stimulate Spo11 to catalyze the DSB formation, as well as mediate removal of Spo11 by Mre11 cleavage. Even before DSB formation, MRX is involved in the recruitment of chromatin remodeling complexes

that rearrange the chromatin around the break (Tsukuda *et al*., 2005). The role of MRX in the resection of ends at DSBs in mitosis and meiosis is unclear.

It appears that the MRX only assist in the 5′ to 3′ resection of DNA, and do not perform the actual 5′ to 3′ generation of ssDNA tails since the removal of MRX from mitotic HR does not eliminate resection, but only delays the process (Ivanov *et al*., 1994). This indicates involvement of a dedicated exonuclease for resection or a functional redundancy in the process. Here the exonuclease Exo1 has been demonstrated to be able to perform 5′to 3′ resection and is thus a likely candidate to participate in resection (Moreau *et al*., 2001). The single-strand tails generated after resection are an important substrate for recombination, however the ssDNA is also susceptible to the formation of secondary structures, which will hamper recombination, and to degradation by nucleases (Bayer *et al*., 1989). This is effectively avoided due to the extensive coating of ssDNA by the trimeric single-strand binding protein RPA (Brill & Stillman, 1991; Alani *et al*., 1992). RPA is an essential component of replication and consist of three conserved subunits Rfa1 (70 kDa), Rfa2 (36 kDa) and Rfa3 (14 kDa). Some non-null alleles of the Rfa1 show recombination and repair deficiency proving the link to HR (Firmenich *et al*., 1995; Smith & Rothstein, 1995). In HR, the presence of RPA inhibits the progression of the strand invasion step as it is strongly bound to DNA and difficult to access by the recombinase Rad51, which is the key factor of strand invasion (Sugiyama & Kowalczykowski, 2002).

Recruitment of the recombinase to processed ends

In order to make RPA disassociate from DNA and thereby relieve the inhibition of Rad51-binding to ssDNA, assistance of the mediator protein Rad52 is required (Sugiyama & Kowalczykowski, 2002). It has been shown that HsRad52 assembles into a heptameric ring structure to be catalytically active (Stasiak *et al*., 2000). Here the role of Rad52 is to win the competition with RPA for the DNA substrate and/or to interact directly with RPA for RPA dissociation from ssDNA supported by the presence of

Rad51 (Sung, 1997a; Sugiyama & Kowalczykowski, 2002). Rad52 recruits Rad51 through their mutual interaction domain, and the loading of Rad51 onto ssDNA is stimulated by the presence of RPA when it is in complex with Rad52 (Sung, 1994).

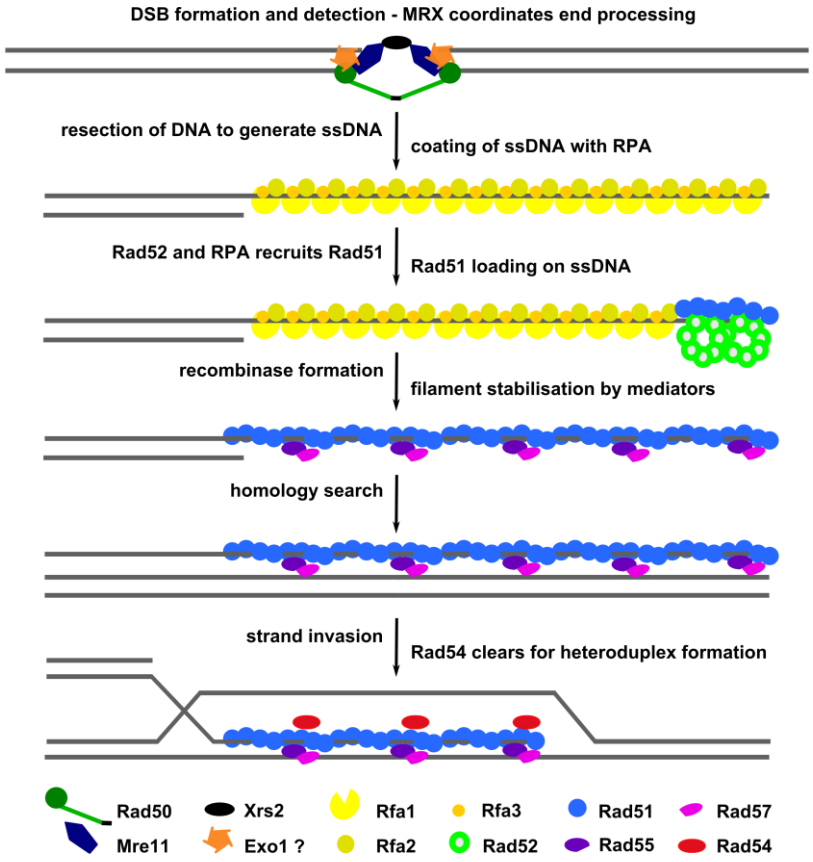

Figure 3.11 Strand invasion. Steps from the DSB detection to the strand invasion are shown (modified from Symington, 2005).

The tight connection is illustrated by the fact that RPA and Rad51 can co-localize with Rad52 in foci (higher ordered structures) both in mitosis and meiosis (Gasior *et al.*, 1998). Rad51 is distributed as catalytically inactive monomers or higher-ordered rings of six Rad51 molecules (Sung & Klein, 2006). Upon assembly of Rad51 on ssDNA, ATP-dependent formation of catalyticly active Rad51 helical nucleoprotein filament (presynaptic filament) takes place.

Rad51 filament formation and strand invasion

Rad51 filament formation is greatly enhanced by the paralogous mediator proteins Rad55 and Rad57. The exact contribution of the Rad55-Rad57 heterodimer is not entirely clear. It may assist Rad52 in relieving the inhibitory effect of Rad51 by RPA, or through stabilization and stimulation at the establishing presynaptic Rad51 filament (Sung, 1997b; Fortin & Symington, 2002). Moreover, Rad51 binds both ssDNA and dsDNA, preferably dsDNA with single-strand overhangs (Mazin *et al*., 2000), but Rad55-Rad57 may promote Rad51 binding to the ssDNA (Fortin & Symington, 2002).

The elevated level of recombination activity in meiosis is assisted by the meiosis-specific homolog of Rad51, Dmc1 (Bishop *et al*., 1992). The actions of Dmc1 are not as well-characterized as for Rad51, but it retains the same principle of higher ordered structure as for Rad51, meaning that Dmc1 also produces an active presynaptic filament (Sung & Klein, 2006). Despite the extensive homology and functional overlap, Rad51 and Dmc1 cannot complement each other completely (Shinohara *et al*., 1997). Rad51 and Dmc1 are assisted in D-loop formation by two SF2 helicases. Rad54 support Rad51, whereas its paralog Rdh54 interacts with both Rad51 and Dmc1 (Sung & Klein, 2006).

Rad54 is believed to be involved in several process steps of HR. In pre-synapsis, Rad54 helps to stabilize the Rad51 filament whereas it in synapsis could use the helicase activity for clearing DNA of nucleosomes, translocating the Rad51 filament and strand opening. Lastly in post-synapsis Rad54 could mediate heteroduplex formation and Rad51 removal (reviewed in Heyer *et al*., 2006). Rad51 is a significant player in HR, however at least one Rad51-independent recombination pathway exists. SSA utilizes the DNA annealing activities of Rad52 and the Rad52 paralog Rad59 as well as Msh2-Msh3 and Rad1-Rad10 (Wu *et al*., 2006). The paralog shows high homology to the N-terminal part of Rad52, but lack the C-terminal part which harbors the RPA and Rad51 interaction domains, therefore, Rad59 cannot substitute for Rad52. Rad51 is also the subject of pathway control mediated by the DNA helicase, Srs2. This control can

determine whether gene conversion is coupled with crossovers or not, which is important to regulate, since inappropriate recombination can result in LOH.

Regulation of crossovers by the Srs2 and Sgs1

Since the occurrence of crossovers can be down regulated by Srs2, this 3′ to 5′ DNA helicase is also termed anti-recombinase. Srs2 intervenes strand invasion by dissolving the Rad51 filament from DNA via ATP hydrolysis (Krejci *et al*., 2003). Srs2 is recruited by SUMOylated PCNA to keep Rad51 from engaging the gaps arising during blockage of replication, thereby promoting the non-recombinogenic translesion synthesis in replication fork restart (Papouli *et al*., 2005). The intimate relations of Srs2 and Rad51 are illustrated by mutations in *RAD51* that act as suppressors of *srs2* mutants resulting in hyperrecombinant strains (Aboussekhra *et al*., 1992). Another DNA helicase with a profound and conserved regulatory role in DNA repair is the RecQ homolog, Sgs1. The proposed action of Sgs1 is to resolve HJ structures in non-crossover products. Sgs1 has shown to perform branch migration of HJs *in vitro*. Indeed, a reverse branch migration of dHJs by sgs1 is thought to converge dHJs, which then can be resolved as a non-crossover by topoisomerase III, Top3, as shown in **Figure 3.12** (Ira *et al*., 2003).

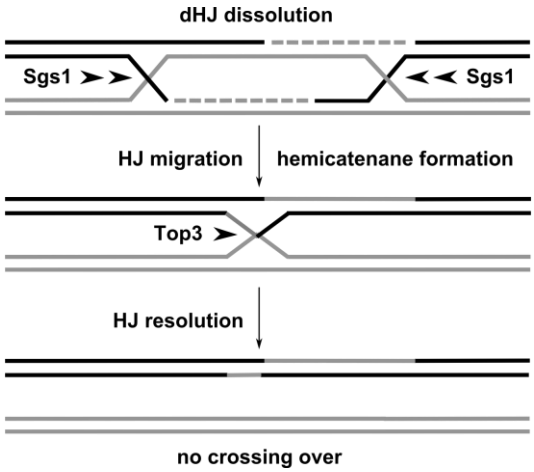

Figure 3.12 Regulation of crossovers by Sgs1-Top3 with hemicatenane formation. Illustration is modified from Sung & Klein, 2006.

This is supported by the fact that branch migration and thus conversion tracts are increased in *sgs1* null strains, which is accompanied by elevated spontaneous recombination. Srs2 and Sgs1 do have distinct functions, but they are, when overexpressed, still able to substitute for each other in the respective deletion strains hereby showing some redundant functions in resolving recombination intermediates (Fabre *et al*., 2002).

Thus, mutations in important recombination proteins *rad51*, *rad52*, *rad55* and rad57 can suppress the defects shown by the *sgs1*Δ*srs2*Δ mutant. Regarding these core functions of HR, yeast has been and still is an excellent model system, however some differences do exist e.g. to mammals and probably even the related filamentous fungi. Therefore the most obvious differences to mammalian HR are briefly outlined below.

Mammalian HR

The RAD51 mediated strand invasion in mammals is supported by five RAD51 paralogs all with 20-30% homology to RAD51. XRCC2 and XRCC3 are most homologous to Rad55 and Rad57, respectively. The three other paralogs RAD51B, RAD51C, and RAD51D are needed for presynaptic filament assembly or stabilization. All together, they form two discrete and active complexes; RAD51C and XRCC3, and RAD51B, RAD51C, RAD51D and XRCC2 (Masson *et al*., 2001). These complexes have shown to have more roles than the strand invasion itself, as was shown that the XRCC3-RAD51C has a role in branch migration and resolution of HJs. Other late roles in recombination appear to apply for all of the paralogs (Liu *et al*., 2004). On the contrary, Rad52 only has a minor role in mammals. The reason for this is that BRCA2 has taken over several functions from Rad52 (Yang *et al*., 2002; San Filippo *et al*., 2006). The sections above have described the DSBR features of HR. This is now followed by the outline of two extremely important functions of HR. The first is DNA replication fork rescue, which is connected to the postreplication repair presented earlier in the chapter.

DNA replication fork rescue by HR

The progression of replication by the DNA polymerase can be stalled when it collides with nicks in the DNA and DNA lesions. This can lead to uncoupling of the replisomes at the leading and lagging strands. If replication is not resumed, it leads to a collapse of the replication fork and a DSB. Thus, cells have a complex and extensive replication fork restart program. Focus will be on the modes of restart that involves recombination as illustrated in **Figure 3.13**, however the other features are addressed elsewhere (Branzei & Foiani, 2007).

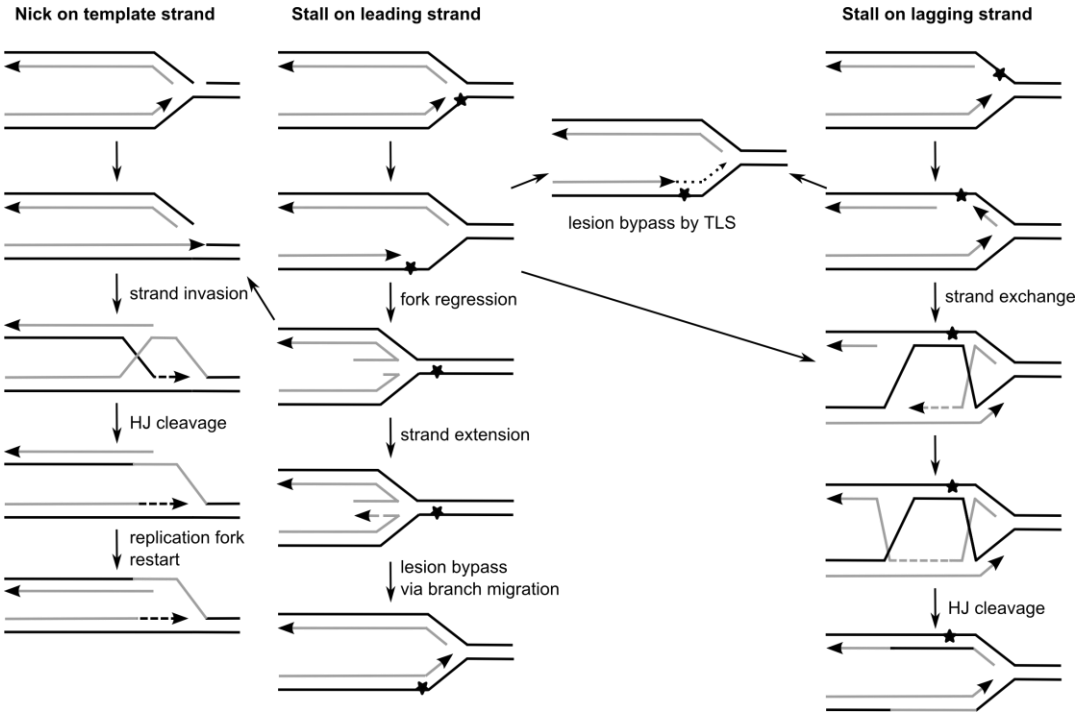

Figure 3.13 Recombination and translesion synthesis in replication fork restart. Nicks and lesions both obstruct fork progression. Besides the three modes of rescuing the stalling DNA polymerase on the leading strand, once the lesion is residing in the duplex, excision repair can fix it. The figure was adapted from Symington, 2005.

As shown in **Figure 3.13**, a nick in the template results in a collapse of the replication fork where the broken chromosomal arm can invade the duplex and by resolving the HJ structure regenerate the replication fork. Lesions can also lead to the stalling of the replication fork. When lesions are located on the leading strand the nascent strands can

pair and the fork regresses. By using the lagging strand as template, DNA synthesis followed by branch migration can lead to lesion bypass. However, lesions on the leading strand can also undergo strand invasion. Lesions on lagging strand results in gapped DNA, which is filled by TLS or via recombination (Symington, 2005; Gangavarapu *et al*., 2007).

Thus, recombination has proven to be vital in the maintenance of replication. As for replication, recombination in also vital for gene targeting, a technology of tremendous importance for manipulating organisms and has potential for future gene therapy.

Gene targeting

The gene-targeting technology is a simple procedure for creating site-directed alterations in the genomes of many organisms. Hence, gene deletions, allele- and promoter replacements, and fluorescent protein tags can be achieved. The DNA substrate for targeting is constructed *in vitro*, e.g. by PCR, and introduced into the cells. It contains target sequences, which are homologous to a certain locus in the genome. Within the cells, the substrates can by recombination integrate at the desired chromosomal target. Principally, two integration approaches of gene-targeting substrates exist depending on their configuration, which are denoted ends-in and ends-out gene targeting, respectively (Hastings *et al*., 1993). Ends-in gene targeting usually employs plasmid substrates, which has been opened by an endonuclease in the targeting sequence as illustrated in **Figure 3.14A**. Thus, the continuity of the targeting sequence has been disrupted. The two separated targeting sequences can integrate as intended when they are pointing towards each other through one crossover and non-crossover event. Hence, the entire sequence from the plasmid including the marker gene will be integrated into the locus targeted flanked by the two alleles of the target sequence. These alleles constitute a direct repeat (DR) that can confer genetic instability and undergo DR recombination via the SSA pathway resulting in the loss of marker and one of the alleles. The ends-out substrates

are pieces of DNA where the selection marker is flanked by the two distinctive sequences that each targets a chromosomal sequence, as shown in **Figure 3.14B**.

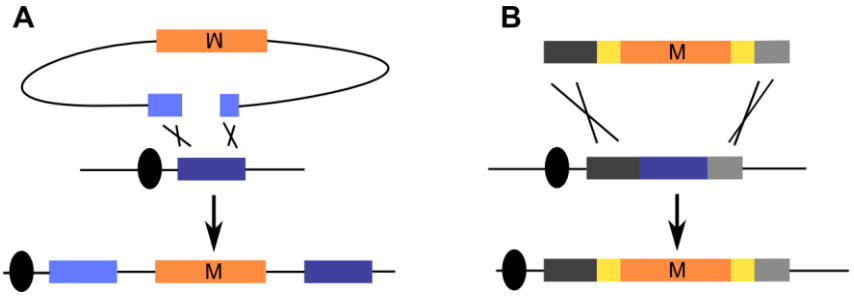

Figure 3.14 Two scenarios for gene targeting. A) Ends-in gene targeting. Here the light blue DNA sequence is a mutated allele that will recombine to the endogenous gene in dark blue located on the chromosome indicated by the centromere (filled oval). One crossover and one non-crossover resolution ensure the integration of mutated allele, either as shown or in the opposite order. The marker gene in orange can be excised after recombination between the two alleles. B) Ends-out gene targeting. In grey, the up- and downstream sequences to the target on the chromosome are flanking the repeats (in yellow) bordering a selection marker. A double crossover event substitutes the target sequence with the genetic marker. The direct repeats located on each side of the marker will facilitate loss of marker by SSA.

Two different mechanisms have been proposed to account for ends-out gene targeting, see **Figure 3.15**. One of these models involves a one-ended invasion of the chromosome by the substrate (Leung *et al.*, 1997). The invasion generates heteroduplex DNA between the target and the exogenous DNA, which spans the entire substrate length. The invading strand is assimilated and the heteroduplex DNA is corrected by the mismatch repair system. The other mechanism is based on a two-ended invasion of the DNA with a final resolution of dHJs resulting in two independent crossover events, replacing the target on the chromosome with the gene-targeting substrate (Hastings *et al.*, 1993; Langston & Symington, 2004). The two modes of ends-out gene targeting described provide a permanent incorporation of exogenous DNA, hence also the genetic marker.

However, the gene-targeting substrates can be elaborated to include features that enable a dynamic exchange of elements at targeted locus. If the DR is located on each side of the marker, it will facilitate loss of marker by SSA, see **Figure 3.11** and Chapters 4 and 5.

This can happen spontaneously as the presence of repeated sequences confer genetic instability. But as described briefly in Chapter 2, counter-selectable markers do exist, that employ both positive and negative selection greatly minimizing the screening efforts. Gene targeting has in yeast been routinely used for almost two decades, as it is extremely efficient due to a prevalent HR. This is accompanied by low requirements in target sequence length which eases the construction of gene-targeting substrates by PCR. Typically, less than a few hundred bp are applied. Inspired by the success in yeast, many laboratories have integrated gene targeting as the primary genetic engineering tool in the closely related filamentous fungi. However, gene targeting in these organisms usually requires more than 1000 bp and the efficiencies are relatively low.

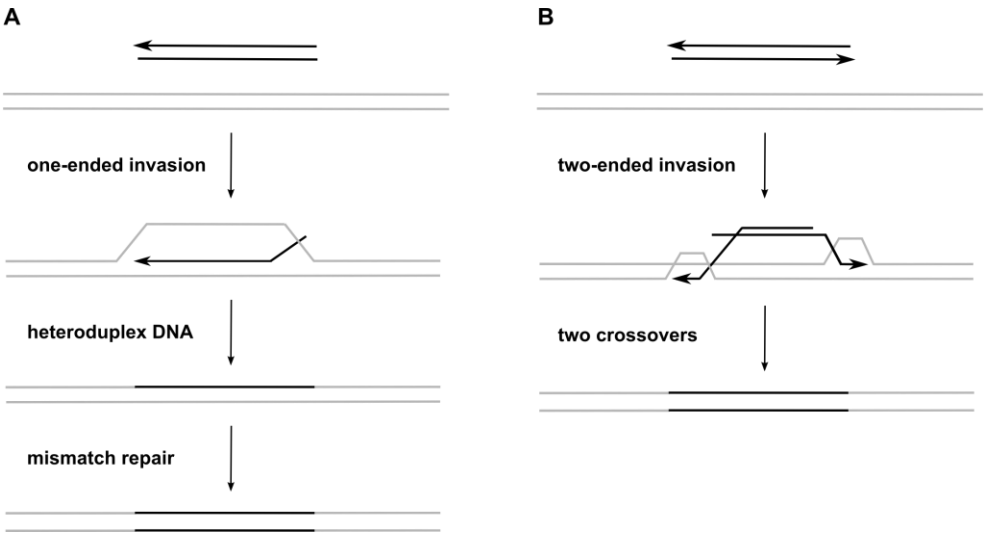

Figure 3.15 Two models for ends-out gene targeting. See text for details, modified from Leung *et al.*, 1997.

In *A. nidulans*, several reports on gene targeting have been published within the last decade (Bird & Bradshaw, 1998; Yang *et al.*, 2004; Yu *et al.*, 2004; Nielsen *et al.*, 2006), including the adaptation of PCR-based bipartite gene targeting from yeast (Erdeniz *et al.*, 1997). This method will be the focus in the remaining part of the chapter and in Chapter 4 and 5, due to the potential it holds for use in organisms such as filamentous fungi. The hallmarks of this technology are the fusion of individual PCR fragments by PCR.

Moreover, the selection marker was truncated to approximately 2/3s of its size, which resulted in 1/3 of the marker now constituted an overlapping and homologous sequence prone for HR. At first, this reduced the risk of PCR-mediated mutations, since the substrate was reduced in length. There proved to be additional advantages, since the HR repair machinery tends to localize in repair foci (Lisby *et al*., 2001), hence the relatively high concentration of targeting substrates within a nucleus could promote recombination between the marker-sequence overlap, and the continued presence of repair protein foci facilitates the completion of gene targeting. The high likelihood of three successive recombination events compared only one as well as the inability of the truncated marker to function at ectopic integrations significantly reduce the number of false-positive transformants, as described in Chapter 4. However, the effort that has probably made the strongest impact on gene-targeting efficiency in fungi was the elimination of NHEJ (Ninomiya *et al*., 2004; Nayak *et al*., 2006).

Performing gene targeting in fungal strains deficient in NHEJ has shown to greatly reduce the random insertions of DNA substrates. The disrupted NHEJ genes have mainly been in one of the genes encoding the Ku heterodimer and DNA ligase 4 (Ninomiya *et al*., 2004; Ishibashi *et al*., 2006, Nayak *et al*., 2006). With NHEJ deficient strains targeting efficiencies of up to 100 % were obtained. Initially, no unwanted phenotype was detected with these strains, but later it has shown not to be without consequences to eliminate NHEJ, since fungal Ku mutants are sensitive to γ-irradiation and contain shortened telomeres (Meyer *et al*., 2007; Steve W. James, pers. comm.). In mammals where gene targeting holds promise as gene therapy, it is even more cumbersome to perform gene targeting than in filamentous fungi and lack of NHEJ is severe and coupled to immune deficiencies and developmental defects (Gu *et al*., 1997; Park & Gerson, 2005). Thus subtle molecular systems are needed to move gene targeting in higher eukaryotes to the next level. This is intimately linked to the comprehensive dissection of the underlying principles and pathways involved in maintaining genome

stability. The following four chapters are the first steps of my contribution to achieving this in a eukaryotic model organism, *A. nidulans*.

References

Aboussekhra, A., Chanet, R., Adjiri, A., and Fabre, F., 1992. Semidominant suppressors of Srs2 helicase mutations of *Saccharomyces cerevisiae* map in the *RAD51* gene, whose sequence predicts a protein with similarities to procaryotic RecA proteins. *Mol. Cell. Biol*., **12**: 3224–3234.

Ahnesorg, P., Smith, P., and Jackson, S.P., 2006. XLF interacts with the XRCC4-DNA ligase IV complex to promote DNA nonhomologous end-joining. *Cell* **124(2)**: 301-313.

Alani, E., Thresher, R., Griffith, J.D., and Kolodner, R.D., 1992. Characterization of DNA-binding and strand-exchange stimulation properties of y-RPA, a yeast single-strand-DNA-binding protein. *J. Mol. Biol*. **227(1)**: 54-71.

Allers, T and Lichten, M., 2001. Differential timing and control of noncrossover and crossover recombination during meiosis. *Cell* **106(1)**: 47-57.

Aparicio, O.M., Billington, B.L., and Gottschling, D.E., 1991. Modifiers of position effect are shared between telomeric and silent mating-type loci in *S. cerevisiae*. *Cell* **66**: 1279–1287.

Bayer, I., Fliess, A., Greipel, J., Urbanke, C., and Maass, G., 1989. Modulation of the affinity of the single-stranded DNA-binding protein of *Escherichia coli* (*E. coli* SSB) to poly(dT) by site-directed mutagenesis. *Eur. J. Biochem*. **179(2)**: 399-404.

Bird, D. and Bradshaw, R., 1997. Gene targeting is locus dependent in the filamentous fungus *Aspergillus nidulans*. *Mol. Gen. Genet*. **255**: 219-225.

Bishop, D. K., Park, D., Xu, L., and Kleckner, N., 1992. *DMC1*: a meiosis-specific yeast homologue of *E. coli recA* required for recombination, synaptonemal complex formation, and cell cycle progression. *Cell* **69**: 439–456.

Boulton, S.J. and Jackson, S.P., 1996a. *Saccharomyces cerevisiae* Ku70 potentiates illegitimate DNA double-strand break repair and serves as a barrier to error-prone DNA repair pathways. *EMBO J.* **15(18)**: 5093-5103.

Boulton S.J. and Jackson S.P., 1996b. Identification of a *Saccharomyces cerevisiae* Ku80 homologue: roles in DNA double strand break rejoining and in telomeric maintenance. *Nucleic Acids Res.* **24(23)**: 4639-4648.

Boulton, S.J. and Jackson, S.P. 1998. Components of the Ku-dependent non-homologous end-joining pathway are involved in telomeric length maintenance and telomeric silencing. *EMBO J.* **17**: 1819–1828.

Branzei, D. and Foiani, M., 2007. Template switching: from replication fork repair to genome rearrangements. *Cell* **131(7)**: 1228-1230.

Brill, S. J., and Stillman, B., 1991. Replication factor-A from *Saccharomyces cerevisiae* is encoded by three essential genes coordinately expressed at S phase. *Genes Dev.* **5**: 1589–1600.

Critchlow, S.E. and Jackson, S.P., 1998. DNA end-joining: from yeast to man. Trends Biochem. Sci. **23(10)**: 394-398.

Daley, J.M., Palmbos, P.L., Wu, D., and Wilson, T.E., 2005. Nonhomologous end joining in yeast. *Annu. Rev. Genet.* **39**: 431-51.

d'Adda di Fagagna, F., Hande, M.P., Tong, W.M., Roth, D., Lansdorp, P.M., Wang, Z.Q., and Jackson, S.P., 2001. Effects of DNA nonhomologous end-joining factors on telomere length and chromosomal stability in mammalian cells. *Curr. Biol.* **11(15)**: 1192-1196.

D'amours, D. and Jackson, S.P., 2002. The Mre11 complex: at the crossroads of DNA repair and checkpoint signalling. *Nat. Rev. Mol. Cell. Biol.* **3(5)**: 317-327.

De Bont, R. and van Larebeke, N., 2004. Endogenous DNA damage in humans: a review of quantitative data. *Mutagenesis* **19(3)**: 169-185.

de Jager, M., van Noort, J., van Gent, D.C., Dekker, C., Kanaar, R., and Wyman, C., 2001. Human Rad50/Mre11 is a flexible complex that can tether DNA ends. *Mol. Cell*. **8(5)**: 1129-1135.

Dernburg, A.F., McDonald, K., Moulder, G., Barstead, R., Dresser, M., and Villeneuve, A.M., 1998. Meiotic recombination in *C. elegans* initiates by a conserved mechanism and is dispensable for homologous chromosome synapsis. *Cell* **94(3)**: 387-98.

Dolling, J.A., Boreham, D.R., Brown, D.L., Raaphorst, G.P., and Mitchel, R.E., 1999. Cisplatin-modification of DNA repair and ionizing radiation lethality in yeast, *Saccharomyces cerevisiae*. *Mutat. Res.* **433(2)**: 127-136.

Dynan, W.S. and Yoo, S., 1998. Interaction of Ku protein and DNA-dependent protein kinase catalytic subunit with nucleic acids. *Nucleic acids res.* **26(7)**: 1551-1559.

Elkind, M.M. & Redpath, J.L. 1977. Molecular and cellular biology of radiation lethality. In Cancer: A comprehensive treatise **6**. Plenum press New York.

Erdeniz, N., Mortensen, U.H., Rothstein, R., 1997. Cloning-free PCR-based allele replacement methods. *Genome Res.* **7(12)**: 1174-1183.

Fabre F, Chan A, Heyer WD, Gangloff S., 2002. Alternate pathways involving Sgs1/Top3, Mus81/ Mms4, and Srs2 prevent formation of toxic recombination intermediates from single-stranded gaps created by DNA replication. *PNAS* **99(26)**: 16887-16892.

Fan, Q.Q. and Petes T.D., 1996. Relationship between nuclease-hypersensitive sites and meiotic recombination hot spot activity at the HIS4 locus of *Saccharomyces cerevisiae*. *Mol. Cell. Biol.* **16(5)**: 2037-2043.

Firmenich, A.A., Elias-Arnanz, M., and Berg, P. A novel allele of *Saccharomyces cerevisiae* RFA1 that is deficient in recombination and repair and suppressible by *RAD52*. *Mol. Cell. Biol.* **15(3)**: 1620-1631.

Fortin, G. S. and Symington, L. S., 2002. Mutations in yeast Rad51 that partially bypass the requirement for Rad55 and Rad57 in DNA repair by increasing the stability of Rad51–DNA complexes. *EMBO J.* **21**: 3160–3170.

Game, J.C. and Mortimer, R.K., 1974. A genetic study of x-ray sensitive mutants in yeast. *Mutat Res.* **24(3)**: 281-292.

Gangavarapu, V., Prakash, S., Prakash, L., 2007. Requirement of RAD52 group genes for postreplication repair of UV-damaged DNA in *Saccharomyces cerevisiae*. *Mol. Cell. Biol.* **27(21)**: 7758-7764.

Gasior, S.L., Wong, A.K., Kora, Y., Shinohara, A., and Bishop, D.K., 1998. Rad52 associates with RPA and functions with Rad55 and Rad57 to assemble meiotic recombination complexes. *Genes Dev.* **12(14)**: 2208-2221.

Godar, D.E., 2005. UV doses worldwide. *Photochem. Photobiol.* **81(4)**: 736-749.

Goldman, G.H. and Kafer, E., 2004. *Aspergillus nidulans* as a model system to characterize the DNA damage response in eukaryotes. *Fung. Genet. Biol.* **41**: 428-442.

Gottlieb, T.M. and Jackson, S.P., 1993. The DNA-dependent protein kinase: requirement for DNA ends and association with Ku antigen. *Cell* **72(1)**: 131-142.

Gu, Y., Seidl, K.J., Rathbun, G.A., Zhu, C., Manis, J.P., van der Stoep, N., Davidson, L., Cheng, H.L., Sekiguchi, J.M., Frank, K., Stanhope-Baker, P., Schlissel, M.S., Roth, D.B.,

Alt, F.W., 1997. Growth retardation and leaky SCID phenotype of Ku70-deficient mice. *Immunity* **7(5)**: 653-665.

Hanawalt, P.C., 1994. Transcription-coupled repair and human disease. *Science* **266(5193)**:1957-1958.

Hastings, P.J., McGill, C., Shafer, B., Strathern, J.N., 1993. Ends-in vs. ends-out recombination in yeast. *Genetics* **135(4)**: 973-980.

Hefferin, M.L. and Tomkinson, A.E., 2005. Mechanism of DNA double-strand break repair by non-homologous end joining. *DNA Repair (Amst)* **4(6)**: 639-648.

Helleday, T., Lo, J., van Gent, D.C., and Engelward, B.P., 2007. DNA double-strand break repair: from mechanistic understanding to cancer treatment. *DNA Repair (Amst)* **6(7)**: 923-935.

Hentges, P., Ahnesorg, P., Pitcher, R.S., Bruce, C.K., Kysela, B., Green, A.J., Bianchi, J., Wilson, T.E., Jackson, S.P., and Doherty, A.J., 2006. Evolutionary and functional conservation of the DNA non-homologous end-joining protein, XLF/Cernunnos. *J. Biol. Chem.* **281(49)**: 37517-37526.

Heyer, W.D., Li, X., Rolfsmeier, M., and Zhang, X.P., 2006. Rad54: the Swiss Army knife of homologous recombination? *Nucleic Acids Res*. **34(15)**: 4115-4125.

Hoeijmakers, J.H., 2001. Genome maintenance mechanisms for preventing cancer. *Nature* **411(6835)**: 366-374.

Ikenaga, M., Ichikawa-Ryo, H., and Kondo, S., 1975. The major cause of inactivation and mutation by 4-nitroquinoline 1-oixde in Escherichia coli: excisable 4NQO-purine adducts. *J. Mol. Biol.* **92(2)**: 341-356.

Inbar, O., Liefshitz, B., Bitan, G., and Kupiec, M., 2000. The relationship between homology length and crossing over during the repair of a broken chromosome. *J. Biol. Chem*. **275(40)**: 30833-30833.

Ira, G., Malkova, A., Liberi, G., Foiani, M., and Haber, J.E., 2003. Srs2 and Sgs1–Top3 suppress crossovers during double-strand break repair in yeast. *Cell* **115**: 401–411.

Ira, G., Pellicioli, A., Balija, A., Wang, X., Fiorani, S., Carotenuto, W., Liberi, G., Bressan, D., Wan, L., Hollingsworth, N.M., Haber, J.E., and Foiani, M., 2004. DNA end resection, homologous recombination and DNA damage checkpoint activation require CDK1. *Nature* **431(7011)**: 1011-1017.

Ishibashi, K., Suzuki, K., Ando, Y., Takakura, C., and Inoue, H., 2006. Nonhomologous chromosomal integration of foreign DNA is completely dependent on MUS-53 (human Lig4 homolog) in *Neurospora*. *PNAS* **103(40)**: 14871-14876.

Ivanov, E.L., Sugawara, N., White, C.I., Fabre, F., and Haber, J.E., 1994. Mutations in XRS2 and RAD50 delay but do not prevent mating-type switching in *Saccharomyces cerevisiae*. *Mol. Cell. Biol.* **14(5)**: 3414-3425.

Kato, T., Todo, T., Ayaki, H., Ishizaki, K., Morita, T., Mitra, S., and Ikenaga, M., 1994. Cloning of a marsupial DNA photolyase gene and the lack of related nucleotide sequences in placental mammals. *Nucleic Acids Res*. **22(20)**: 4119-4124.

Keeney, S., Giroux, C.N., Kleckner, N., 1997. Meiosis-specific DNA double-strand breaks are catalyzed by Spo11, a member of a widely conserved protein family. *Cell* **88(3)**: 375-384.

Keeney S., 2001. Mechanism and control of meiotic recombination initiation. *Curr. Top. Dev. Biol*. **52**: 1-53.

Kidwell M.G., 2002. Transposable elements and the evolution of genome size in eukaryotes. *Genetica* **115(1)**: 49-63.

Krejci, L., Van Komen, S., Li, Y., Villemain, J., Reddy, M.S., Klein, H., Ellenberger, T., and Sung, P., 2003. DNA helicase Srs2 disrupts the Rad51 presynaptic filament. *Nature* **423**: 305–309.

Kupiec, M., 2000. Damage-induced recombination in the yeast *Saccharomyces cerevisiae*. *Mutat. Res.***451(1-2)**: 91-105.

Langston, L. D. and Symington, L.S., 2004. Gene targeting in yeast is initiated by two independent strand invasions. *PNAS* **101**: 15392-15397.

Lawrence, C., 1994. The RAD6 DNA repair pathway in *Saccharomyces cerevisiae*: what does it do, and how does it do it? *Bioessays* **16(4)**: 253-258.

Leung, W., Malkova, A., and Haber, J.E., 1997. Gene targeting by linear duplex DNA frequently occurs by assimilation of a single strand that is subject to preferential mismatch correction. PNAS **94(13)**: 6851-6856.

Lewis, L. K. and Resnick, M. A., 2000. Tying up loose ends: nonhomologous end-joining in *Saccharomyces cerevisiae*. *Mutat. Res.* 451: 71-89.

Lindahl, T. 1993. Instability and decay of the primary structure of DNA. *Nature* **362(6422)**: 709-715.

Lisby, M., Rothstein, R., and Mortensen, U.H., 2001. Rad52 forms DNA repair and recombination centers during S phase. *PNAS* **98(15)**: 8276-8282.

Liu, Y., Masson, J.Y., Shah, R., O'Regan, P., and West, S.C., 2004. RAD51C is required for Holliday junction processing in mammalian cells. *Science* **303**: 243–246.

Ma, J.L., Kim, E.M., Haber, J.E., and Lee, S.E., 2003. Yeast Mre11 and Rad1 proteins define a Ku-independent mechanism to repair double-strand breaks lacking overlapping end sequences. *Mol. Cell. Biol*. **23(23)**: 8820-8828.

Masson, J.Y., Tarsounas, M.C., Stasiak, A.Z., Stasiak, A., Shah, R., McIlwraith, M.J., Benson, F.E., and West, S.C., 2001. Identification and purification of two distinct complexes containing the five RAD51 paralogs. *Genes Dev*. **15**: 3296–3307.

Mazin, A.V., Zaitseva, E., Sung, P., and Kowalczykowski, S.C., 2000. Tailed duplex DNA is the preferred substrate for Rad51 protein-mediated homologous pairing. *EMBO J*. **19(5)**: 1148-1156.

Moreau, S., Morgan, E.A., and Symington, L.S., 2001. Overlapping functions of the *Saccharomyces cerevisiae* Mre11, Exo1 and Rad27 nucleases in DNA metabolism. *Genetics* **159(4)**: 1423-1433.

Nayak, T., Szewczyk, E., Oakley, C.E., Osmani, A., Ukil, L., Murray, S.L., Hynes, M.J., Osmani, S.A., and Oakley, B.R., 2006. A versatile and efficient gene-targeting system for *Aspergillus nidulans*. *Genetics* **172(3)**: 1557-1566.

Nielsen, M.L., Albertsen, L., Lettier, G., Nielsen, J.B., and Mortensen, U.H., 2006. Efficient PCR-based gene targeting with a recyclable marker for *Aspergillus nidulans*. *Fungal. Genet. Biol*. **43(1)**: 54-64.

Ninomiya, Y., Suzuki, K., Ishii, C., and Inoue, H., 2004. Highly efficient gene replacements in *Neurospora* strains deficient for nonhomologous end-joining. *PNAS* 101: 12248-12253.

Paillard, S. and Strauss, F., 1991. Analysis of the mechanism of interaction of simian Ku protein with DNA. *Nucleic Acids Res.* **19(20)**: 5619-5624.

Palmbos, P.L., Daley, J.M., and Wilson, T.E., 2005. Mutations of the Yku80 C terminus and Xrs2 FHA domain specifically block yeast nonhomologous end joining. *Mol. Cell. Biol.* **25(24)**: 10782-90.

Papouli, E., Chen, S., Davies, A.A., Huttner, D., Krejci, L., Sung, P., Ulrich, H.D., 2005. Crosstalk between SUMO and ubiquitin on PCNA is mediated by recruitment of the helicase Srs2p. *Mol. Cell*. **19(1)**: 123-133.

Pâques, F. and Haber J.E., 1999. Multiple pathways of recombination induced by double-strand breaks in *Saccharomyces cerevisiae*. *Microbiol. Mol. Biol. Rev.* **63(2)**: 349-404.

Park, Y. and Gerson, S.L., 2005. DNA repair defects in stem cell function and aging. *Annu. Rev. Med*. **56**: 495-508.

Povirk, L.F., 1996. DNA damage and mutagenesis by radiomimetic DNA-cleaving agents: bleomycin, neocarzinostatin and other enediynes. *Mutat. Res*. **355(1-2)**: 71-89.

Powell, C., Swenberg, J., and Rusyn, I., 2005. Expression of base excision DNA repair genes as a biomarker of oxidative DNA damage. *Cancer Lett.* **229(1)**: 1-11.

Prakash, S., Johnson, R.E., and Prakash, L., 2005. Eukaryotic translesion synthesis DNA polymerases: specificity of structure and function. *Annu. Rev. Biochem*. **74**: 317-353.

Rothkamm, K. and Löbrich, M., 2003. Evidence for a lack of DNA double-strand break repair in human cells exposed to very low x-ray doses. PNAS **100(9)**: 5057-5062.
Sancar, G.B., 2000. Enzymatic photoreactivation: 50 years and counting. *Mutat. Res*. **451(1-2)**: 25-37.

San Filippo, J., Chi, P., Sehorn, M.G., Etchin, J., Krejci, L., and Sung, P., 2006. Recombination mediator and Rad51 targeting activities of a human BRCA2 polypeptide. *J. Biol. Chem*. **281(17)**: 11649-11657.

Scherer, S. and R.W. Davis., 1979. Replacement of chromosome segments with altered DNA sequences constructed in vitro. *PNAS* **76**: 4951–4955.

Shinohara, A., Gasior, S., Ogawa, T., Kleckner, N., and Bishop, D.K., 1997. *Saccharomyces cerevisiae recA* homologues *RAD51* and *DMC1* have both distinct and overlapping roles in meiotic recombination. *Genes Cells.* **2(10)**: 615-629.

Shore, D., 2000. The Sir2 protein family: A novel deacetylase for gene silencing and more. *PNAS* **97(26)**: 14030-14032.

Shuman, S., Glickman, M.S., 2007. Bacterial DNA repair by non-homologous end joining. *Nat. Rev. Microbiol.* **5**: 852-861.

Sinha, R.P. and Häder, D.P., 2002. UV-induced DNA damage and repair: a review. *Photochem. Photobiol. Sci.* **1(4)**: 225-236.

Smith, J. and Rothstein, R., 1995. A mutation in the gene encoding the *Saccharomyces cerevisiae* single-stranded DNA-binding protein Rfa1 stimulates a *RAD52*-independent pathway for direct-repeat recombination.
Mol. Cell. Biol. **15(3)**: 1632-1641.

Stasiak, A.Z., Larquet, E., Stasiak, A., Müller, S., Engel, A., Van Dyck, E., West, S.C., and Egelman, E.H., 2000. The human Rad52 protein exists as a heptameric ring. *Curr. Biol.* **10(6)**: 337-340.

Sugasawa, K., Okamoto, T., Shimizu, Y., Masutani, C., Iwai, S., and Hanaoka, F., 2001. A multistep damage recognition mechanism for global genomic nucleotide excision repair. *Genes Dev.* **15(5)**: 507-521.

Sugawara, N. and Haber J.E., 1992. Characterization of double-strand break-induced recombination: homology requirements and single-stranded DNA formation. *Mol. Cell. Biol.* **12(2)**: 563-575.

Sugawara, N., Pâques, F., Colaiácovo, M., and Haber, J.E., 1997. Role of *Saccharomyces cerevisiae* Msh2 and Msh3 repair proteins in double-strand break-induced recombination. *PNAS* **94(17)**: 9214-9219.

Sugiyama, T. and Kowalczykowski, S.C., 2002. Rad52 protein associates with replication protein A (RPA)-single-stranded DNA to accelerate Rad51-mediated displacement of RPA and presynaptic complex formation. *J. Biol. Chem.* **277(35)**: 31663-31672.

Sung, P., 1994. Catalysis of ATP-dependent homologous DNA pairing and strand exchange by yeast RAD51 protein. *Science* **265**: 1241–1243.

Sung, P., 1997a. Function of yeast Rad52 protein as a mediator between replication protein A and the Rad51 recombinase. *J. Biol. Chem*. **272**: 28194-28197.
Symington, L.S., 2002. Role of RAD52 epistasis group genes in homologous recombination and double-strand break repair. *Microbiol. Mol. Biol. Rev.* **66(4)**: 630-670.

Sung, P., 1997b. Yeast Rad55 and Rad57 proteins form a heterodimer that functions with replication protein A to promote DNA strand exchange by Rad51 recombinase. *Genes Dev.* **11**: 1111–1121.

Sung, P. and Klein, H., 2006. Mechanism of homologous recombination: mediators and helicases take on regulatory functions. *Nat. Rev. Mol. Cell. Biol.* **7(10)**: 739-750.

Symington, L.S., 2002. Role of RAD52 epistasis group genes in homologous recombination and double-strand break repair. *Microbiol. Mol. Biol. Rev.* **66(4)**: 630-670.

Symington, L.S., 2005. Focus on recombinational DNA repair. *EMBO Rep*. **6(6)**: 512-517.

Szostak, J.W., Orr-Weaver, T.L., Rothstein, R.J., and Stahl, F.W., 1993. The double-strand-break repair model for recombination. *Cell* **33(1)**: 25-35.

Teo, S.H. and Jackson, S.P., 2000. Lif1p targets the DNA ligase Lig4p to sites of DNA double-strand breaks. *Curr. Biol.* **10(3)**: 165-168.

Trujillo, K.M. and Sung, P., 2001. DNA structure-specific nuclease activities in the *Saccharomyces cerevisiae* Rad50*Mre11 complex. *J. Biol.Chem*. **276(38)**: 35458-35464.

Tsukuda, T., Fleming, A.B., Nickoloff, J.A., and Osley, M.A., 2005. Chromatin remodelling at a DNA double-strand break site in *Saccharomyces cerevisiae. Nature* **438(7066)**: 379-383.

Usui T., Ohta, T., Oshiumi, H., Tomizawa, J., Ogawa, H., and Ogawa, T., 1998. Complex formation and functional versatility of Mre11 of budding yeast in recombination. *Cell* **95**: 705-716.

Valencia, M., Bentele, M., Vaze, M.B., Herrmann, G., Kraus, E., Lee, S.E., Schär, P., and Haber, J.E., 2001. *NEJ1* controls non-homologous end joining in *Saccharomyces cerevisiae. Nature* **414(6864)**: 666-669.

Walker, J.R., Corpina, R.A., and Goldberg, J., 2001. Structure of the Ku heterodimer bound to DNA and its implications for double-strand break repair. *Nature* **412 (6847)**: 607-14.

Ward, J.F., 2000. Complexity of damage produced by ionizing radiation. *Cold. Spring Harb. Symp. Quant. Biol*. **65**:377-382.

Wilson, D.M. and Thompson, L.H., 1997. Life without DNA repair. *PNAS* **94(24)**: 12754-12757.

Wiseman, H and Halliwell, B., 1996. Damage to DNA by reactive oxygen and nitrogen species: role in inflammatory disease and progression to cancer. *Biochem J.* **313(Pt 1)**:17-29.

Wu, Y., Sugiyama, T., and Kowalczykowski, S.C., 2006. DNA annealing mediated by Rad52 and Rad59 proteins. *J. Biol. Chem.* **281(22)**: 15441-15449.

Würtele, H., Little K.C.E., and Chartrand, P., 2003. Illegitimate DNA integration in mammalian cells. *Gene Therapy* **10**: 1791–1799.

Yamaguchi-Iwai, Y., Sonoda, E., Buerstedde, J.M., Bezzubova, O., Morrison, C., Takata, M., Shinohara, A., and Takeda., S., 1998. Homologous recombination, but not DNA repair, is reduced in vertebrate cells deficient in RAD52. *Mol Cell Biol.* **18**: 6430-6435.

Yang, H., Jeffrey, P.D., Miller, J., Kinnucan, E., Sun, Y., Thoma, N.H., Zheng, N., Chen, P.L., Lee, W.H., and Pavletich, N.P., 2002. BRCA2 function in DNA binding and recombination from a BRCA2-DSS1-ssDNA structure. *Science* **297(5588)**: 1837-1848.

Yang, L., Ukil, L., Osmani, A., Nahm, F., Davies, J., De Souza, C.P., Dou, X., Perez-Balaguer, A., and Osmani, S.A., 2004. Rapid production of gene replacement constructs and generation of a green fluorescent protein-tagged centromeric marker in *Aspergillus nidulans*. *Eukaryot. Cell* **3**: 1359-62.

Yu, J.H., Hamari, Z., Han, K.H., Seo, J.A., Reyes-Dominguez, Y., and Scazzocchio, C., 2004. Double-joint PCR: a PCR-based molecular tool for gene manipulations in filamentous fungi. *Fungal Genet. Biol*. **41**: 973-81.

Chapter 4

Efficient PCR-based gene targeting with a recyclable marker for *Aspergillus nidulans*

Available online at www.sciencedirect.com
ScienceDirect
Fungal Genetics and Biology 43 (2006) 54–64
FUNGAL GENETICS AND BIOLOGY

Efficient PCR-based gene targeting with a recyclable marker for *Aspergillus nidulans*

Michael L. Nielsen, Line Albertsen, Gaëlle Lettier, Jakob B. Nielsen, Uffe H. Mortensen*

Center for Microbial Biotechnology, BioCentrum-DTU, Technical University of Denmark, Building 223, DK-2800 Kgs. Lyngby, Denmark

Received 20 July 2005; accepted 19 September 2005
Available online 11 November 2005

Abstract

The rapid accumulation of genomic sequences from a large number of eukaryotes, including numerous filamentous fungi, has created a tremendous scientific potential, which can only be realized if precise site-directed genome modifications, like gene deletions, promoter replacements, in frame GFP fusions and specific point mutations can be made rapidly and reliably. The development of gene-targeting techniques in filamentous fungi and other higher eukaryotes has been hampered because foreign DNA is predominantly integrated randomly into the genome. For *Aspergillus nidulans*, we have developed a flexible method for gene targeting employing a bipartite gene-targeting substrate. This substrate is made solely by PCR, which obviates the need for bacterial subcloning steps. The method reduces the number of false positives and can be used to produce virtually any genome alteration. A major advance of the method is that it allows multiple subsequent genome manipulations to be performed as the selectable marker is recycled.

Keywords: Gene targeting; Filamentous fungi; *Aspergillus nidulans*; Homologous recombination; Genome integration; Deletion; Point mutation

1. Introduction

In recent years, the complete genome sequences of a number of filamentous fungi, including that of the model fungus, *Aspergillus nidulans*, have become available (reviewed in Archer and Dyer, 2004). This has created a tremendous potential to obtain insight into many important aspects of fungal biology such as transcriptional regulation, secondary metabolite production, cellular differentiation, tissue specialization, hyphal growth and pathogenicityin. Experimentally, this potential can only be fully exploited if precise genome modifications like gene deletions, promoter replacements in frame GFP fusions and specific point mutations can be made. This has been demonstrated for the yeast, *Saccharomyces cerevisiae*, where the combination of a complete genome sequence and efficient gene-targeting methods has made this organism the genetically best characterized eukaryote. Moving from unicellular to multicellular model organisms, *A. nidulans* is a good choice since gene-targeting success rates are typically quite high, lying in the range of 10-50%, which is orders of magnitudes higher than for most other multicellular eukaryotes (Schaefer, 2001). Although, most types of genome manipulations have been reported for *A. nidulans*, the methods often employ, several cumbersome *Escherichia coli* based cloning steps and therefore the development of versatile cloning-free method is

* Corresponding author. Fax: +45 4588 4148.
E-mail address: um@biocentrum.dtu.dk (U.H. Mortensen).

1087-1845/$ -see front matter ©2005 Elsevier Inc. All rights reserved. doi:10.1016/j.fgb.2005.09.005

desirable. To avoid bacterial cloning, three similar PCR-based methods have recently been successfully used to perform gene deletions and promoter replacements in *A. nidulans* using a one step gene replacement strategy (Yang et al., 2004; Yu et al., 2004, Zarrin et al., 2004). In all three methods, the final gene-targeting substrate is generated by combining three overlapping fragments in a subsequent PCR reaction. A simpler and more flexible PCR-based method, which allows the selectable marker to be recycled, has previously been developed for *S. cerevisiae* (Erdeniz et al., 1997). The method employs PCR to generate two composite DNA fragments, here termed a bipartite gene-targeting substrate, that are fused *in vivo* by homologous recombination (HR) to form the active gene-targeting substrate. In this method, the selectable marker is flanked by a direct repeat, which allows multiple rounds of gene targeting to be performed in the same strain as the marker can be excised via direct-repeat recombination. Furthermore, integration as well as direct-repeat recombination events are easily scored as a selectable/counter-selectable marker is used. This method has been used to create gene deletions, point mutations, allele replacements and GFP fusions (Erdeniz et al., 1997; Lisby et., 2001; Reid et al., 2002a,b). The only prerequisite for each class of genome modification is a vector that serves as a template for constant parts of the bipartite gene-targeting substrate. In the present study, we demonstrate that this gene-targeting scheme can be adapted to *A. nidulans* to efficiently create gene deletions and point mutations. Furthermore, we show that the use of bipartite substrates results in a higher frequency of correct targeting events compared to that obtained with the corresponding continuous substrates.

2. Materials and methods

2.1. Strains, media and plasmids

The *A. nidulans* strain, IBT 27263, (*argB2*, *pyrG89*, *veA1*) was used for all gene-targeting experiments. The strain is derived from GO51 of the Glasgow strain collection. Solid and liquid media were made according to Clutterbuck (Clutterbuck, A.J., 1974). 5-fluoroorotic acid (5-FOA) was from Sigma. 5-FOA medium was made by adding filter-sterilized 5-FOA to a final concentration of 1.3 mg/ml to minimal medium supplemented with 10 mM uridine, 10 mM uracil, 4 mM L-arginine and 2% agar cooled to 50ºC after autoclavation. *E. coli* strain DH5α was used as host for plasmid construction. Plasmids pUC57 and pUC18 were obtained from Fermentas and New England Biolabs (NEB), respectively. Plasmid pDJB2 contains *pyr-4* of *N. crassa* (Ballance and Turner., 1985) and pYA11 harbors both *argB* and *yA* of *A. nidulans* (Aleksenko and Ivanova, 1998).

2.2. Oligonucleotides, PCR and Cloning

A linker, d(pGGGTACCC) containing a *Kpn*I cut site was obtained from NEB. Oligonucleotides were supplied by MWG-Biotech AG and are listed in Table 1.

PCR was performed using the Expand High Fidelity PCR kit from Roche according to manufacturer's recommendations. All PCR products were purified from agarose gels using a GFX purification kit (Amersham Pharmacia).

Table 1
Oligonucleotides used in this study

Primer	Usage	Sequence
M1	Recyclable primers for gene targeting	catggcaattcccggggatc**GCCGGC** **AATTCTTTTAGGTAGC**
M2		**CCAGAAGCAGTACACGGC**
M3		**GTTGTCTGCTTGCGCTTCTTC**
M4		catggtggtcagctggaat**TCCTCC** **GCCATTTCTTATTCCC**
R1		catggcaattcccggggatc**TGGAT** **AACCGTATTACCGCC**
R2		catggtggtcagctggaatt**TGCCAA** **GCTTAACGCGTACC**
D1	Deletion of *radC*	aattccagctgaccaccatg**CACTAT** **CGACCTCGTCTTATGC**
D2		**GGATACTCCTGAATCTCGAC**
U1		**CGCCTTCGGATCGATGAG**
U2		gatccccgggaattgccatgCGACTG CATCCGTACTAGCAGTCTGATGCG **TGTGATGCTTGCCGGGCC**
Y1	Mutagenesis in *yA*	aattccagctgaccaccatg**CAAA** **TGTTCTATCATGGGGGC**
Y2		gatccccgggaattgccatg**GGTTG** **ATTGGGAATATGTAGTTC**
O1	Cloning	cgctatattaccctgttatccctagc gtaact**CGGCAGATTTTCTGT** **GAAGAG**
O2		agttacgctagggataacagggtaat atagcg**CGAGCGAGGTCTCAA** **CAAC**
O3		ATCATTGCTGCAGCATCGAT **TCCTCCGCCATTTCTTA**
O4		TACTTCTAGAACCTAGG**GCCGGCAA** **TTCTTTTTAGGTAG**
O5		AGCAATGCATCTGGAGAATCGAT **AAATGTTCTATCATGGGGGC**
O6		GATGCATGCCTGGAGACTAGT**GGTT** **GATTGGGAATATGTAGTTC**
O7		ACCTGAAGCTTAACGCGTACCCGGGAA GATCT**CATGGTCATAGCTGTTTCCTG**
O8		ACTGGCATGCAGCGGCCGCAGCTAG CACAATTGAGGCGCGCC **GAGCTGATACCGCTCGCCGC**
O9	Probe P4	**TGGGTTGAACCGCTTACTCAG**
O10		**CAGCTGCAGCATGAAATCCAG**

All sequences are shown in 5′–3′ direction. Bases shown in bold capitals anneal to the template DNA. Sections of the oligonucleotides in lower case characters represent fusion tags.

Plasmid construction was performed using standard methods (Sambrook and Russell, 2001) and all inserted PCR fragments were sequenced by MWG-Biotech AG.

pYA11-*Kpn*I served as PCR template for the mutant allele *yA*-*Kpn*I (see Section 2.3) and was constructed by ligating a phosphorylated *Kpn*I linker, see above, into the *Sma*I restriction site of pYA11. The *Kpn*I site is situated 401 bp downstream of the ATG of *yA* and causes a frameshift mutation.

pYA11-I-*Sce*I served as PCR template for the mutant allele *yA*-I-*Sce*I (see Section 2.3) and was constructed by inserting a *yA*-I-*Sce*I containing PCR fragment digested with *Mfe*I and *Nhe*I into a *Mfe*I-*Nhe*I vector fragment of pYA11. This PCR fragment was generated in two steps. First, two PCR fragments were made in separate reactions using primer pairs (Y1 and O1) and (Y2 and O2), respectively, and pYA11 as template. Second, these two fragments were fused via 32 bp I-*Sce*I sequences (Moure et al., 2003; Plessis et al., 1992) present in their ends using the primer pair Y1 and Y2 by PCR. In pYA11-I-*Sce*I, the 32 bp I-*Sce*I recognition sequence is located 1579 bp downstream of the ATG of *yA* and causes a frameshift mutation.

pRSub3 was used to produce targeting fragments described in Section 2.4 and was constructed in three steps. First, a 1.4 Kb PCR fragment, which contained the entire *N. crassa pyr-4* marker, was generated by the primer pair O3 and O4 using pDJB2 as template. This fragment was digested with *Xba*I and *Pst*I and inserted into an XbaI-PstI vector fragment of pUC57 to produce pRSub1. Next, a 2146 bp PCR fragment was generated by using the primer pair O5 and O6 and pYA11-*Kpn*I as template. This fragment, which contains the *yA*-*Kpn*I allele and a *Bpm*I recognition sequence just downstream of the *yA* locus, was digested with *Cla*I and *Sph*I and inserted into a *Cla*I-*Sph*I pRSub1 vector fragment to produce pRSub2. Finally, the 2146 bp PCR fragment obtained above was digested with *Nsi*I and *Spe*I to release a fragment containing the *yA*-*Kpn*I allele and a *Bpm*I recognition sequence just upstream of the *yA* locus. This fragment was inserted into an *Nsi*I-*Avr*II vector fragment of pRSub2 to produce pRSub3, see Fig. 1.

pDEL1 served as PCR template for the marker-containing fragments of the bipartite substrates for the *radC* deletion (see Section 2.3). The vector contains the *pyr-4* marker and a 290 bp direct repeat and was constructed in 3 steps. First, the *Xma*I site of pUC18 was destroyed by digesting the plasmid by *Xma*I, filling out the ends by Klenow polymerase (Large Fragment from NEB) followed by religation of the blunt ends to produce pJST1. Next, a 290 bp fragment, which was generated by PCR using the primer pair O7 and O8 and pJST1 as template, was digested by *Hind*III and *Sph*I and inserted into a *Hind*III-*Sph*I vector fragment of pJST1 to form pJSH1. Finally, an *Xba*I and *Pst*I fragment isolated from pRSub1, which contains the entire pyr-4 gene, was inserted into an *Xba*I-*Pst*I vector fragment of pJSH1 to yield pDEL1.

2.3. PCR-based bipartite substrates for gene-targeting experiments

The two marker-containing fragments of the bipartite substrates were amplified by PCR using pDEL1 as template. Specifically, for creating deletions, the primer pairs (M3 and R1) and (M2 and R2) were used for the upstream and downstream fragments, respectively; and for making point mutations, primer pairs (M1 and M3) and (M2 and M4) were used for the upstream and downstream fragments, respectively.

To delete *radC* in the genome, The upstream (2088 bp) and downstream (2033 bp) specific targeting sequences flanking radC were PCR amplified from genomic DNA using the primer pairs (U1 and U2) and (D1 and D2), respectively. The 5' flanking targeting sequence was fused to the upstream marker fragment (described above) by PCR using primers U1 and M3. The 3' flanking sequence was fused to the downstream marker fragment by using primers M2 and D2.

For creating genomic point mutations in *yA*, mutant *yA* alleles were amplified from either pYA11-*Kpn*I or pYA11-I-*Sce*I using the primers, Y1 and Y2. In each case, the resulting fragment was fused to both the upstream and the downstream

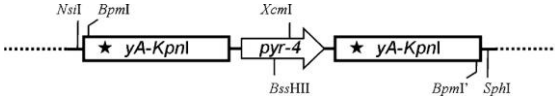

Fig. 1. A graphical representation showing the relevant features of pRSub3. The location of the *pyr-4* gene is given as an open arrow and the location of the *yA* targeting sequences as open boxes. The stars indicate the position of the new *Kpn*I site. The positions of relevant restriction enzyme cut sites are indicated. *Bpm*I and the enzyme pair *Nsi*I and *Sph*I are used to produce outer homologous and non-homologous substrate-ends, respectively. *Bpm*I recognizes an asymmetric sequence and the cuts produced from the sites with the orientations CTTGAG and CTCAAG are labeled *Bpm*I and *Bpm*I', respectively. The actual *Bpm*I recognition sites are located outside the *yA* targeting sequences as this enzyme cuts 16 bp downstream of CTTGAG and 14 bp upstream of CTCAAG.

central marker fragment using primer pairs (U1 and M3) and (M2 and D2), respectively, in two independent reactions.

2.4. Gene-targeting substrates derived from pRSub3

pRSub3 is used as a source of both bipartite and complete gene-targeting substrates. Depending on the choice of restriction enzymes, substrates with homologous or non-homologous ends can be produced. Substrates with homologous ends were generated by exploiting the fact that the two asymmetric *Bpm*I recognition sites in pRSub3 are located so that *Bpm*I cuts inside the *yA* targeting sequence even though its recognition sequence is located outside the *yA* targeting sequence (see Fig. 1). Specifically, double digestions with *Bpm*I/*Xcm*I and *Bss*HII/*Bpm*I generated the 3.9 Kb upstream and 3.7 Kb downstream fragments of the bipartite substrate, respectively, while *Bpm*I digestion alone gives the 7.1 Kb, continous substrate. Substrates with non-homologous ends were generated by exploiting the fact that *Nsi*I and *Sph*I cleaves pRSub3 outside *yA* leaving 18 bp of non-homologous sequences in both ends of the substrate. Specifically, double digestions with *Nsi*I/*Xcm*I and *Bss*HII/*Sph*I were performed to yield the fragments of the bipartite substrate while a double digestion with *Nsi*I/*Sph*I was performed to generate the continous substrate.

2.5. Transformation and selection of direct-repeat recombinants

Genetic transformation of *A. nidulans* protoplasts was preformed as previously described (Johnstone et al., 1985), except that protoplasting was achieved by using the enzyme, Glucanex, (Novozymes A/S), at a concentration of 40 mg/ml in protoplasting buffer. All transformations were performed with 10^7 protoplasts in 100 μl transformation buffer (Johnstone et al., 1985). For experiments using PCR derived fragments, 1-2 μg DNA was used unless otherwise indicated. In experiments where the efficiency of the two plasmid derived substrate types, continuous and bipartite, are compared, the same amount of DNA was used (in a range of 0.3-1 μg DNA).
Transformants were purified by streaking out spores to obtain single colonies on selective minimal medium. From these, direct repeat recombinants were selected by plating approximately 10^6 spores on 5-FOA containing plates and incubated at 37°C for 3-4 days. The resulting recombinants were further purified by streaking out spores on a fresh 5-FOA containing plate.

2.6. Southern blot hybridization

Genomic DNA from *A. nidulans* strains was isolated either as previously described (Blin and Stafford, 1976) or using the FastDNA spin kit from Qbiogene, Inc. For each sample, 2 μg genomic DNA was digested with appropriate restriction enzyme(s). Blotting was done as described by Sambrook and Russell (Sambrook and Russell, 2001) using RapidHybe™ hybridization buffer (Amersham Pharmacia) for probing. Probes for detecting the *radC* locus were: Probe P1, a 2088 bp PCR fragment amplified from genomic DNA using primer pair U1 and U2 and Probe P2, a 2033 bp PCR fragment made using primer pair D1 and D2. Probes for detecting the *yA* locus were: Probe P3, a 1461 bp fragment of *yA*, generated from pRSub2 by *Bam*HI digestion and Probe P4, a 361 bp fragment, made by PCR from genomic DNA using the primer pair O9 and O10. All probes were radioactively labeled with [α-^{32}P]-dCTP by random priming using Rediprime II kit (Amersham-Pharmacia).

3. Results

We were interested in developing a versatile PCR-based gene-targeting system for *A. nidulans*, where the selectable marker can be recycled. Such a system has previously been developed and successfully used to create genome modifications like gene deletions, point mutations and GFP fusions in *S. cerevisiae*. (Erdeniz et al., 1997; Reid et al., 2002a,b). The system is based on a bipartite gene-targeting substrate in which each of the two fragments carries a targeting sequence as well as a part of a selectable marker gene. None of the two individual fragments contain a functional marker, but if the fragments fuse by HR via overlapping marker sequences, a complete and functional marker is generated after co-transformation as shown in Fig. 2A and B. In addition, the bipartite substrate is designed so that a direct repeat is formed when it is integrated into the genome. This feature allows the marker to be eliminated in a subsequent direct-repeat recombination event, thereby permitting several rounds of gene targeting using the same marker. In *S. cerevisiae*, the *Kluyveromyces lactis URA3* gene is often used as the marker, since it only rarely recombines with the

endogenous *URA3* gene (Bailis and Rothstein, 1990). Transformants can easily be selected on media lacking uracil, and direct-repeat recombinants can be identified by counter selecting on media containing 5-FOA. Similar advantages can be obtained for *A. nidulans* by using the *URA3* homolog, *pyr-4*, from *N. crassa* (Ballance and Turner, 1985). Accordingly, we tested the possibility of adapting the bipartite gene-targeting method to *A. nidulans* using *pyr-4* as a marker. Specifically, we tested whether it could be used to make gene deletions and point mutations. For this purpose, a general vector, pDEL1 containing *pyr-4* flanked by a 290 bp direct repeat was constructed, see Section 2 and Fig. 2C. pDEL1 serves as the template for all constant parts of the bipartite gene-targeting fragments. These fragments can be used in any gene-deletion and in any point-mutation experiment.

3.1. PCR generated bipartitet gene-targeting substrates can be used for gene deletion

First we tested the possibility of deleting a gene using a bipartite PCR derived gene-targeting substrate in *A. nidulans* by deleting *radC* (AN4407.2), a gene putatively involved in DNA repair (Goldman and Kafer, 2004). pDEL1 was used as a template in two independent PCR reactions to generate the constant segments of the bipartite substrate that contain the marker and the repetitive sequences (see, Fig. 2C). In parallel, two specific targeting fragments flanking *radC* were generated by PCR using genomic DNA as template. The bipartite gene-targeting substrate was completed in a second and final round of PCR. This was achieved by fusing the fragment containing the 2/3 upstream part of the *pyr-4* marker gene with the upstream *radC* targeting fragment. Similarly, the fragment containing the 2/3 downstream part of the *pyr-4* marker was fused to the downstream *radC* targeting fragment. A specific fusion of two PCR fragments was possible as the fragments contained identical sequences in their ends, see Fig. 2C. Such ends were generated by using primer pairs where one of the primers is an adaptamer, a chimeric oligonucleotide where the 3'-end acts as a normal PCR primer and the 5'-end contains a specific fusion-tag, see Fig. 2C and Erdinez et al. (1997).

The bipartite gene-targeting substrate was transformed into *A. nidulans* and twelve transformants were obtained. In two of these transformants, *radC* was shown to be replaced by *pyr-4* as assessed by a PCR assay (data not shown). These two strains were transferred to media containing 5-FOA to select for direct-repeat recombinants. The 5-FOA treatment produced numerous candidates, which were purified and shown to be incapable of growth in the absence of uracil. After an initial PCR screen, one of the direct-repeat recombinants was selected for characterization by Southern blot hybridization. For the potential *radCΔ* strain, a single fragment was detected corresponding to the fragment size expected if a single repeat unit has replaced *radC*, see Fig. 3. We therefore conclude that both *radC* and the *pyr-4* marker had been successfully deleted from the genome. A biological characterization of the resulting *radC*Δ strain will be described elsewhere.

3.2. PCR generated bipartite gene-targeting substrates can be used to create point mutations

An experiment was performed to investigate the versatility of the bipartite method by attempting to introduce point mutations into the genome. In the present study, we use the term "point mutation" in the broad sense as it covers introduction of restriction enzyme cut sites into the genome. The scheme for introducing point mutations into the genome is similar to the one described for gene deletions above, except that the direct repeat is now constituted by two identical targeting sequences, which contain the mutation (Fig. 2B and C). After transformation and integration of the bipartite substrate, the original allele is replaced by the selective marker flanked by a direct repeat of the mutant allele. In a subsequent direct repeat recombination event, the marker and one repeat are excised from the genome, leaving a single copy of the mutant allele. However, integration of the gene-targeting substrate may also occur in such a way that only one of the two repeats contains the mutant allele. This has been observed in *S. cerevisiae*, especially when the mutation is located close to the outer end of the substrate (Erdeniz et al., 1997). If only one repeat contains the mutation, screening amongst the direct-repeat recombinants derived from the primary transformant is necessary to identify strains containing the desired genomic alteration.

M.L. Nielsen et al. /Fungal Genetics and Biology 43 (2006) 54-64

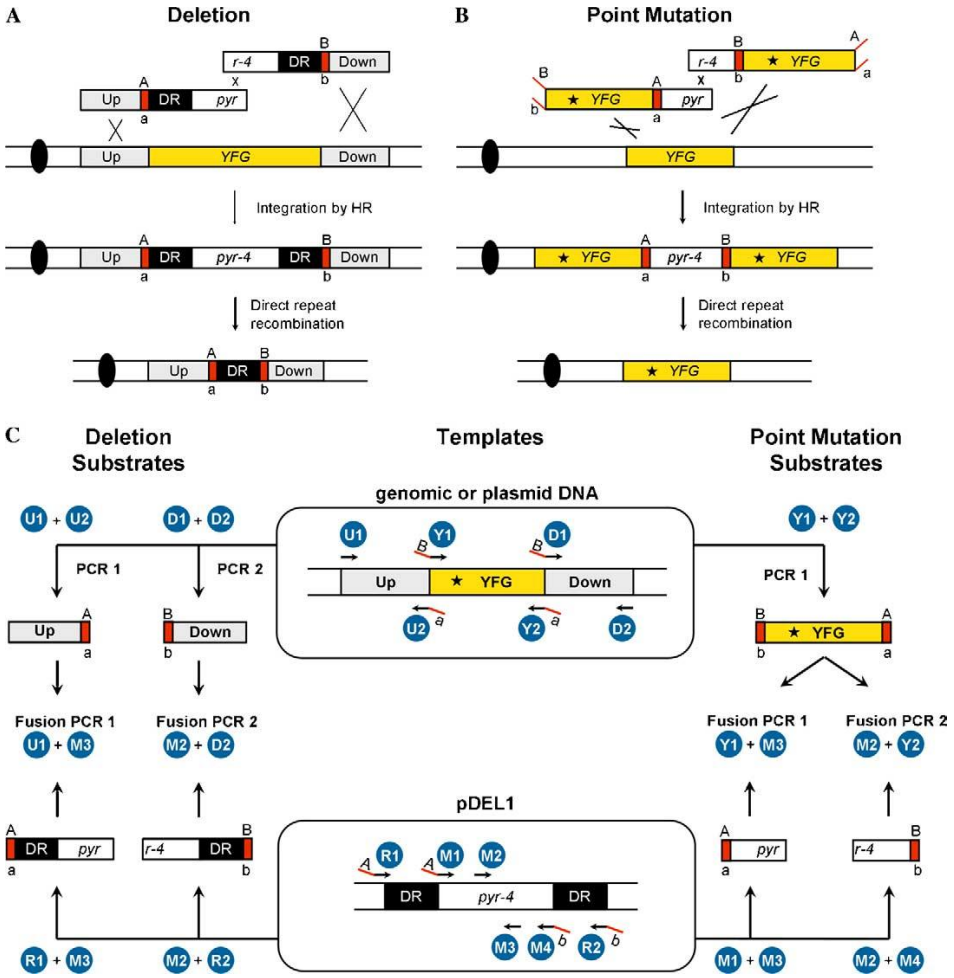

Fig. 2. Integration of bipartite gene-targeting substrates and subsequent direct-repeat recombination events to (A) delete your favorite gene, *YFG* (shown as an orange box), or (B) create a point mutation in the endogenous copy of *YFG*. *In vivo* recombination between two PCR fragments generates a functional, selectable *N. crassa pyr-4* gene. In panel A, recombination between each fragment and the homologous chromosomal locus, via the two targeting sequences Up and Down (shown as grey boxes), results in deletion of *YFG* and insertion of *pyr-4*, shown as white box, flanked by a direct repeat (shown as black boxes labeled DR). The chromosome is illustrated by two parallel fat lines with a solid black oval at the end, representing the centromere. After subsequent direct-repeat recombination, the *pyr-4* marker is excised leaving only a single DR sequence and the strain is ready for a new round of *pyr-4* based gene targeting. Red boxes and lines are fusion tags, which are used during the construction of the gene-targeting substrate, see panel C. In panel B, recombination between each fragment and the homologous chromosomal locus results in a duplication of *YFG* where both copies contain a point mutation depicted with an asterisk. During the integration, the two non-homologous fusion tags **A** and **B** are deleted from the ends of the fragments. After the subsequent direct-repeat recombination event, the point mutation is retained in the genome whereas the *pyr-4* marker is lost, thus, preparing the strain for a new round of *pyr-4* based gene targeting. (C) Construction of bipartite gene-targeting substrates by two subsequent rounds of PCR reactions. The positions of individual primers are illustrated as arrows. Arrows with a red extension are adaptamers, see Section 2, and the red section illustrates the part of the primer that is used in a subsequent fusion PCR reaction. In adaptamers, the sequence **A** is complementary to the sequence **a**, and **B** is complementary to **b**. Sequences **A** and **B** are not related. The names of primers are given in blue circles. In experiments designed to delete *YFG* (left side of the figure), the first round of PCR amplifies the two targeting sequences, Up and Down, in two individual PCR reactions using the primer pairs (U1 and U2) and (D1 and D2) and either genomic or plasmid DNA as template. Note that D1 and U2 are adaptamers. In parallel, two fragments containing *pyr-4* and repeat sequences are generated by using the primer pairs (R1 and M3) and (M2 and R2) with pDEL1 as template. Only the relevant part of pDEL1 is shown including the position of the direct repeats, DR, and the *pyr-4* marker gene. Note that R1 and R2 are adaptamers. In the second round of PCR, the fusion PCR, the appropriate PCR fragments are fused in two independent reactions that involve primer pairs (U1 and M3) and (M2 and D2) to complete construction of the bipartite gene- targeting substrate for deletion of *YFG*. In experiments designed to introduce a point mutation in *YFG* (right side of the figure), the first round of PCR amplifies the *YFG* open reading frame (or a section of *YFG* if the gene is not essential) that will act as the targeting sequence and, which contains the desired alteration. The YFG fragment is generated in a single PCR reaction using the adaptamer pair Y1 and Y2 and either genomic or plasmid DNA as template. In parallel, two fragments containing *pyr-4* sequences are generated by using the primer pairs (M1 and M3) and (M2 and M4) and pDEL1 as template. Note that M1 and M4 are adaptamers. In the second round of PCR, the fusion PCR, the appropriate PCR fragments are fused in two independent reactions that involve primer pairs (Y1 and M3) and (M2 and Y2) to complete construction of a bipartite gene-targeting substrate designed to introduce a point mutation into *YFG*.

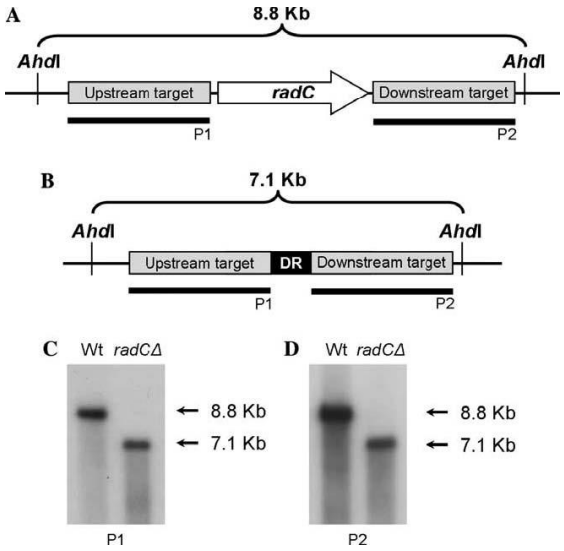

Fig. 3. Deletion of the *radC* locus. (A and B) Graphical representations of the *radC* locus before and after deletion of the *radC* open reading frame, respectively. In panel A, the *radC* open reading frame is illustrated as an open arrow and in panel B the repeat that remains after direct repeat recombination is shown as a black box labeled DR. The up- and downstream targeting sequences are shown as grey boxes and the positions of relevant restriction enzyme cut sites and the predicted fragment size of a digest are indicated. The positions of the two probes, P1 and P2, are shown as thick black lines. (C and D) Southern blot analysis of the *radC* locus in a wild-type strain (lane marked Wt) and in a *radC* deletion strain (lane marked *radCΔ*). The probe used for a specific analysis is shown below each panel. Small arrows point to relevant fragment sizes.

Construction of the bipartite gene-targeting substrate for point mutations requires a total of three PCRs compared to the four needed to create the corresponding substrate for gene deletions. This is because only a single specific targeting fragment is required, which is generated in one PCR by using a single pair of adaptamers, Y1 and Y2 in Fig. 2C. The targeting fragment is then fused to both of the two fragments, which contain the overlapping parts of *pyr-4*, in two PCRs to complete formation of the bipartite substrate. In this case, the outer ends of the bipartite substrate contain adaptamer sequences that are not homologous to the target site (Fig. 2B). Such ends could potentially impede efficient homologous integration as they need to be removed by nucleases during the integration process. Alternatively, a bipartite substrate with homologous outer ends can be made if the targeting sequence is generated in two parallel PCR reactions by two primer pairs, where each pair consists of a regular primer and an adaptamer. Next, the resulting two fragments are fused to the *pyr-4* containing fragments in the same way as described for gene deletion substrates. However, in a large scale genome modification experiment, it may be important to limit costs by using as few primers and PCRs as possible. For this reason, we addressed the possibility of using bipartite substrates containing non-homologous adaptamer derived sequences in the outer ends.

To test the possibility of introducing specific point mutations into the genome by using a bipartite gene-targeting substrate we attempted to insert new restriction enzyme cut sites into the *yA* locus (AN6635.2). *yA* was selected for this analysis as a strain with a dysfunctional *yA* gene develops yellow, instead of the usual green conidiospores (O'Hara and Timberlake, 1989) allowing an easy way to score gene-targeting events. When the outcome of the targeting event produces a direct repeat where both copies contain a mutated *yA* allele, the transformants are yellow. In the cases, where only one of the repeats contains the mutation, transformants develop green conidia and cannot be distinguish from strains resulting from ectopic integration events. However, gene-targeted strains can easily be identified after the selection for direct-repeat recombinants since many yellow clones will develop. Accordingly, the ability of a transformant to produce yellow colonies after direct-repeat recombination was used to assess whether it was the result of a gene-targeting event.

Two different alleles of *yA*, *yA-Kpn*I and *yA*-I-*Sce*I, were chosen for the point-mutation experiment. These alleles were amplified by PCR from the plasmids, pYA11-*Kpn*I and pYA11-I-*Sce*I. For each allele, the PCR product was fused to the two overlapping *pyr-4* containing fragments in two individual PCRs and the resulting bipartite gene-targeting substrates were co-transformed into *A. nidulans*. Only few of the primary tranformants produced the yellow phenotype expected for events where the integration at *yA* contained the mutation in both repeats. Especially with the *yA-Kpn*I substrate none of the seven primary transformants were yellow, and with the *yA*-I-*Sce*I substrates 10 out of 35 were yellow (Table 2). The remaining primary transformants were green. Next all transformants were plated on 5-FOA plates. As expected, yellow primary transformants produced only yellow direct-repeat recombinants. In addition, many of the green primary transformants were capable of producing yellow direct-repeat recombinants demonstrating that they were the result of a gene-targeting event. Of the 7 and 25 green transformants obtained with the *yA-Kpn*I and the *yA*-I-*Sce*I substrates, respectively, 4 and 16

Table 2
Introduction of restriction enzyme cut sites into *yA* using PCR generated bipartite gene-targeting substrates

Site introduced	Trial	Number of transformants		Gene-targeting efficiency (%)
		Total	Yellow on 5-FOA	
*Kpn*I	1	5 (0)[a]	3	60
	2	2 (0)	1	50
	Total	7 (0)	4	57
I-*Sce*I	1	3 (0)	1	33
	2	2 (1)	2	100
	3[b]	30 (9)	23	77
	Total	35 (10)	26	74

[a] The number of primary transformants producing yellow spores are shown in parenthesis.
[b] Four micrograms of substrate was used in this experiment.

could produce yellow colonies. In total, with bipartite substrates containing the *yA*-*Kpn*I and the *yA*-I-*Sce*I alleles, 57 and 74% of all primary transformants, respectively were able to form yellow conidia, see Table 2. The remaining primary transformants (43 and 26%, respectively) never develop yellow conidia after 5-FOA treatment indicating that they were the results of an ectopic integration event. These results indicate that the *yA* locus had been targeted at a high frequency.

The status of the *yA* locus in four direct-repeat recombinants, two from each point mutation experiment, was analyzed by PCR. In all four cases, the size of the resulting *yA* fragment was identical to the one obtained from a wild-type strain, and subsequent digestion of the fragment by either *Kpn*I or I-*Sce*I indicated that the desired point mutation had been correctly created in the genome (data not shown). Next, the two potential *yA*-*Kpn*I strains were analyzed by Southern blot analysis to conWrm that they were the result of successful gene-targeting events. Genomic DNA from each strain was either digested with *Hpa*I, which cuts outside the targeted area, or co-digested with *Hpa*I and *Kpn*I, where the latter only cleaves the *yA* *Hpa*I fragment if the *yA*-*Kpn*I allele is present (Fig. 4A). The blots were analyzed using two different probes. The first probe, P3, hybridizes to the *yA* specific targeting sequence of the bipartite substrate and therefore detects the *yA* locus as well as any additional ectopically integrated gene-targeting substrates (if any are present). On the other hand, the second probe, P4, detects only the *yA* locus as it hybridizes to a region of *yA* that is not included in the gene-targeting substrate. This experiment is designed to show whether the fragments detected in the previous experiment are generated from the *yA* locus. For the two mutant strains, probe P3 only detected a single fragment for *Hpa*I digested samples (Fig. 4B). The size of this fragment was identical to the fragment detected by probe P4 (Fig. 4C). As expected, these fragments were in the same position as the *yA* fragments detected in DNA from a wild-type strain by probes P3 and P4. This demonstrates that direct-repeat recombination was successfully achieved and rules out the possibility that integration of the bipartite substrate at the *yA* locus was accompanied by any additional ectopic integration events. Furthermore, for the *Hpa*I–*Kpn*I digested samples, hybridization with probes P3 and P4 showed that the *yA* *Hpa*I fragment from the mutant strains could be cleaved by *Kpn*I (Figs. 4D and E). Accordingly, the *yA*-*Kpn*I allele was successfully inserted into *yA* of both mutant strains. A similar Southern blot analysis was performed for the two potential *yA*-I-*Sce*I mutant strains. Likewise, the analysis confirmed that correct point

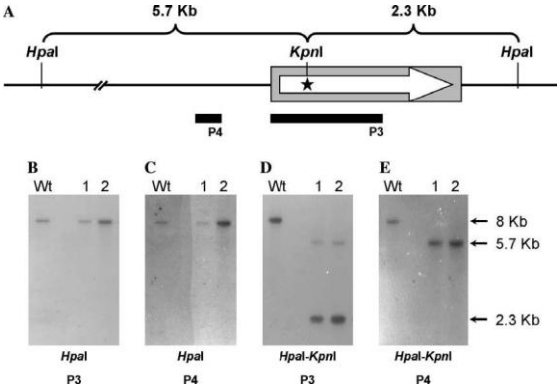

Fig. 4. Insertion of a novel *Kpn*I site in the endogenous *yA* by the use of a bipartite gene-targeting substrate generated by PCR. (A) Graphical representation of the *yA* locus. The *yA* open reading frame is illustrated as an open arrow, the location of the new *Kpn*I site as a star and the sequence used in the targeting substrate is shown as a grey box. The positions of relevant restriction enzyme cut sites and the predicted fragment sizes of a digest are indicated. The positions of the two probes, P3 and P4, used for Southern blot analysis are shown as thick black lines. (B, C, D, and E) Southern blot analysis of the *yA* locus in a wild-type strain (lane marked Wt) and in two mutated strains (lanes 1 and 2). The restriction enzyme(s) used for a specific analysis and the probe used to detect the relevant fragments are shown below each panel. Small arrows point to relevant fragment sizes.

mutations had been created in the two strains after direct-repeat recombination (data not shown). Overall these results show that bipartite PCR generated gene-targeting substrates can be successfully used to make point mutations in the genome

3.3. Bipartite gene-targeting substrates increase successfully targeting compared to continuous gene-targeting substrates

Encouraged by the results above, a more careful analysis of the point-mutation gene-targeting method was performed to determine whether bipartite substrates were targeting the desired locus as efficiently as traditional continuous gene-targeting substrates. We also addressed whether the presence of non-homologous adaptamer sequences in the ends of point-mutation substrates reduced the gene-targeting efficiency. However, the targeting efficiencies of different PCR generated substrates are not easily comparable as they may contain different degrees of PCR generated errors. To solve this problem, a plasmid, pRSub3, was constructed from which all combinations of substrate fragments can be liberated, including versions where the outer substrate-ends are either homologous or non-homologous to the target site (Fig. 1 and Section 2).

Transformation of *A. nidulans*, with the four different substrate types rarely produced yellow primary transformants. In fact only one out of a total of 42 primary transformants obtained was initially yellow. This is similar to the result obtained by the PCR derived *yA-Kpn*I bipartite substrate (see Section 3.2). Transformation with substrates containing non-homologous ends produced slightly lower numbers of transformants compared to the numbers achieved by substrates containing homologous ends. However, the gene-targeting efficiencies determined for the two substrate types were identical, Table 3. We then compared the gene-targeting efficiencies obtained with bipartite substrates with those obtained with continuous substrates. The numbers of transformants obtained using bipartite substrates were reduced approximately twofold compared to those obtained with the corresponding continuous substrates (Table 3). In contrast, the gene-targeting efficiencies obtained with bipartite substrates were two- to threefold higher compared to those obtained with the continuous substrates (Table 3). The average gene-targeting efficiency for integrating the *yA-Kpn*I allele using a bipartite gene-targeting plasmid (pRSub3) derived substrate was 62%. This is similar to the efficiencies obtained when PCR derived bipartite substrates were used to create *yA-Kpn*I strains (57%) and *yA*-I-*Sce*I strains (74%), compare Table 2 and 3.

Table 3
Introduction of a *Kpn*I site into endogenous *yA* by gene-targeting. Comparison of the efficiency obtained by bipartite- and continuous gene-targeting substrates derived from pRSub3

Substrate	End-types	Number of transformants	Yellow on 5-FOA	Gene targeting efficiency (%)
Bipartite	H[a]	5 (1)[b]	3	60
	NH	8 (0)	5	63
	Total	13 (1)	8	62
Continuous	H	17 (0)	5	30
	NH	12 (0)	2	17
	Total	29 (0)	7	24

[a] H are homologous- and NH are non-homologous ends.
[b] The number of primary transformants producing yellow spores are shown in parenthesis.

To confirm that all yellow direct-repeat recombinants presented in Table 3 were due to correct targeting of *yA*, all transformants were analyzed by Southern blot analysis. First, we investigated the status of the *yA* locus before direct-repeat recombination. In this case, a 12.2 kb *Hpa*I fragment is expected if the substrate is integrated at *yA* by HR, see Fig. 5A. In transformants obtained with continuous as well as with bipartite gene-targeting substrates, *Hpa*I fragments larger than 12.2 kb were often observed indicating that additional DNA was inserted at the *yA* locus, Fig. 5B. The larger fragments may be due to polymerization of gene-targeting fragments by non-homologous end-joining. If this happens prior to integration at *yA* by HR, several gene-targeting fragments can simultaneously be integrated at the *yA* locus. However, after integration at *yA*, the polymer will always contain an outer direct repeat. Accordingly, the desired genomic alteration may still be obtained from such transformants by direct-repeat recombination. To test this possibility, one randomly selected yellow colony from each of the 15 yellow direct-repeat recombinants presented in Table 3 was subjected to Southern blot analysis. In all cases, only the desired genomic alteration was left in the genome (Figs. 6A, B, C, and data not shown). Apparently, direct-repeat recombination generally results in complete removal of all additional sequences that integrated at the locus. Based on these results, we conclude that non-homologous ends in the gene-targeting substrate do not adversely affect the gene-targeting efficiency nor do they result in any unwanted ectopic co-integration events.

M.L. Nielsen et al. /Fungal Genetics and Biology 43 (2006) 54-64

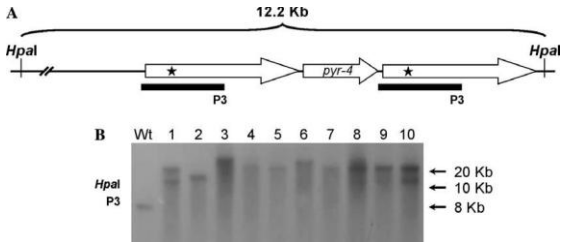

Fig. 5. Analysis of the *yA* locus after transformation with a plasmid derived bipartite gene-targeting substrate. (A) A graphical representation of the structure of the *yA* locus after integration of the bipartite gene-targeting substrate by mechanisms that only involve HR. The two *yA* open reading frames are illustrated by large open arrows, the *pyr-4* marker gene is shown as a small open arrow and the location of the new *Kpn*I site as a star. The position of *Hpa*I cut sites and the predicted fragment size of the digest is indicated. The positions of the probe, P3, used for Southern blot analysis are shown as thick black lines. (B) Southern blot analyses of the *yA* locus in 10 transformed strains. The wild-type locus is included for comparison (lane marked Wt). The analyses of DNA from transformants obtained by continuous and bipartite substrates containing homologous ends are shown in lane 1 and lanes 2–4, respectively; and by continuous and bipartite substrates containing non-homologous ends are shown in lanes 5–8 and 9–10, respectively. For each lane the genomic DNA was *Hpa*I digested and probed with P3. Small arrows to the right of each panel point to relevant fragment sizes.

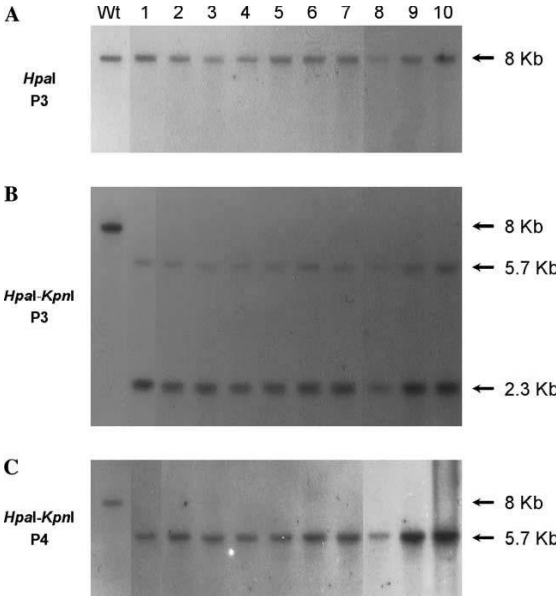

Fig. 6. Analysis of the *yA* locus after transformation with a plasmid derived bipartite gene-targeting substrate and after elimination of the *pyr4* marker by subsequent direct-repeat recombination. For a graphical representation of the *yA* locus after direct-repeat recombination including the positions of the probes, P3 and P4, and predicted fragment sizes of relevant digests, see Fig. 4A. (A, B, and C) Southern blot analyses of the *yA* locus in 10 transformed strains after selection for direct-repeat recombinants. The wild-type locus is included for comparison (lane marked Wt). The analyses of DNA from transformants obtained by continuous and bipartite substrates containing homologous ends are shown in lane 1 and lanes 2–4, respectively; and by continuous and bipartite substrates containing non-homologous ends are shown in lanes 5–8 and 9–10, respectively. The restriction enzyme(s) used for a speciWc analysis and the probe used to detect the relevant fragments are shown to the left of each panel. Small arrows to the right of each panel point to relevant fragment sizes.

4. Discussion

With the increasing availability of fully sequenced fungal genomes, the demand for efficient gene-targeting methods for filamentous fungi has increased. In the present study, we have adapted a PCR-based gene-targeting method from *S. cerevisiae*, which can be used to create virtually any genome modification, in *A. nidulans* and demonstrated that it works efficiently for creating gene deletions and point mutations. The ability to create specific point mutations allows for a more detailed analysis of enzymatic activities e.g., by construction of separation of function mutants or construction of genes encoding a mutant protein where the capacity for a posttranslational modification has been altered. Even essential genes can be manipulated this way if the resulting point mutation is not lethal. In this case, it is important to note that the direct repeat used to introduce the mutation needs to cover the entire open reading frame of the gene of interest. This way, one repeat unit consisting of the entire mutated open reading frame will be in the normal position with respect to the original promoter of the gene.

After integration of the gene-targeting substrate, the selective marker will be flanked by a direct repeat. This is an important feature of the method and it provides three main advantages. First, since the marker can be eliminated by direct-repeat recombination, it allows iterative gene-targeting experiments to be performed as the marker can be recycled. Hence, the genome of a progenitor strain can be manipulated an unlimited number of times. Second, in the scheme used to introduce a deletion, one of the direct-repeat sequences remains in the genome after the procedure is completed. It is

therefore easy to adjust the procedure to allow construction of fusion genes, e.g., to tag proteins with GFP or to allow promoter swapping. The only requirement is a vector where the *pyr-4* marker is flanked by the relevant sequence as a direct repeat, e.g., by the sequence encoding GFP or by the promoter sequence of choice. Third, in methods, where the selective marker gene remains at the target locus after integration, transcription from the marker gene may influence the state of the chromatin structure at the targeted region. Accordingly, the phenotype of a given mutation inserted by such a method could be influenced by this effect as the regulation of neighbor genes may be affected. This problem is minimized in the method presented here as the marker is eliminated by direct-repeat recombination.

In the method, gene-targeting is achieved by co-transformation with a bipartite gene-targeting substrate. This allows PCR construction of substrates where the marker is flanked by large targeting sequences that help to increase the efficiency of the directed integration process (Bird and Bradshaw, 1997). The bipartite substrate is made via two successive PCRs. In contrast, construction of the corresponding continuous substrate generally requires three successive PCRs or a second reaction where three PCR fragments are fused simultaneously. Since DNA polymerases are not error free, an additional round of PCR increases the possibility of the final targeting substrate containing unwanted mutations. More importantly, PCR amplification of a large continuous fragment that contains a direct repeat is difficult and often results in production of a small byproduct, which results from PCR recombination between the repetitive sequences (Meyerhans et al., 1990). The bipartite method circumvents this problem because each repeat is amplified in separate reactions.

A successful gene-targeting event using a bipartite gene-targeting substrate requires that three HR events take place. At first glance, this hardly seems favorable given that in *A. nidulans* non-homologous end-joining rather than HR is the predominant process for integration of recombinant DNA (Goldman et al., 2002). However, since bipartite substrates only produce transformants if the marker is reconstituted by HR it may be envisioned that this HR event may channel the entire substrate into the HR pathway. Mechanistically this is feasible since in organisms ranging from *S. cerevisiae* to mammals DNA double strand breaks, DSBs, are repaired in large protein structures termed repair centers (reviewed in Lisby and Rothstein, 2005) Importantly, when multiple DNA DSBs are introduced in *S. cerevisiae*, the resulting DNA ends are typically localized in a single repair center (Lisby et al., 2003). Therefore, when the bipartite substrate is fused in the cell by HR in a DNA repair center, the two outer ends of the substrate may likely be embedded in the same center, which is specialized for HR. If so, the entire substrate may preferentially proceed in the HR pathway and integrate at the desired location. In agreement with this view, the gene-targeting efficiency determined for bipartite substrates is threefold higher compared to the efficiency obtained by the corresponding continuous gene-targeting substrate. A higher ratio of correctly to ectopically integrated transformants means less cumbersome screening to identify desired transformants. At the same time, we note that the overall transformation efficiency obtained with bipartite substrates is reduced compared to the efficiency obtained with continuous substrates. This may be due to the fact that ectopic integration of the individual fragments of a bipartite substrate cannot produce viable transformants. Thus, the increased gene-targeting efficiency obtained with bipartite substrates may simply reflect a reduced number of ectopic integrants.

The activity of the non-homologous end-joining pathway may be visible in some of the integrations at the *yA* locus. In the Southern blot analyses in Fig. 5B showing the configuration of the *yA* locus after transformation, it was interesting to note that in lanes 1, 3, 8, 9, and 10 the *yA* specific probe hybridizes to two restriction fragments, when only a single band was expected. This would typically be interpreted as a result of ectopic integration. However, given that the subsequent Southern blot analyses (Figs. 6A, B, and C) of the same strains after elimination of the *pyr-4* marker in all cases fail to show any evidence of ectopic integration, it is highly unlikely that ectopic integration could account for the additional band in the transformants. Perhaps, they may be explained as the result of different degrees of repeat loss, caused by the instability of large tandem repeats during shake Xask growth of mycelia prior to genomic DNA isolation.

In genome-wide gene-modification projects, it may be important to reduce costs for primers and PCR. The use of adaptamers is well suited for this purpose as previously described for *S. cerevisiae* (Reid et al., 2002a,b). For example, in a gene

deletion project the number of targeting fragments can be reduced by 50% if entire intergenic regions are amplified by adaptamers and used as targeting sequences. This is possible as the same fragment can be used to target the upstream gene as well as the down stream gene. Similarly, in projects where only one specific targeting sequence is needed, like in substrates for making point mutations, the targeting fragment can be created using a single adaptamer pair to reduce costs as two primers and one PCR can be saved for every point mutation strain to be created. A consequence of using adaptamer pairs to generate targeting sequences is that the final gene-targeting substrate will contain short adaptamer derived sequences in the outer ends, which are not homologous to the genomic target sequence. In *S. cerevisiae* such ends are efficiently removed by the Rad1/Rad10 endonuclease (Sung et al., 1993; Tomkinson et al., 1993; Ivanov and Haber, 1995). Since a *RAD1* homolog (AN3620.1) is present in the *A. nidulans* genome (Goldman and Kafer, 2004), we reasoned that a similar activity would be present in *A. nidulans*. In agreement with this, we show that the presence of non-homologous ends does not seem to influence the gene-targeting efficiency. We conclude that it is possible to take advantage of adaptamers for making gene-targeting substrates for *A. nidulans*.

The bipartite method presented here is extremely flexible and can easily be adapted to perform genome manipulations like promoter replacements and GFP tagging. It is suitable for large scale genome alteration projects since the substrates are PCR based and the method reduces the screening required to find correct integrants. Recently, key genes, *mus51* (a *KU70* homolog) and *mus-52* (a *KU80* homolog), in the non-homologous end-joining repair pathway have been deleted in *N. crassa*. Such strains have shown gene-targeting efficiencies approaching 100% (Ninomiya et al., 2004). If similar mutant strains were available for *A. nidulans*, the bipartite method could easily be adapted to a high throughput gene-targeting scheme. In addition, it may eliminate polymerization of gene-targeting substrates and thereby eliminate the need to verify that unwanted sequences are left at the target locus after direct-repeat recombination.

Acknowledgements

This work was supported by the Danish Research Agency to UHM and the Danish Biotech Research Academy, FOBI to G.L. The Technical University of Denmark for Ph.D. grants to G.L. and J.B.N. We thank Jesper Storm and Maya Pedersen for skilful technical assistance, and Gerald Hofmann and Iben Plate for critically reviewing this manuscript.

References

Aleksenko, A., Ivanova, L., 1998. In vivo linearization and autonomous replication of plasmids containing human telomeric DNA in *Aspergillus nidulans*. Mol. Gen. Genet. 260, 159-164.

Archer, D.B., Dyer, P.S., 2004. From genomics to post-genomics in *Aspergillus*. Curr Opin Microbiol. 7, 499-504.

Bailis, A.M., Rothstein., R., 1990. A defect in mismatch repair in *Saccharomyces cerevisiae* stimulates ectopic recombination between homeologous genes by an excision repair dependent process. Genetics 126, 535–547.

Ballance, D. J., Turner, G., 1985. Development of a high-frequency transforming vector for *Aspergillus nidulans*. Gene. 36, 321-331.

Bird, D., Bradshaw, R., 1997. Gene targeting is locus dependent in the filamentous fungus *Aspergillus nidulans*. Mol. Gen. Genet. 255, 219-225.

Blin, N., Stafford, D.W., 1976. A general method for isolation of high molecular weight DNA from eukaryotes. Nucleic Acids Res. 3, 2303-2308.

Clutterbuck, A.J., 1974. In: King, R.C. (Ed.), Handbook of genetics, Plenum Press, New York, NY., pp. 447-510.

Erdeniz, N., Mortensen, U.H., Rothstein, R., 1997. Cloning-free PCR-based allele replacement methods. Genome Research 7, 1174-1183.

Goldman, G.H., McGuire, S.L., Harris, S.D., 2002. The DNA damage response in filamentous fungi. Fungal Genet. Biol. 35, 183-195.

Goldman, G.H., Kafer, E., 2004. *Aspergillus nidulans* as a model system to characterize the DNA damage response in eukaryotes. Fungal Genet. Biol. 41, 428-442.

Ivanov, E.L., Haber, J.E., 1995. RAD1 and RAD10, but not other excision repair genes, are required for double-strand break-induced recombination in *Saccharomyces cerevisiae*. Mol. Cell Biol. 15, 2245-2251.

Johnstone, I.L., Hughes, S.G., Clutterbuck, A.J., 1985. Cloning an *Aspergillus nidulans* developmental gene by transformation. EMBO J. 4**,** 1307-1311.

Lisby, M., Mortensen, U.H., Rothstein, R., 2003. Colocalization of multiple DNA double-strand breaks at a single Rad52 repair centre. Nat. Cell Biol. 5, 572-577

Lisby, M., Rothstein, R., Mortensen, U.H., 2001. Rad52 forms DNA repair and recombination centers during S phase. Proc. Natl. Acad. Sci. USA 98, 8276-8282.

Lisby, M., Rothstein, R., 2005. Localization of checkpoint and repair proteins in eukaryotes. Biochimie 87, 579-589.

Meyerhans, A., Vartanian, J.P., Wain-Hobson, S., 1990. DNA recombination during PCR. Nucleic Acids Res. 18, 1687-1691.

Moure, C.M., Gimble, F.S., Quiocho, F.A., 2003. The crystal structure of the gene targeting homing endonuclease I-SceI reveals the origins of its target site specificity. J. Mol. Biol. 5, 685-95.

Ninomiya, Y., Suzuki, K., Ishii, C., Inoue, H., 2004. Highly efficient gene replacements in Neurospora strains deficient for nonhomologous end-joining. Proc. Natl. Acad. Sci. USA 101, 12248-12253.

O'Hara, E. B., Timberlake, W.E., 1989. Molecular characterization of the *Aspergillus nidulans yA* locus. Genetics 121, 249-254.

Plessis, A., Perrin, A., Haber, J.E., Dujon, B., 1992. Site-specific recombination determined by I-*Sce*I, a mitochondrial group I intron-encoded endonuclease expressed in the yeast nucleus. Genetics 130, 451–460.

Reid, R.J., Lisby, M., Rothstein, R., 2002a. Cloning-free genome alterations in *Saccharomyces cerevisiae* using adaptamer-mediated PCR. Methods Enzymol. 350, 258-277.

Reid, R.J., Sunjevaric, I., Keddache, M., Rothstein, R., 2002b. Efficient PCR-based gene disruption in Saccharomyces strains using intergenic primers. Yeast 19, 319-328.

Sambrook, J., Russell, D.W., 2001. Molecular cloning a laboratory manual. Cold Spring Harbor Laboratory Press, Cold Spring Harbor, NY.

Schaefer, D.G., 2001. Gene targeting in *Physcomitrella patens*. Curr. Opin. Plant. Biol. 4, 143-150.

Sung, P., Reynolds, P., Prakash, L., Prakash, S. 1993. Purification and characterization of the *Saccharomyces cerevisiae* RAD1/RAD10 endonuclease. J. Biol. Chem. 268, 26391-26399.

Tomkinson, A.E., Bardwell, A.J., Bardwell., L., Tappe, N.J., Friedberg, E.C., 1993. Yeast DNA repair and recombination proteins Rad1 and Rad10 constitute a single-stranded-DNA endonuclease. Nature. 362, 860-862.

Yang, L., Ukil, L., Osmani, A., Nahm, F., Davies, J., De Souza, C.P., Dou, X., Perez-Balaguer, A., Osmani, S.A., 2004. Rapid production of gene replacement constructs and generation of a green fluorescent protein-tagged centromeric marker in *Aspergillus nidulans*. Eukaryot. Cell 3, 1359-62.

Yu, J.H., Hamari, Z., Han, K.H., Seo, J.A., Reyes-Dominguez, Y., Scazzocchio, C., 2004. Double-joint PCR: a PCR-based molecular tool for gene manipulations in filamentous fungi. Fungal Genet. Biol. 41, 973-81.

Zarrin, M., Leeder, A.C., Turner, G., 2005. A rapid method for promoter exchange in *Aspergillus nidulans* using recombinant PCR. Fungal Genet. Biol. 42, 1-8.

Spore-PCR on *Aspergillus* conidia

The bipartite gene-targeting technology presented in this chapter offers the advantage of higher gene-targeting efficiency than the continuous fragments. However, the efficiency is still not 100 %, and therefore some false positive transformants are obtained. To verify transformants, PCR and/or Southern analysis are usually performed based on purified gDNA. This step however is time consuming, and I set out to establish the simplest possible PCR based analysis of transformant genotypes by adding the spores directly to the PCR mix prior to PCR. The method has proven to be attractive and thus has potential for high throughput applications.

In 1993, Aufauvre-Brown and co-workers performed PCR directly on processed *A. fumigatus* conidia, but the method has not gained much popularity. I have successfully modified and adapted the method for use with *A. nidulans* conidia, and subsequently we have made successful runs with *A. oryzae* conidia, and optimized the method for high reliability and success with green, yellow and white *A. nidulans* conidia. The method allows rapid PCR screening of colonies, e.g. after transformation or counter-selection events. The average success rate of the spore-PCR ranges from 50 to 100 % depending on the reaction.

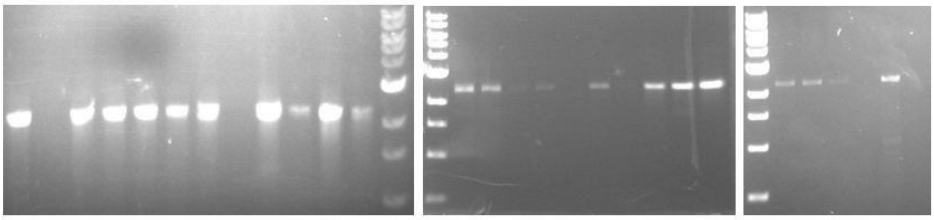

Figure 4.1 Spore-PCR of the *ligD* locus (left) and *nkuA* locus (middle and right) in different strains. The picture on the right shows three reactions by *Taq* and *Paq* 5000, respectively. 15-20 µL of sample were loaded on the agarose gel.

Procedure

Spore-PCR was made directly from conidia picked from the vegetative mycelium. The reactions were mainly catalyzed by the *Taq* polymerase (Sigma), however it was also

possible to use a low-price polymerase *Paq* 5000 (Stratagene) as seen in **Figure 4.1**. The reaction mixture for a *Taq* based reaction was composed of the following; 1x PCR buffer, 1.5 mM – 2.1 mM $MgCl_2$, Primers from 0.2 µM, and 0.03 U polymerase/µL. For DNA templates, spores were transferred from the colony (e.g. with a sterile pipette tip) directly to the PCR reaction mix. Picking spores should be done by gently touching the conidiophores at the periphery of the colonies (the spores on the tip should be slightly visible to the naked eye). The number of spores added to the PCR tube, which has given the best results are 10^3 -10^5 spores per 50 µL, which also depends on the pigmentation of conidia. A dilution series of the PCR reaction mix including the spores can be made to fine-tune the optimal number of spores. The direct transfer of spores avoids additional dilution of conidia, and the long primary denaturation step (15 min.) makes pre-processing of conidia unnecessary (**Figure 4.2**). Load at least 15-20 µL of sample on the agarose gel.

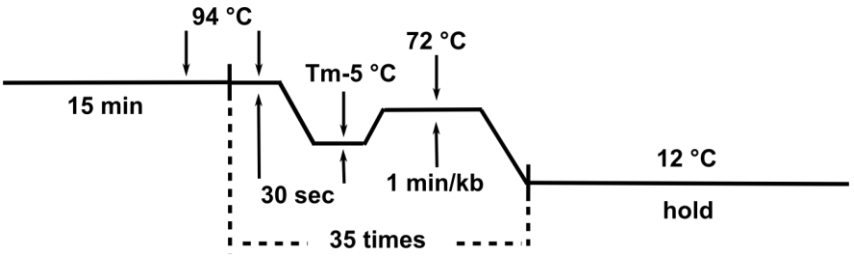

Figure 4.2 *Taq* polymerase spore-PCR.

The method was published on-line in May 2007 at the Fungal Genetics Stock Center homepage http://www.fgsc.net/Aspergillus/.

References

Aufauvre-Brown, A., Tang, C.M., and Holden, D.W., 1993. Detection of gene-disruption events in *Aspergillus* transformants by polymerase chain reaction direct from conidiospores. *Curr. Genet.* **24**: 177-178.

Chapter 5

Transient disruption of non-homologous end-joining facilitates targeted genome manipulations in the filamentous fungus *Aspergillus nidulans*

Available online at www.sciencedirect.com

ScienceDirect

Fungal Genetics and Biology 45 (2008) 165–170

FUNGAL GENETICS AND BIOLOGY

Technological Advancement

Transient disruption of non-homologous end-joining facilitates targeted genome manipulations in the filamentous fungus *Aspergillus nidulans*

Jakob B. Nielsen, Michael L. Nielsen, Uffe H. Mortensen *

Center for Microbial Biotechnology, BioCentrum-DTU, Technical University of Denmark, Building 223, DK-2800 Kgs. Lyngby, Denmark

Received 24 May 2007; accepted 9 July 2007
Available online 20 July 2007

Abstract

We have developed a transiently disrupted *nkuA* system in *Aspergillus nidulans* for efficient gene targeting. The *nkuA* disruption was made by inserting a counter-selectable marker flanked by a direct repeat (DR) composed of *nkuA* sequences. In the disrupted state, the non-homologous end-joining (NHEJ) activity is abolished and gene targeting can be performed with success rates identical to those obtained with permanent *nkuA* knock-out strains. When gene targeting is complete, the functional *nkuA* allele can be re-established via a simple selection step, thereby eliminating the risk that defective NHEJ influences subsequent analyses of the manipulated strain. Our system will facilitate construction of large numbers of defined mutations in *A. nidulans*. Moreover, as the system can likely be adapted to other filamentous fungi, we expect it will be particularly beneficial in species where NHEJ cannot be restored by sexual crossing.

Keywords: Gene targeting; Filamentous fungi; *Aspergillus nidulans*; Non-homologous end-joining; Transient disruption; Direct-repeat recombination

1. Introduction

The availability of numerous fungal genomes (Galagan et al., 2003, 2005; Machida et al., 2005; Nierman et al., 2005; Pel et al., 2007) provides a tremendous potential for accelerating fungal research and has spurred a rapid development of gene-targeting technologies including methods allowing gene-targeting substrates to be efficiently made by PCR (Yang et al., 2004; Yu et al., 2004; Nielsen et al., 2006). The major break-through in gene targeting for filamentous fungi was obtained in *Neurospora crassa* by eliminating the NHEJ activity, thus achieving gene-targeting efficiencies of more than 90% (Ninomiya et al., 2004). Similar results have since been presented for five different aspergilli (Krappmann et al., 2006; Nayak et al., 2006; Takahashi et al., 2006; Meyer et al., 2007). However, the fact that such strains lack an important DNA repair pathway needs to be considered as it may impact fitness. In *Saccharomyces cerevisiae* aspects of the phenotype of *yku70* or *yku80* deletion strains include genomic instability, shorter telomeres and inviability at 37°C

* Corresponding author. Fax: +45 4588 4148.
E-mail address: um@biocentrum.dtu.dk (U.H. Mortensen).

1087-1845/$ -see front matter ©2007 Elsevier Inc. All rights reserved. doi:10.1016/j.fgb.2007.07.003

(reviewed in Fisher and Zakian, 2005). Furthermore, in mammals, Ku70$^{-/-}$ cells are sensitive to γ-rays and Ku70$^{-/-}$ knock-out mice show the severe combined immunodeficiency, SCID, phenotype (Reviewed in Park and Gerson, 2005). Although the phenotype of NHEJ deficient filamentous fungi has initially been reported to be modest showing no altered morphology compared to wild-type strains and relative mild sensitivities to genotoxins such as MMS and UV (Ninomiya et al., 2004; Nayak et al., 2006) it is likely that more careful analyses will reveal undesired defects. For example, recent studies have shown that deletion of *kusA* in *Aspergillus niger* causes sensitivity towards γ-irradiation (Meyer et al., 2007) and like *S. cerevisiae*, *Aspergillus nidulans nkuA*Δ display shortened telomeres (Steven W. James, personal communication). Therefore, when gene targeting has been completed in an NHEJ deficient strain it is advisable to restore the NHEJ activity before further characterization of the mutant strain. This can be done by time consuming sexual backcrossing or, if this is not possible, by an additional round of gene targeting. To facilitate gene targeting with NHEJ deficient strains, we have developed a system based on transiently disrupted *nkuA* strains using *A. nidulans* as a model organism for filamentous fungi. In this system, *nkuA* function can be rapidly regenerated by a simple selection scheme after the desired genetic manipulations have been completed in the NHEJ deficient state.

2. Materials and methods

2.1. Strains, media and plasmids

The *A. nidulans* strain IBT27263, (*argB2, pyrG89, veA1*) was used as wild-type strain and was the basis for all strain constructions. The strain is derived from G051 (Clutterbuck, 1974) of the Glasgow strain collection. *A. niger* genomic DNA for PCR was obtained from strain BO1 (Pedersen et al., 2000). The IBT27263 derivatives *nkuA-trL* and *nkuA-trS* have been deposited in the IBT Culture Collection at BioCentrum-DTU, Lyngby, Denmark as IBT28737 and IBT28738, respectively. *Escherichia coli* strain DH5α was used to propagate all plasmids. Minimal media (MM) contained 1% glucose, 10 mM $NaNO_3$,1x salt solution (Cove, 1966) and 2% agar for solid media. MM was supplemented with 10 mM uridine (Uri), 10 mM uracil (Ura), 4 mM L-arginine (Arg) when necessary. For counter-selection with 5-fluoroorotic acid (5FOA, Sigma–Aldrich), filter-sterilized 5-FOA was added to MM at a final concentration of 1.3 mg/ml. Plasmid pDEL1 contains *pyr-4* from *N. crassa* and is flanked by a direct repeat (Nielsen et al., 2006) and pYA11 harbors both *argB* and *yA* of *A. nidulans* (Aleksenko and Ivanova, 1998). The vector pCR2.1-A*fpyrG* (kindly provided by A.A. Brakhage) carries *pyrG* from *A. fumigatus*. pDEL2 was made by replacing the N. crassapyr-4 marker by *pyrG* from *A. fumigatus.* Specifically, a fragment containing the *pyrG* ORF as well as 368bp up-and 156bp downstream of this ORF was amplified from pCR2.1-A*fpyrG* by PCR using the primers R1 + R2, see below and Supplementary table 1. This fragment was digested with NotI and XbaI and inserted into the *Not*I–*Xba*I vector fragment of pDEL1 to produce pDEL2. Restriction enzymes and T4 DNA ligase were from New England Biolabs and Sigma–Aldrich, respectively.

2.2. PCR, Southern blot and sequencing analyses

All oligonucleotides (MGW Biotech or Sigma-Aldrich) used in the present study are listed in Supplementary table 1. Diagnostic Spore-PCR reactions were made directly from green conidiospores using 800 spores, 1x PCR buffer (including 1.5 mM $MgCl_2$), 0.2 mM dNTP, 1.5 U Taq polymerase (Sigma-Aldrich) and 0.2 μM of each primer in a total volume of 50 μl. When analyzing yellow colonies, 400 spores were added to each reaction. Reaction conditions were: A denaturation step (94°C, 15 min) followed by 35 PCR cycles (94°C, 30 sec; 52°C, 30 sec and 72°C, 3 min) and finally an extension step (72°C for 5 min). All fragments for gene-targeting substrates or for sequencing were made using the Phusion polymerase (Finnzymes) according to manufacturer's recommendations and purified using illustra™ DNA and Gel band purification kit (GE Healthcare).

Genomic DNA for Southern blot analysis and template for PCR reactions was extracted using the FastDNA® SPIN for Soil Kit (MP Biomedicals, LLC.). For each Southern blot sample, 2 μg genomic DNA was digested with *Eco*RV. Blotting was performed as described by Sambrook and Russell (2001). For detecting the *nkuA* locus, a 2431 bp PCR fragment generated by primers D1 and D2 was radioactively labeled with α-^{32}P-dCTP by random priming using Rediprime II™ kit (GE

Healthcare) and used as probe in RapidHyb hybridization buffer (GE Healthcare). Sequencing of PCR fragments obtained from genetically engineered strains was performed by MWG Biotech.

2.3. Transformation and gene-targeting experiments

Protoplasting and gene-targeting procedures were as described previously (Nielsen et al., 2006). The complete deletion of *nkuA* (*nkuA*Δ, AN7753.2) and *yA* (*yA*Δ, AN6635.2) ORFs as well as construction of the transient *nkuA* disruption strains, *nkuA-trL* and *nkuA-trS*, were performed using bipartite gene-targeting substrates (Nielsen et al., 2006). Each part of a bipartite substrate (a and b) consists of a targeting sequence and a marker sequence, which were individually amplified by PCR using the primer pairs presented in Supplementary table 2. Next, to complete each substrate, an upstream targeting sequence was fused to an upstream marker sequence to form part a, and the downstream marker sequence to the downstream targeting sequence to form part B, see Supplementary table 2, in a second PCR reaction via adaptamers (Erdeniz et al., 1997; Nielsen et al., 2006).

The marker *argB* (GenBank accession No. M19158) was amplified from *A. niger* genomic DNA. pDEL2 was used as template for amplifying the *pyrG* fragments for deletion of *nkuA* whereas pCR2.1-Af*pyrG* was used as template for the amplification of the *pyrG* fragments in the substrates for the transient disruption of *nkuA*. For each gene-targeting experiment, 2 - 4 μg of PCR generated DNA was used. Transformants were purified by streaking out spores on selective minimal medium. To generate the *nkuA*Δ strain, 10^6-10^8 spores were plated on solid medium containing 5-FOA for counter-selection of the *pyrG* marker (Oakley et al., 1987; Nielsen et al., 2006) and incubated at 37°C for 3-4 days.

2.4. Estimation of mitotic direct repeat recombination frequencies

To estimate the direct repeat recombination frequencies in the *nkuA-trL* and *nkuA-trS* strains, nine independent trials were performed for each strain. As a standard, colonies were grown to a diameter of 1.5 cm and all conidiospores harvested. Approximately 200 spores were plated on MM+Ura+Uri+Arg to evaluate the germination efficiency of the strain and a dilution series of the remaining spores were plated on 5-FOA medium to select for recombinants. After incubation at 37ºC for 3 days, colonies were counted and DR recombination frequencies were calculated for each strain. The recombination frequency presented for each strain is the median number of the nine trials.

3. Results and discussion

In order to develop a transformation system with gene-targeting frequencies similar to those achieved in *nkuA* knock-out strains, but without deleting *nkuA* permanently, we disrupted *nkuA* by a counter-selectable marker flanked by an *nkuA* based DR as indicated by horizontal arrows in Fig. 1a. In the NHEJ deficient state, the strain can be further genetically engineered by gene targeting with a success rate similar to *nkuA*Δ strains in which the entire *nkuA* ORF has been deleted. After the desired genome alterations have been carried out, *nkuA* can be regenerated to its wild-type state by DR recombination (Fig. 1b). Identification of wild-type *nkuA* strains is simple as the marker between the DR is counter-selectable. In the system presented here, we have used *pyrG* as DR recombinants can be selected in the presence of 5-FOA (Oakley et al., 1987).

3.1. Design, construction and verification of nkuA deficient strains

A homolog of *ku70*, *nkuA*, has been identified in *A. nidulans* (AN7753.2, Nayak et al., 2006). To construct a disruption of *nkuA* containing an *nkuA* based DR, we used a strategy employing a bipartite gene-targeting substrate. The two targeting sequences of the substrate, nkuA-5´ and nkuA-3´, see Supplementary table 2, share a common *nkuA* sequence that constitutes the DR after integration at the *nkuA* locus (see Fig. 1a). In the design of nkuA-5´ and nkuA-3´ two issues need to be considered. First, since the gene-targeting substrate only disrupts the *nkuA* locus in our system, the possibility exists that NHEJ activity is not completely abolished. In this context, we note that a small C-terminal truncation of human Ku70 has previously been shown to retain some activity (Jin and Weaver, 1997). Second, the stability of the *nkuA*-based DR needs to be sufficiently high to ensure that the vast majority of the nuclei in the culture contains the *nkuA* disruption, but not so

J.B. Nielsen et al. /Fungal Genetics and Biology 45 (2008) 165–170

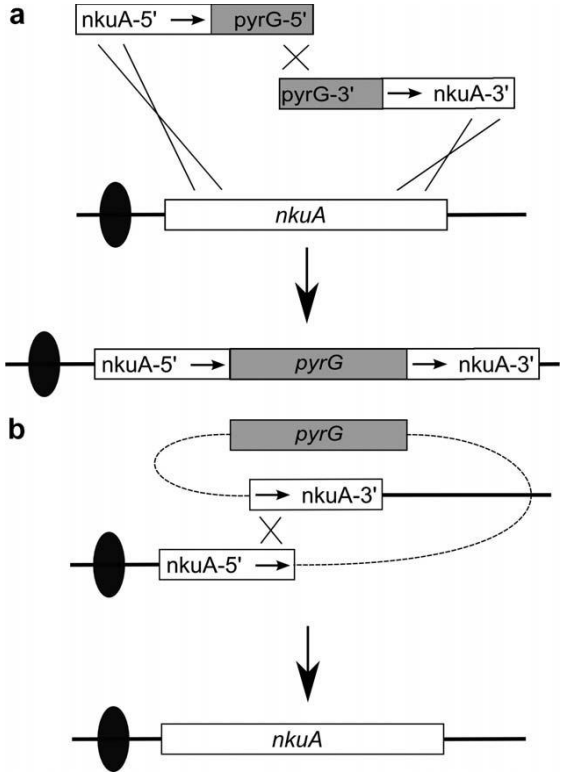

Fig. 1. The strategies for construction of a transiently disrupted *nkuA* strain (a) and for subsequent regeneration of a functional *nkuA* gene (b). (a) A bipartite gene-targeting substrate, see Section 2.3, is transformed into the wild-type strain. In the present system, the selectable marker is *pyrG* from *A. fumigatus*. Fusion and genomic integration of the substrate by homologous recombination results in a disrupted *nkuA* allele. Since, the nkuA-5´- and nkuA-3´ targeting sequences overlap, a DR is formed as indicated by horizontal arrows. In this state, the strain can be used for further gene-targeting experiments. (b) When the desired genetic manipulations have been carried out, the *nkuA* locus is restored by DR recombination. DR recombinants can be selected in the presence of 5-FOA as this recombination event eliminates the *pyrG* marker. The stippled lines do not represent DNA, but rather acts to demonstrate how DNA sections are connected.

stable that counter selection by 5-FOA will identify mutations in *pyrG* rather than DR recombinants. Thus, the position of the counter-selectable marker in the disrupted *nkuA* locus and the size of the DR may influence gene-targeting success rates. Accordingly, two transient disruptions of *nkuA* were constructed, see below, where the position and the proportions of the *nkuA* DR in the targeting substrate were varied. The two transient *nkuA* disruptions were named *nkuA-trL* and *nkuA-trS* as they contain a long, 882 bp, and a short, 143 bp, DR, respectively. In *nkuA-trL* the position of the *pyrG* marker results in an *nkuA* C-terminal truncation lacking 146 aa residues. Similarly, the other *nkuA* disruption strain, *nkuA-trS*, lacks 301 aa residues.

Transformants obtained with the gene-targeting substrates designed to generate *nkuA-trL* and *nkuA-trS* were screened by PCR to identify candidates where *nkuA* was targeted. One putative candidate for each strain was subjected to Southern blotting and analyzed in parallel with a wild-type and an *nkuA*Δ strain, Fig. 2a-d. In contrast to wild-type strains, the 4.7 kb *nkuA* containing fragment was lacking in the three *nkuA* mutant strains indicating that the *nkuA* locus was correctly targeted. Moreover, each *nkuA* mutant strain produced a novel fragment diagnostic of the genomic composition of *nkuA*Δ (2.9 kb), *nkuA-trS* (6.8 kb) and *nkuA-trL* (7.5 kb) strains. Lastly, all regions of the *nkuA-trS* and *nkuA-trL* loci corresponding to PCR derived gene-targeting substrates were sequenced and no mutations resulting from PCR errors were identified.

3.2. Fidelity of nkuA direct repeat recombination and stability of nkuA direct repeats

A key feature in the transient *nkuA* system is the reversibility from a disrupted *nkuA* allele to wild-type *nkuA* through a recombination event between the repeated *nkuA* sequences. Therefore, the fidelity of DR recombination and the stability of the DRs in the two transiently disrupted *nkuA* strains were evaluated. For each strain, DR recombinants were selected on 5-FOA medium and the composition of the *nkuA* locus was analyzed for more than 26 randomly picked colonies in a PCR test. In all cases, the 5-FOA resistant colonies were the result of DR recombination and not due to mutation of *pyrG* (data not shown). One DR recombinant, *nkuA-trS-r*, was further analyzed by Southern blot hybridization. As expected, this strain yielded a 4.7 kb fragment representing the wild-type *nkuA* locus (Fig. 2d). Moreover, the entire *nkuA* locus of this DR recombinant was amplified by PCR and sequenced. No deviations from the *nkuA* wild-type sequence were detected (data not shown) showing that DR recombination was accurately performed in this strain. The stability of the DR in the two transiently disrupted *nkuA* strains was evaluated by determining DR recombination frequencies. With *nkuA-trS* and *nkuA-trL* strains, 5-FOA resistant spore-colonies developed with frequencies of 1.5×10^{-6} and 2.5×10^{-5}, respectively. Hence, the DRs in both strains are sufficiently stable to allow large amounts of

J.B. Nielsen et al. /Fungal Genetics and Biology 45 (2008) 165–170

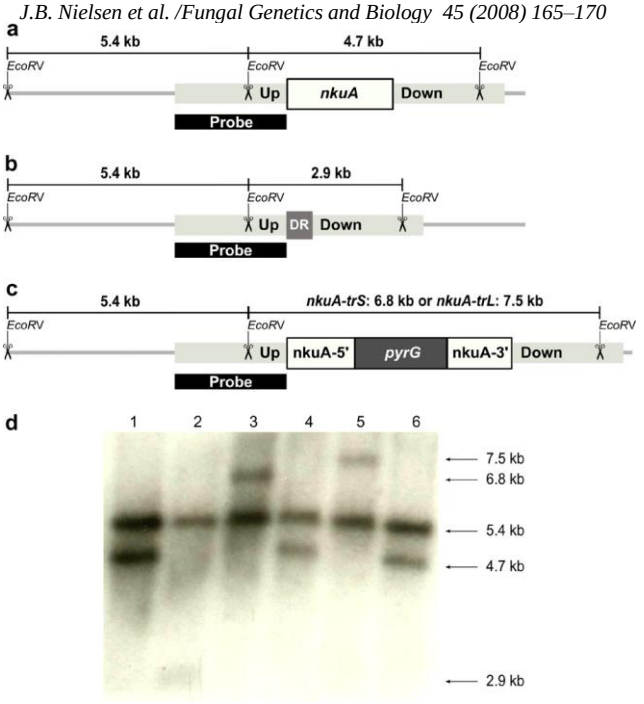

Fig. 2. Structure of the *nkuA* locus in wild-type and *nkuA* mutant strains. Graphical representation of the structure of the *nkuA* locus in (a) wild-type, (b) *nkuA*Δ and (c) transient *nkuA* disruption strains. The latter (c), represents two strains, *nkuA-trS* and *nkuA-trL*, which differ with respect to the size of the *nkuA* repeated sequences and to the position of the *pyrG* marker, see text. The positions of the probe, of *Eco*RV cut sites and the predicted sizes of the two *Eco*RV fragments detected by the probe are indicated for each strain. (d) Southern blot analysis of the *nkuA* locus of wild-type and *nkuA* mutant strains as well as of the strain *nkuA-trS-r*, which is derived from *nkuA-trS* by DR recombination. Lanes 1-6: wild-type, *nkuA*Δ, *nkuA-trS*, *nkuA-trS-r*, *nkuA-trL* and wild-type.

Table 1
Gene targeting in wild-type and *nkuA* disrupted strains

Strain	Number of transformants		
	Yellow	Green	Total
WT	0	22	22
*nkuA*Δ	27	1	28
nkuA-trS	37	2	39
nkuA-trL	40	1	41
nkuA-trS-r	0	42	42
nkuA-trL-r	0	89	89

protoplasts to be generated without any significant risk that gene targeting will occur in a nucleus with an *nkuA* wild-type background. On the other hand, DR recombination is not so infrequent that wild-type *nkuA* strains are difficult to obtain after gene targeting has been completed. In conclusion, both transiently disrupted *nkuA* strains are suitable for gene-targeting experiments.

3.3. Gene targeting is efficient in the transient nkuA strains

The *nkuA-trS* and *nkuA-trL* strains were compared to *nkuA*Δ for gene-targeting efficiency. As target gene we chose the laccase I gene, *yA*, as defects in this gene results in yellow, rather than the wild-type green conidia (O'Hara and Timberlake, 1989) hence, providing a simple read-out for gene-targeting efficiency (Nielsen et al., 2006). In these experiments we used a bipartite gene-targeting substrate designed to delete *yA*, see Supplementary table 2 and Section 2.3. The two targeting sequences of this substrate are composed of roughly 1 kb of up- and downstream *yA* sequences, respectively. *argB* from *A. niger* was used as a heterologous marker to select for integration of gene-targeting substrates. The substrate was transformed into wild-type, *nkuA*Δ, *nkuA-trL* and *nkuA-trS* strains. All transformants obtained with the wild-type strain were green indicating that they did not result from integration by gene-targeting (Table 1). The low gene-targeting efficiency (< 4%) is likely due to the length of the targeting sequences, 1 kb, which is suboptimal for gene targeting in wild-type *A. nidulans* strains (Bird and Bradshaw, 1997; Yu et al. 2004). In agreement with others (Ninomiya et al., 2004; Nayak et al., 2006) we find that even with suboptimal gene-targeting substrates, high targeting efficiencies are obtained in NHEJ deficient strains. Thus, using the *yA* gene-targeting substrate targeting efficiencies of ≥ 95% were obtained with *nkuA*Δ strains demonstrating the

robustness of this method for efficient gene targeting. Importantly, the same advantage is obtained by using *nkuA-trS* and, *nkuA-trL* strains as most transformants produced yellow colonies indicating gene-targeting efficiencies of ≥ 95%. This result shows that NHEJ is eliminated in the two transiently disrupted *nkuA* strains. In addition, it confirms that the transient *nkuA* strains are sufficiently stable during transformation to allow efficient gene targeting. As a final control, we transformed the *yA* gene-targeting substrate into two strains, *nkuA-trS-r* and *nkuA-trL-r*, in which the disrupted *nkuA* genes was regenerated by DR recombination. No yellow spores were obtained with these strains and like wild-type strains the gene-targeting efficiency was less than 4%. Hence, the ability to perform NHEJ is restored in *nkuA-trS-r* and *nkuA-trL-r*.

4. Concluding remarks

In the present study, we have presented a simple strategy allowing genetic manipulations to be efficiently performed in a transiently disrupted NHEJ background, which can be restored to wild type rapidly and easily via a simple counter-selection procedure. In the system presented here, the final strain will be *pyrG* deficient. We note that for some experiments missing this gene function may also interfere with subsequent analyses. In this case, it may be advisable to disrupt *nkuA* with a different marker. We are currently, exploring the possibility of using a marker cassette containing both the *E. coli hph* gene and the herpes simplex virus type 1 thymidine kinase gene (Lupton et al., 1991, Krappmann et al., 2005) conferring hygromycin resistance and sensitivity to nucleoside analogs such as 5-Fluoro-2'-deoxyuridine, respectively. We expect that transient *nkuA* disrupted strains will further speed up the current revolution in reverse genetics in filamentous fungi. Especially, we envision that it will facilitate large scale genome manipulation projects as well as gene targeting in fungal species where NHEJ cannot be restored by sexual crossing.

Acknowledgements

This work was supported by the Danish Research Council for Technology and Production Sciences (U.H.M). We thank Steven W. James for sharing insight into telomere lengths in *A. nidulans nkuA* strains prior to publication and for critical reading of this manuscript. We thank Simo Abdesamad Jakobsen for excellent technical assistance, and Jimmy Hoffmann Hansen and Stig Rattleff for constructing the pDEL2.

Appendix A. Supplementary data

Supplementary data associated with this article can be found, in the online version, at doi:10.1016/j.fgb.2007.07.003.

References

Aleksenko, A., Ivanova, L. 1998. In vivo linearization and autonomous replication of plasmids containing human telomeric DNA in *Aspergillus nidulans*. Mol. Gen. Genet. 260, 159-164.

Bird, D., Bradshaw, R., 1997. Gene targeting is locus dependent in the filamentous fungus *Aspergillus nidulans*. Mol. Gen. Genet. 255, 219-225.

Clutterbuck, A. J., 1974. *Aspergillus nidulans*. In: King, R.C. (Ed.), Handbook of genetics, vol. 1. Plenum Publishing Corp., NY, pp. 447-510.

Cove, D.J., 1966. The induction and repression of nitrate reductase in the fungus *Aspergillus nidulans*. Biochim. Biophys. Acta 113, 51-56.

Erdeniz, N., Mortensen, U.H., Rothstein, R., 1997. Cloning-free PCR-based allele replacement methods. Genome Res. 7, 1174-1183.

Fisher, T.S., Zakian, V.A., 2005. Ku: A multifunctional protein involved in telomere maintenance. DNA repair 4, 1215-1226.

Galagan, J.E. *et al*., 2003. The genome sequence of the filamentous fungus *Neurospora crassa*. Nature 442, 859-868.

Galagan, J.E. *et al*., 2005. Sequencing of *Aspergillus nidulans* and comparative analysis with *A. fumigatus* and *A. oryzae*. Nature 438, 1105-1115.

Jin, S., Weaver, D.T., 1997. Double-strand break repair by Ku70 requires heterodimerization with Ku80 and DNA binding functions. EMBO journal 16, 6874-6885.

Krappmann, S., Bayram, O., Braus, G.H., 2005. Deletion and allelic exchange of the *Aspergillus fumigatus veA* locus via a novel recyclable marker module. Eukaryot. Cell. 4, 1298-1307.

Krappmann, S., Sasse, C., Braus, G., 2006. Gene targeting in *Aspergillus fumigatus* by homologous recombination is facilitated in a nonhomologous end-joining-deficient genetic background. Eukaryot. Cell 5, 212-215.

Lupton, S.D., Brunton, L.L., Kalberg, V.A., Overell, R.W., 1991. Dominant positive and negative selection using a hygromycin phosphotransferase-thymidine kinase fusion gene. Mol. Cell. Biol. 11, 3374-3378.

Machida, M. *et al*., 2005.Genome sequencing and analysis of *Aspergillus oryzae*. Nature 438, 1157-1161.

Meyer, V., Arentshorst, M., El-Ghezal, A., Drews, A.C., Kooistra, R., Van den Hondel, C.A., Ram, A.F., 2007. Highly efficient gene targeting in the *Aspergillus niger kusA* mutant. J. Biotechnol. 128, 770-775.

Nayak, T., Szewczyk, E., Oakley, C.E., Osmani, A., Ukil, L., Murray, S.L., Hynes, M.J., Osmani, S.A., Oakley, B.R., 2006. A versatile and efficient gene targeting system for *Aspergillus nidulans*. Genetics 172, 1557-1566.

Nielsen, M.L., Albertsen, L., Lettier, G., Nielsen, J.B., Mortersen U.H., 2006. Efficient PCR-Based gene targeting with a recyclable marker for *Aspergillus nidulans*. Fung. Genet. Biol. 43, 54-64.

Nierman, W.C. *et al*., 2005. Genomic sequencing of the pathogenic and allergenic filamentous fungus *Aspergillus fumigatus*. Nature 438, 1151-1156.

Ninomiya, Y., Suzuki, K., Ishii, C., Inoue, H., 2004. Highly efficient gene replacements in *Neurospora* strains deficient for nonhomologous end-joining. Proc. Natl. Acad. Sci. USA 101, 12248-12253.

Oakley, B.R., Rinehart, J.E., Mitchell, B.L., Oakley, C.E., Carmona, C., Gray, G.L., May, G.S., 1987. Cloning, mapping and molecular analysis of the *pyrG* (orotidine-5´-phosphate decarboxylase) gene of *Aspergillus nidulans*. Gene 61, 385-399.

O'Hara, E.B., Timberlake, W.E., 1989. Molecular Characterization of *Aspergillus nidulans yA* locus. Genetics 121, 249-254.

Park, Y., Gerson, S.L., 2005. DNA repair defects in stem cell function and aging. Annu. Rev. Med. 56, 495-508.

Pel, H.J, *et al*., 2007. Genome sequencing and analysis of the versatile cell factory *Aspergillus niger* CBS 513.88. Nat. Biotechnol. 25, 211-231.

Perdersen, H., Beyer, M., Nielsen, J., 2000. Glucoamylase production in batch, chemostat and fedbatch cultivations by an industrial strain of *Aspergillus niger*. Appl. Microbiol. Biotechnol. 53, 272-277.

Sambrook, J., Russell, D.W., 2001 Molecular cloning a laboratory manual. Cold Spring Harbor Laboratory Press, Cold Spring Harbor, NY.

Takahashi, T., Masuda, T., Koyama, Y., 2006. Enhanced gene targeting frequency in *ku70* and *ku80* disruption mutants of *Aspergillus sojae* and *Aspergillus oryzae*. Mol. Genet. Genomics 275, 460-470.

Yang, L., Ukil, L., Osmani, A., Nahm, F., Davies, J., De Souza, C.P., Dou, X., Perez-Balaguer, A., Osmani, S.A., 2004. Rapid production of gene replacement constructs and generation of a green fluorescent protein-tagged centromeric marker in *Aspergillus nidulans*. Eukaryot. Cell 3, 1359-1362.

Yu, J.H., Hamari, Z., Han, K.H., Seo, J.A., Reyes-Dominguez, Y., Scazzocchio, C., 2004. Double-joint PCR: a PCR-based molecular tool for gene manipulations in filamentous fungi. Fung. Genet. Biol. 41, 973-981.

J.B. Nielsen et al. /Fungal Genetics and Biology 45 (2008) 165–170

Supplementary table 1. Oligonucleotides used in the study

Code	Usage	Sequence[a]
T1	**Disruption of *nkuA***	ATGGCCGACGACTATCGCGA
T2		**GTGAAGAGCATTGTTTGAGGC**-AGCACGTACATGGATTCGGA
T3		**GCCTCCTCTCAGACAGAAT**-TTCGGAGCACTAAAACTCAC
T4		CTAGAACTTCGTCTCAAGTAAC
T5		**GTGAAGAGCATTGTTTGAGGC**-GTGAAGCAAACCTGGTCC
T6		**GCCTCCTCTCAGACAGAAT**-CGTCAAGAGTCGGCGAGA
D1	**Deletion of *nkuA***	GGCTGCAGACGTAGCATC
D2		**GATCCCCGGGAATTGCCATG**-GGCGTCTTGAATACAACTGGGG
D3		**AATTCCAGCTGACCACCATG**-CTAGTTGTGACTCTGTTGTCGGT
D4		CTCCACTCTGGACTATCCTCC
C1	**PCR-check of *nkuA***	GAGGTTACCTCAGATCTTG
C2		CGAGTGCACAGCACAGCTG
D5	**Deletion of *yA***	GTGGGTTGAACCGCTTACTCAG
D6		**GATCCCCGGGAATTGCCATG**-CCCGGAGGAATCAAAATGACGC
D7		**AATTCCAGCTGACCACCATG**-GTTTGGGATTCTTAGGTGAGCTC
D8		GGTCAAAACTGCATCGGCGTTG
M1	**Recyclable *pyrG* marker**	GCCTCAAACAATGCTCTTCAC
M2		GGAAGAGAGGTTCACACC
M3		TGATACAGGTCTCGGTCCC
M4		ATTCTGTCTGAGAGGAGGC
M5		**CATGGCAATTCCCGGGGATC**-TGGATAACCGTATTACCGCC
M6		**CATGGTGGTCAGCTGGAATT**-TGCCAAGCTTAACGCGTACC
M7	**ASN*argB* marker**	**CATGGCAATTCCCGGGGATC**-CCTGCCAGTGAGGCTACCC
M8		CCCTTCGGCGTAGCAACAGC
M9		CCGCATTTCCACCGAAGGC
M10		**CATGGTGGTCAGCTGGAATT**-CATCGGCTTCCCGGCTGC
R1	**pDEL2 construction**	TCTAGACGTGGAGTTACCAGTGATTG
R2		GCGGCCGCCTTGCTAGATGACTGGTAGG

[a] All sequences are shown in 5´-3´direction. Sections of the oligonucleotides in bold represent fusion tags.

Supplementary table 2. PCR fragments for bipartite gene-targeting substrate construction

Final strain	Substrate part[a]	Targeting sequences[a]		Marker sequences[a]	
		Fragments	**Primers[b,c]**	**Fragments**	**Primers[b,c]**
nkuA-trL	A	nkuA-trL-5´	*T1*+T2	AFpyrG-tr-5´	M1+*M2*
	B	nkuA-trL-3´	T3+*T4*	AFpyrG-tr-3´	*M3*+M4
nkuA-trS	A	nkuA-trS-5´	*T1*+T5	AFpyrG-tr-5´	M1+*M2*
	B	nkuA-trS-3´	T6+*T4*	AFpyrG-tr-3´	*M3*+M4
***nkuA*Δ**	A	nkuA-Up	*D1*+D2	AFpyrG-5´	M5+*M2*
	B	nkuA-Dw	D3+*D4*	AFpyrG-3´	*M3*+M6
***yA*Δ**	A	yA-Up	*D5*+D6	ASNargB-5´	M7+*M8*
	B	yA-Dw	D7+*D8*	ASNargB-3´	*M9*+M10

[a] see Section 2.3

[b] see Supplementary table 1

[c] italicized primers are used to fuse corresponding targeting- and marker sequences to create the bipartite substrate by PCR.

Transient NHEJ disruption in *Aspergillus*

The work published in Chapter 5 provides proof of concept for the transient disruption of NHEJ gene can be used for greatly improving the gene-targeting efficiency in *A. nidulans* as well as rapidly regenerating full NHEJ activity. One of the overall aims is to transfer the technology to other species by the use of universal selection-marker cassettes that can be used in virtually all fungal systems. Thus, efficient marker systems are essential in this establishment.

The *pyrG* marker was the ideal choice as a marker for the transient *nkuA* system as described in the paper, due to the stable two-way selection. Furthermore, orthologs of this gene exist in all fungi tested, which has enabled the use of heterologous systems. However, the *pyrG* marker has been reported to have limited use in pathogenic models and industrial species. For example, the *pyrG* homolog *URA3* of *C. albicans* have shown to give differentiated expression at various locations in the genome, which affected the virulence of the strains (Lay *et al*., 1998). Therefore, new counter-selectable markers have to be implemented to supplement the use of *pyrG*, or to replace *pyrG* in situations where the application of strains with the corresponding auxotrophy is not convenient. Three systems with alternative counter-selection are currently under investigation in *A. nidulans* for use with the transient disruption technology. All three systems employ bacterial or viral genes, and are under control of the *A. nidulans gpdA* promoter and *trpC* terminator. One of the systems employs the bi-functional fusion product of the hygromycin resistance gene, *hph*, coupled to the thymidine kinase (*TK*) from the Herpes simplex virus (Lupton *et al.,* 1991). This construct was inserted into the pAN7-1 vector and flanked by the abovementioned regulatory sequences. Furthermore, the equivalent systems were made with solely *TK* and *sacB* from *B. subtilis*. The latter encodes the levansucrase enzyme that has been shown to cause lethality in bacteria by low concentrations of sucrose (Ried & Collmer, 1987). This is attractive since the price of sucrose is considerably lower than anti-metabolites, such as the 5-FOA and 5-fluoro-2′-

deoxyuridine (5-FUdR) for *pyrG* and *TK*, respectively. These three solutions are currently under investigation in *A. nidulans*, and the strategies are summarized in **Figure 5.1**.

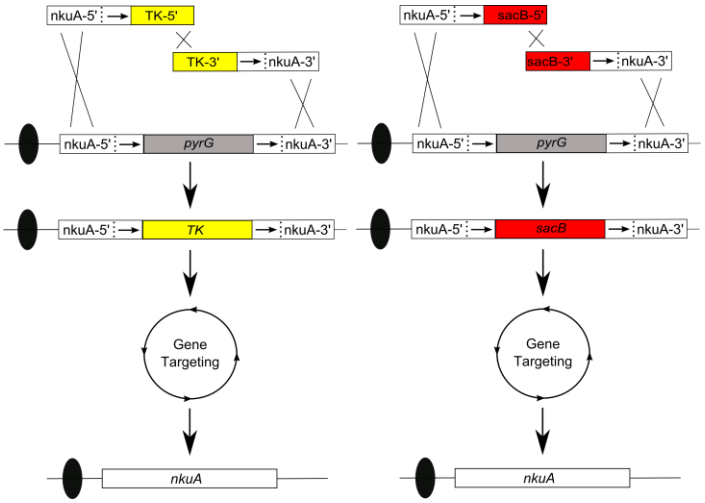

Figure 5.1 Replacement of *pyrG* in *nkuA* with either *TK* or *sacB*. The selection of *pyrG* replacements can be selected with 5-FOA. Loss of TK is detected with 5-FUDR, whereas *sacB*⁺ cells are sensitive to sucrose. Further, when *TK* is fused to *hph* it allows selection for integrants with hygromycin as well as excision of the disruption cassette 5-FUDR.

The transient disruption has been implemented in the opportunistic pathogen *A. fumigatus* and currently under implementation in the cell factory *A. niger*. The disruption of *akuA* in *A. fumigatus* with *pyrG* from *A. nidulans* has been constructed and verified by Southern analysis. Further analysis is carried out by Dr. Thorsten Heinekampp, HKI Jena.

References

Lay, J., Henry, L.K., Clifford, J., Koltin, Y., Bulawa, C.E., and Becker, J.M. Altered expression of selectable marker *URA3* in gene-disrupted *Candida albicans* strains complicates interpretation of virulence studies. *Infect Immun*. **66(11)**: 5301-5306.

Lupton, S.D., Brunton, L.L., Kalberg, V.A., and Overell, R.W., 1991. Dominant positive and negative selection using a hygromycin phosphotransferase-thymidine kinase fusion gene. *Mol Cell Biol*. **11(6)**: 3374-3378.

Ried, J. L. and Collmer., A., 1987. An *nptI-sacB-sacR* cartridge for constructing directed, unmarked mutations in gram-negative bacteria by marker exchange-eviction mutagenesis. *Gene* **57**: 239–246.

Chapter 6

The role of *radC* in homologous recombination and DNA repair in *Aspergillus nidulans*

The role of *radC* in homologous recombination and DNA repair in *Aspergillus nidulans*

Gaëlle Lettier‡†, Michael L. Nielsen‡, Jakob B. Nielsen, Katrine H. Brogaard, Simo A. Jakobsen and Uffe H. Mortensen*

Running head: The role of *radC* in *Aspergillus nidulans*

Center for Microbial Biotechnology, BioCentrum-DTU, Technical University of Denmark, Denmark.

‡These authors contributed equally to this work.

† Present address: Biotech Research and Innovation Centre (BRIC), Ole Maaløes Vej 5, 2200 København N, Denmark.

*Corresponding author. Technical University of Denmark, BioCentrum-DTU, Center for Microbial Biotechnology, DK-2800 Lyngby, Denmark.

Tel.: +45 4525 2701; Fax: +45 4588 4148

E-mail: um@biocentrum.dtu.dk

Summary

Homologous recombination, HR, contributes in the repair of a variety of DNA lesions including meiotic and mitotic DNA double-strand-breaks, DSBs, and in restarting stalled and collapsed replication forks. In the yeast, *S. cerevisiae*, Rad52 is important for all processes that depend on HR. However, its role seems to have changed in evolution, so it has a prominent role in yeast and a less prominent role in vertebrates displaying only mild phenotypes. To investigate how the functions of Rad52 have evolved it is interesting to evaluate the role of Rad52 in other organisms. Here we have determined the role of the Rad52 homolog RadC in a number of different repair processes in the filamentous fungus, *A. nidulans*. Like for *S. cerevisiae rad52*Δ strains, we find that *A. nidulans radC*Δ strains are sterile and highly sensitive to methyl methanesulfonate (MMS) and hydroxyurea (HU) suggesting involvement of RadC in the repair of replication induced lesions. Similar to vertebrates devoid of Rad52 functions, we find that *radC*Δ strains are resistant to γ-ray induced DNA damage suggesting that other pathways have evolved to cope with such lesions. Moreover, like in vertebrates, gene targeting is reduced, but not abolished, in *radC*Δ strains, indicating that a RadC independent pathway for recombinational repair must be present in *A. nidulans*. Taken together the role of RadC in DNA repair appears to be intermediate to that found for *S. cerevisiae* and for vertebrates.

Introduction

Homologous recombination (HR) is an essential process for maintaining the integrity of the genome of eukaryotes. For example, in meiotic cells it is required for proper chromosome segregation and in mitotic cells it plays important roles in DNA repair and in restarting stalled replication forks (24). In the budding yeast *Saccharomyces cerevisiae*, genes involved in HR belong to the *RAD52* epistasis group. The defining member of this group, *RAD52*, plays a central role in HR as it encodes the only dedicated recombination protein, required for all types of HR (41, 64). Accordingly, when compared to the other genes in this group, deletion of *RAD52* results in the most severe phenotype, including dramatic reductions in meiotic and mitotic HR, growth and sporulation defects and extreme sensitivity to γ-rays and genotoxins like the DNA alkylating agent methyl methanesulfonate (MMS) (reviewed by (23)).

Homologs of *RAD52* have been identified in other yeasts and in organisms like filamentous fungi, fish, chicken, mouse and human, (2, 3, 6, 35, 40, 50, 56, 65, 70). However, sequence analyzes of the different Rad52 homologs show that only the N-terminus of the protein is highly conserved as the middle and C-terminal regions show little sequence identity. Nevertheless, the overall domain organization, except the position of the nuclear localization signal (NLS), is similar in *S. cerevisiae* and vertebrate Rad52 (18, 22, 32-34, 42, 45, 55, 57, 59, 60, 65) and the biochemical functions appear conserved (18, 32, 33, 42, 47, 58, 60). In spite of this, it is therefore surprising that the defects shown by chicken DT40 cells, mouse ES cells and mice lacking Rad52 are modest (49, 72) compared to those of *S. cerevisiae rad52*Δ strains, suggesting that the role of Rad52 in HR and DNA double-strand break (DSB) repair is less important in higher eukaryotes. To investigate how the role of Rad52 has evolved during evolution, we have assessed the importance of the Rad52 homolog RadC in the filamentous fungus, *Aspergillus nidulans* in these processes. By analyzing the performance of a *radC*Δ mutant in a number of different repair processes we show that *radC*Δ strains display a phenotype intermediate to that of *S. cerevisiae* and vertebrates.

MATERIALS AND METHODS

Strains, media and plasmids. The *A. nidulans* strain, IBT27263, (*argB2*, *pyrG89*, *veA1*) was used as reference strain and IBT28010 (*argB2*, *pyrG89*, *veA1, radC*Δ) (37) as *radC*Δ strain in all experiments concerning haploid strains. In the addition, strains IBT26134 (*pantoA10*, *veA1*) and IBT28539 (*argB2*, *pantoA10*, *veA1*, *yA-Kpn*I, *radC*Δ) were used for the sexual crosses. All strains are available from the IBT Culture Collection at BioCentrum-DTU, Lyngby, Denmark. *S. cerevisiae* strains W1588-4C (74) and UM270-44A (this study) are isogenic to W303-1A (69) except that they are *RAD5* and *RAD5*, *rad52*::*HIS5*, respectively. *Escherichia coli* strain DH5α was used to propagate plasmids.

Minimal medium (MM) and complete medium (CM) were made according to Clutterbuck (7) except that the salts solution was made according to Cove (8). MM and CM were supplemented with 10 mM uridine, 10 mM uracil, 4 mM L-arginine when necessary. CM containing bleomycin, MMS or HU were made by adding either bleocin (Cat. Nr. 203408, Calbiochem), MMS (M4016, Sigma-Aldrich) or HU (H8627, Sigma-Aldrich), respectively, to CM containing 2% agar after it had cooled down to 50°C subsequent to autoclavation.

The plasmid pJET-kat1 was constructed by inserting a PCR fragment containing a *yA::pyrG* disruption into pJET1 (Fermentas GMBH) by blunt-end insertion. Specifically, this insertion contains 2506 bp of sequence upstream of the *yA* ORF, followed by the *pyrG* marker casette from *A. fumigatus*, and 2346 bp of sequence downstream of the *yA* ORF.

cDNA analysis. The *radC* mRNA transcript was analyzed using the SMART RACE cDNA amplification kit (Clontech Laboratories Inc., Mountain View USA.). cDNA for both 5' and 3' amplification was prepared according to the recommendations of the manufacturer. The template was total RNA extracted from exponentially growing mycelia in minimal medium. 5' cDNA was generated by PCR using a single *radC* internal reverse primer (5'-GAGGAAGCTGCTGCCCTTCAAGCAC-3') and the universal primer mix supplied with the kit. The PCR products were inserted into the pGEM-T vector (Promega Corp., Madison, USA.) and transformed into *E. coli*. The

resulting inserts were sequenced (MWG-Biotech AG, Ebersberg, Germany). Cloned 3' end cDNA fragments were obtained in a similar manner using *radC* specific primers (5'-ATCGCCAGAAACCCGTTTGAGGAAGCC-3' and 5'-AACGCGCTCTGCGGAACTTCGGC-3').

Sensitivity to DNA damaging agents. Sensitivity to bleomycin, MMS and HU was tested by spotting 5 μl of serial 10-fold dilutions of conidial suspensions on solid CM containing the genotoxin. To test for sensitivity towards γ- and UV-irradiation, conidial suspensions were spotted on complete medium as described above, and the plates were incubated for approximately two hours at room temperature before irradiation with different doses of γ- or UV-irradiation. γ-irradiation was performed using the gamma cell irradiator at the Radiation Research Department at Risø National Laboratory (Roskilde, Denmark). UV irradiation was performed using a Stratalinker UV Crosslinker 1800 from Stratagene (La Jolla, California, USA). In this case, plates were kept in total darkness at all stages after irradiation by wrapping plates with aluminum foil. All strains exposed to genotoxins and irradiation were incubated at 37°C for 3 days before photography.

Gene targeting assay. The 6 kb linear DNA fragment used as gene-targeting substrate to delete *yA* was liberated from plasmid pJET-kat1 by *Nru*I digestion and purified using illustra™ DNA and Gel band purification kit (GE Healthcare). The resulting fragment consists of the selectable marker, *pyrG*, flanked by a 2.4 and a 1.5 kb, up- and downstream *yA* targeting sequence, respectively. Protoplasting and gene-targeting procedures were as described previously (37) using 2 μg of the gene-targeting substrate, and subsequently selecting for uracil/uridine prototrophy. The gene-targeting efficiency of a strain (*pyrG*$^{-}$ and *yA*$^{+}$) is determined as the ratio of yellow transformants (*pyrG*$^{+}$ and *yA*$^{-}$) to the total number of transformants.

Analysis of meiosis in *radC*Δ strains. Meiosis was investigated by sexual crossing of *A. nidulans* strains. This was performed by plating 10^6 conidia of each parental strain in a circle with a diameter of about 3.5 cm in the center of a plate containing solid MM. Since the two haploid strains used in a cross contained complementary marker gene

combinations, none of the parental strains are able to grow on MM and a 0.5 cm^3 cube of solid complete media was therefore placed in the center of the plate to allow initial germination and growth. In cases where the two parental strains had a common auxotrophy (for example, *argB2*), the minimal medium was supplemented accordingly. After 2-3 days incubation at 37°C, the plates were sealed with two layers of parafilm, wrapped in aluminum foil to induce meiosis and incubated for an additional 14 days. Plates were then examined for number and size of the cleistothecia formed. The ascospore content of cleistothecia was determined microscopically and the presence of viable spore by plating on CM.

Growth rate determination. The growth rates of *radC* and *radC*Δ strains in liquid culture were determined as follows. 3 ml of conidia spores (from a solution with a density of OD_{600} = 0.1) were inoculated in triplicate into 100 ml of liquid MM supplemented with arginine, uridine and uracil and incubated at 37°C with shaking. After 12 hours incubation, 1 ml of biomass was sampled every 1.5 hours and filtered from the broth using nitrocellulose filters (pore size 0.45 μm). Biomass was determined applying the sample to pre-dried filters. Filters were washed with distilled water and dried on the filter for 15 min in a microwave-oven at 150 W before determining the mass of applied biomass. Subsequently, cell mass concentration was calculated as mg/L.

RESULTS

cDNA sequence analysis of the *radC* gene. The annotation of *A. nidulans radC* (AN4407.3) available from the Broad Institute (http://www.broad.mit.edu) describes a gene interrupted by four introns and containing an ORF predicted to encode a protein of 582 amino acid residues. This is more than 100 residues longer than both *S. cerevisiae* and human Rad52, and this prompted us to confirm the annotation, experimentally. We isolated mRNA from *A. nidulans* strain, IBT27263, and performed 5' and 3' RACE (see Experimental procedures). In order to locate the putative translation start site of the *radC* mRNA transcript, five individual subcloned 5' cDNA fragments were sequenced. Since all fragments started within a narrow 25 nucleotide region, we assume that the mRNA

transcription start site is located immediately upstream of this region. If true, the first 5' ATG in frame with a large ORF within these fragments represents the most likely translation start site of RadC (Fig. S1). This translation start site is upstream of the ATG suggested by the AN4407.3 annotation and it adds a novel 8 nucleotide exon and a 68 nucleotide intron to the *radC* gene. Moreover, translation from this ATG extends the N-terminus of RadC by sixteen residues. To support our annotation, we compared the upstream region of *radC* with fourteen other fungal *RAD52* homologs, including six from aspergilli (Fig. 1A). In agreement with our annotation, this alignment shows that all fungal sequences in this analysis contain a putative eight nucleotide exon similar to the one we have identified for *A. nidulans radC*. This exon has been uncovered in eight of the fourteen published annotations. Moreover, as the fifteen N-termini produced from the ATG in this exon are highly conserved (Fig. 1B) we conclude that it is expressed and that it defines the N-terminus of these Rad52 homologues. Sequencing of the central part of the *radC* cDNA demonstrated that the last intron of *radC* is three nucleotides larger than predicted by the AN4407.3 annotation (Fig. S1). Finally, 3' RACE of the *radC* messenger reveals that polyadenylation occurs 344 nucleotides downstream of the TAA stop codon (Fig. S1). Together our cDNA sequencing results predict that RadC is composed of 597 amino acid residues. Only the N-terminal 1/3 of Rad52 is highly conserved during evolution (34). In this context, we note that compared to the smaller Rad52 species from *S. cerevisiae* and vertebrates, most of the additional residues present in the larger fungal Rad52 species are located downstream of the highly conserved N-terminus. Lastly, we note the presence of a putative NLS in the very C-terminal end of RadC. This is similar to its proposed position in vertebrates (65) (Fig. S2), but not to its position in *S. cerevisiae* Rad52 where it is located in the middle part of the protein (45).

Growth and spore formation of the *radC*Δ strain. For *S. cerevisiae,* several laboratories have reported, around a two-fold reduction in growth rate for cells lacking Rad52 (11, 44, 63). In contrast, we find that the *radC*Δ mutation does not appear to affect growth in liquid medium (see Experimental procedures) as the doubling times of *radC*Δ and wild-type strains during the early exponential growth phase are 88 ± 8 and 83 ± 4

minutes, respectively. In agreement with this result, when *radC*Δ strains were incubated as three point stabs on agar plates and incubated at 25°C, 30°C or 37°C, colonies developed at similar rates compared to wild-type strains (Fig. 2). However, unlike the wild-type strains that are green due to formation of conidiospores, *radC*Δ colonies appear pale indicating that spore formation is impaired in *radC*Δ strains. In accordance with this observation, *radC*Δ colonies produce about 3% of the wild-type amount of conidia at 37°C, see Table 1. At 30°C, where *A. nidulans* strains grow slower, *radC*Δ colonies appear greener and at this temperature they produce around 20% of the wild-type amount of conidia.

The response of the *radC*Δ strain to genotoxins. In *S. cerevisiae*, loss of Rad52 activity, results in cells that are highly sensitive to γ-irradiation and to MMS (14, 46, 48). In contrast, Rad52 appears to play little or no role in the repair of these types of damage in chicken or mammalian cells (49, 72). To understand the role of *A. nidulans* RadC in DNA repair and to address whether this role is more similar to its role in *S. cerevisiae* or in higher eukaryotes, we tested the ability of *radC*Δ mutant strains to survive exposure to a number of DNA damaging agents, including γ-rays and MMS, in spot assays. Firstly, the sensitivity of *radC*Δ mutant strains to γ-ray induced DNA DSBs was investigated. As control and for comparison, *S. cerevisiae* wild-type and *rad52*Δ strains were also included in the analysis. The *A. nidulans* and the *S. cerevisiae* strains were irradiated simultaneously to ensure that both cell types received the same amount of irradiation. As expected, the *S. cerevisiae rad52*Δ strain was extremely sensitive to γ-irradiation see Fig. 3. For example, at 40 krad, the viability was reduced by more than six orders of magnitude compared to wild-type strains. In contrast, both *A. nidulans radC* and *radC*Δ strains were equally resistant to γ-irradiation indicating that RadC does not contribute significantly in the repair of γ-ray induced damage in mitotic cells. To further investigate the ability of *A. nidulans* strains in repairing DNA DSBs, *radC*Δ and wild-type strains were plated on solid medium containing bleomycin (Fig. 3). In this case, we observed that survival of *radC*Δ strains were much reduced compared to wild-type.

Thus, the ability to survive chronic DNA DSB formation, unlike the ability to survive a single dose of γ-ray induced damage, depends on RadC activity.

Next, *radC* and *radC*Δ strains were challenged by chronic exposure to the DNA alkylating agent MMS. This treatment dramatically reduced survival of *radC*Δ strains compared to wild-type strains Fig. 4. Hence, the role of RadC in the repair of γ-ray induced damage appears similar to that observed in vertebrates, whereas its role in the repair of MMS induced damage is similar to that in *S. cerevisiae*. We also tested the ability of *radC*Δ mutants to survive UV-irradiation and chronic exposure to HU (Fig. 4). Compared to wild-type strains we find that HU severely affects the viability of *radC*Δ strain whereas UV-irradiation only causes a minor reduction in survival of the mutant strains.

Efficiency of gene targeting in the *radC*Δ strains. The role of Rad52 in HR appears different between *S. cerevisiae* and vertebrates. Specifically, when HR is evaluated in an "ends-out" gene targeting assay (64), Rad52 is essential for gene targeting in *S. cerevisiae* (25, 52, 53), but not in mouse and chicken cells where the gene-targeting efficiency is reduced about three-fold in the absence of Rad52 (49, 72). To investigate the role of RadC in HR in *A. nidulans* we evaluated the efficiency of ends-out gene targeting using a linear DNA substrate designed to delete *yA* (see Experimental procedures). *yA* was chosen as target gene as *yA*Δ strains produce yellow rather than wild-type green conidiospores (39). This provides a simple read-out of gene-targeting efficiency since transformation with a *yA* knockout gene-targeting substrate results in yellow transformants if the substrate integrates by HR and in green transformants if it integrates by NHEJ (37). When wild-type strains were transformed with the gene-targeting substrate 11% of the transformants were yellow (Table 2). In contrast, with *radC*Δ strains approximately 1% of the transformants were yellow indicating that the gene targeting efficiency is 10-fold reduced in the absence of RadC. Accordingly, like in vertebrates, RadC plays an important, but not essential, role in HR.

Analysis of meiosis in the *radC*Δ mutant. In *S. cerevisiae* and most sexually reproducing eukaryotes, recombination is very frequent during meiosis as it ensures the

correct pairing and segregation of homologous chromosomes during the first meiotic division (27). Meiotic recombination is a well-regulated event that includes programmed formation of multiple DNA DSBs at chromosomal hot spots in a process involving the evolutionarily conserved topoisomerase type II-like protein, Spo11 (21). In *S. cerevisiae*, *rad52*Δ strains are sterile as they fail to repair Spo11-induced DNA DSBs (23). In contrast, *RAD52*$^{-/-}$ mice are fertile, (49) even though successful meiotic divisions, like in *S. cerevisiae*, depends on the formation of a large number of Spo11 induced DNA DSBs (10). Therefore, the importance of Rad52 during meiosis appears reduced in mice compared to in *S. cerevisiae*. Since meiotic recombination is frequent in *A. nidulans* (68) and since it contains a Spo11 homolog (AN8259.1) (16) it is reasonable to assume that DNA DSBs are also produced during meiosis in *A. nidulans*. We therefore investigated the role of RadC during meiosis in *A. nidulans*. Accordingly, sexual crosses were carried out using wild-type and *radC*Δ strains. When two wild-type strains or one wild-type and one *radC*Δ strain were mated, cleistothecia developed within 14 days and ascospores were abundant and viable as expected. However, when two *radC*Δ strains were crossed, cleistothecia were scarce and abnormally small after 14 days of incubation (Fig. 5) and further incubation did not change this result. Moreover, out of 30 tested cleistothecia obtained from *radC*Δ strains, none contained ascospores. These results suggest that RadC, like Rad52 in *S. cerevisiae*, is required in meiosis at a step prior to ascospore formation and that a single functional *radC* copy within the dikaryon is sufficient to ensure successful meiotic divisions.

DISCUSSION

The overall pathways for HR and DNA DSB repair generally appear conserved through evolution, however, the individual contributions of specific proteins may vary from organism to organism. For example, the role of the Rad52 protein has changed from being essential in *S. cerevisiae* to playing only a minor role in vertebrates. In the present study, we have characterized a *RAD52* homolog, *radC*, in *A. nidulans* and investigated its role in this organism. Moreover, aspergilli encompass species that are

pathogens as well as species that are important producers of industrially relevant compounds and it is therefore important to address how this group of fungi performs HR and DNA DSB repair. Indeed, in the case of industrial strains, understanding these repair mechanisms may be used to develop more genetically stable producer strains; and in the case of pathogenic strains, it may provide new antifungal drug targets.

An important function of HR is to repair DNA DSBs. In organisms with a sexual cycle, this function is most pronounced during meiosis where hundreds of programmed DNA DSBs are induced by Spo11 (4, 20). The fact that a Spo11 homolog exists in *A. nidulans* strongly suggests that DNA DSB induced HR takes place during meiosis in *A. nidulans*. Recombinational repair of these DNA DSBs likely require RadC function as *radC*Δ strains fail to develop sexual spores. In mitotic cells, accidental DNA DSBs occur at a low frequency due to e.g. irradiation and the presence of reactive oxygen species (41, 64). In contrast to meiotic DNA DSBs, repair of these breaks take place in competition with NHEJ based repair pathways (1). Gene-targeting experiments in different filamentous fungi including *A. nidulans* have indicated that DNA DSBs are predominantly repaired by NHEJ (19, 36, 37, 71). This view is supported by the finding that a NHEJ deficient *A. niger* strain, *kusA*Δ, is γ-ray sensitive (31). In agreement with this, we find that RadC appears to play little or no role in repair of γ-ray induced DNA DSBs. If the NHEJ pathway repairs most of these breaks in *A. nidulans*, this pathway, unlike in *S. cerevisiae*, has evolved to efficiently repair the frayed DNA ends that are produced by γ-rays (26). In higher eukaryotes, NHEJ dependent repair of such ends are facilitated by the activity of the Artemis/DNA-PK complex (5, 30). However, we note that these proteins have not yet been identified in *A. nidulans*. Alternatively, damaged DNA ends may be processed by the MRX complex to facilitate repair by NHEJ (73) more efficiently in *A. nidulans* than in *S. cerevisiae*.

The preference for a DNA DSB repair pathway may depend on the position of the cell in the cell cycle. Hence, in many organisms, including *C.albicans, Schizosaccharomyces pombe* and mammals, it has been shown that NHEJ and HR are active in G1 and S/G2/M cells, respectively (6, 12, 51, 73). If this is also true for *A. nidulans*, significant death of

S/G2/M *radC*Δ cells after γ-irradiation could be masked by surviving G1 cells, if the latter represent a large fraction of the cells in the population. This view is supported by the fact that *radC*Δ strains are sensitive to chronic exposure to bleomycin, hence, requiring repair of DNA DSB generated in all phases of the cell cycle.

Another important function of HR is to overcome replication stress. HU has been shown to produce stalled replication forks, accumulation of single stranded DNA and even DNA breaks; and re-initiation of replication is believed to occur via an HR-dependent mechanism (28, 62, 66). Similarly, replication of DNA that has been exposed to the DNA alkylating agent MMS leads to lesions that interfere with the replication machinery and require HR for repair (29). Here, we show that *radC*Δ strains, like *rad52*Δ *S. cerevisiae* strains, are hypersensitive to both MMS and HU, strongly suggesting an essential role of RadC in repair of replication stress induced lesions. HR deficient *S. cerevisiae* strains are often mildly UV sensitive indicating that UV-rays occasionally produce damage that requires repair by HR. Such lesions may be stalled replication forks resulting from pyrimidine dimers that escaped repair via the nucleotide excision repair pathway prior to replication (61). Considering that *radC*Δ strains are mildly UV-sensitive, a similar scenario may apply for *A. nidulans*.

Rad52 species are conserved from *S. cerevisiae* to humans, but it is clear that, the importance of Rad52 in HR repair has changed during evolution towards a central role in *S. cerevisiae* and a more modest role in vertebrates. The extremes appear to be *S. pombe* encoding two full length Rad52 homologs (9); and plants and invertebrates that do not seem to contain Rad52 homologs. In the present study we have aimed at clarifying the roles of RadC in DNA metabolism in the filamentous fungus *A. nidulans*. We show that with respect to growth, gene-targeting efficiency and repair of γ-ray induced damage it is similar to vertebrates; but, with respect to repair of MMS induced damage and gametogenesis it appears similar to that of *S. cerevisiae*. This contrasts the role of Rad52 in another filamentous fungus, *Neurospora crassa*, which is distantly related to *A. nidulans* (15). In the absence of Rad52 activities, this fungus displays a phenotype close to that of *S. cerevisiae* as *N. crassa mus-11* deficient strains are infertile and sensitive to γ-irradiation

(50, 54). Moreover, no ends-out gene-targeting transformants were obtained in these strains (17, 38). Hence, the role of Rad52 has not only evolved differently between *S. cerevisiae* and vertebrates, but also within the fungal kingdom.

In vertebrates, the lack of a prominent phenotype in the absence of Rad52 has been explained by existence of other proteins with similar functions, e.g. XRCC3 and BRCA2 (43, 67) and that these proteins may compensate for each other. This is supported by the fact that combined Rad52 and XRCC3 deficiency is lethal in chicken DT40 cells (13). In this context it is interesting to note that ends-out gene targeting is not completely abolished in *radC*Δ strains indicating that a RadC independent pathway for HR exists in *A. nidulans*. Since sequence comparisons so far have failed to identify any homologs of XRCC3 and BRCA2 in *A. nidulans* (16) another protein with Rad52-like functions may have evolved in *A. nidulans* to take over part of its functions. On the other hand, the observation that Rad52 species in filamentous fungi typically are around 100 amino-acid residues longer than homologs identified in other species suggests that Rad52 may have gained functions different from those known in *S. cerevisiae* and vertebrates. For example, RadC appears to play a role in development of asexual spores, a cell type, which is not formed in *S. cerevisia*e or in vertebrates. Further investigations into fungal DNA repair biology may address these intriguing possibilities.

ACKNOWLEDGEMENTS

This work was supported by the Danish Research Council for Technology and Production Sciences (U.H.M). We thank Arne Miller and co-workers at the Radiation Research Department at Risø National Laboratory for access to the gamma cell, and the members of the Mortensen laboratory for critically reading this manuscript.

FIGURE LEGENDS

FIG. 1. The position of the start codon in *radC*. A. Nucleotide alignment of *RAD52* homologs from fifteen fungal species. Nucleotides representing the first intron in each sequence is omitted, except for the two first and the two last nucleotides of each intron.

The numbers in bracket provide the total size of the introns in nucleotides. ATGs as suggested by GenBank annotations are shown in gray boxes, whereas the ATG in *radC* determined in the present study is shown in a black box. Below, a schematic representation of the position of the novel exon and intron determined in the present study relative to the *radC* sequence. Novel translated nucleotides as predicted by our analysis are indicated by gray bars. Translated nucleotides according to the Broad annotation (AN4407.3) are indicated as a black bar. B. An alignment of the putative amino acid sequences (aa) predicted by using the ATG determined in the present study as translation start site. The methionine of the translation start in *A. nidulans* determined in the present study is indicated by a black box. Conserved amino acid residues are shaded. Methionines predicted as the first amino acid residue in Rad52 homologs by the Broad annotations are indicated in bold. For *A. nidulans* the location of novel amino-acid residues predicted by our analysis, as well as those predicted by the Broad annotation, are illustrated schematically as a gray and a black bar, respectively, below the sequences.

FIG. 2. Conidiospore formation, but not colony growth, is impaired in *radC*Δ strains. Wild-type and *radC*Δ strains were incubated as three point stabs on agar plates and incubated at 25°C, 30°C or 37°C as indicated. Magnifications of sections, indicated as squares, of colonies grown at 37°C are shown to the right.

FIG. 3. Sensitivity of *radC*Δ strains to γ-irradiation and bleomycin. A. Strains were spotted as serial 10-fold dilutions on solid medium and subjected to γ-irradiation, or (B) spotted on medium containing bleomycin. γ-iray doses and bleomycin concentrations are indicated above panels.

FIG. 4. Sensitivity of *radC*Δ strains to MMS, HU and UV-irradiation. The toxicity of a number of genotoxins was evaluated in spot assays. Strains were spotted as serial 10-fold dilutions on solid medium containing MMS and HU (upper panels) at the

genotoxin concentrations indicated. The same dilutions were spotted on solid medium and subjected to UV-irradiation at the doses indicated (lower panels).

FIG. 5. RadC is required for development cleistothecia. Comparison of cleistothecia produced by wild-type (A) and *radC*Δ (B) strains on solid medium. Comparison of isolated and purified cleistothecia obtained from wild-type (C) and *radC*Δ (D) strains. Typical representatives of size-variation of cleistothecia in wild-type and *radC*Δ strains are shown and their frequency in the population in percentage is indicated for each type above panels. A scale bar representing 1 mm is presented below panel D.

Fig. S1. Summary of the results obtained from sequencing *radC* cDNA. Only selected sequence is shown. Nucleotides typed in capitals have been confirmed by sequencing and lower case indicates sequences inferred from the genomic sequence. Black boxes with super scripted numerals indicate the start of five different 5′ RACE clones. For each amino acid encoding triplet, the residue is given as single letter code. Novel residues are shown in bolded italics. The novel intron is bounded by grey boxes. The ATG annotated as the start codon of radC by the Broad annotation is shown in bold. The stop TAA stop-codon is shown. The final intron is one codon longer than previously annotated indicated by gta. The polyadenylation site is indicated with asteriks.

Fig. S2. *radC* contains a putative nuclear localization signal (NLS) in the C-terminal at approximately the same position as vertebrate genes. **A**. Alignment of the C- terminal taken from Takahashi and Dawid, 2005. The black bar indicates the location of the NLS for four vertebrate genes as determined by Takahashi and Dawid. B. Alignment of *A. nidulans radC*. The black bar indicates a pat7 NLS signal predicted by the online software PSORT II (Hicks,G.R. and Raikhel,N.V. Ann. Rev. Cell Dev. Biol., 11, 155, 1995).

REFERENCES

1. **Allen, C., J. Halbrook, and J. A. Nickoloff**. 2003. Interactive competition between homologous recombination and non-homologous end joining. Mol Cancer Res. **1**:913-920.

2. **Bendixen, C., I. Sunjevaric, R. Bauchwitz, and R. Rothstein**. 1994. Identification of a mouse homologue of the Saccharomyces cerevisiae recombination and repair gene, RAD52. Genomics **23**:300-303.

3. **Bezzubova, O. Y., H. Schmidt, K. Ostermann, W. D. Heyer, and J. M. Buerstedde**. 1993. Identification of a chicken RAD52 homologue suggests conservation of the RAD52 recombination pathway throughout the evolution of higher eukaryotes. Nucleic Acids Res **21**:5945-5949.

4. **Borde, V.** 2007. The multiple roles of the Mre11 complex for meiotic recombination. Chromosome. Res. **15**:551-563.

5. **Burma, S., B. P. Chen, and D. J. Chen**. 2006. Role of non-homologous end joining (NHEJ) in maintaining genomic integrity. DNA Repair (Amst) **5**:1042-1048.

6. **Ciudad, T., E. Andaluz, O. Steinberg-Neifach, N. F. Lue, N. A. Gow, R. A. Calderone, and G. Larriba**. 2004. Homologous recombination in Candida albicans: role of CaRad52p in DNA repair, integration of linear DNA fragments and telomere length. Mol Microbiol. **53**:1177-1194.

7. **Clutterbuck, A. J.** 1974. Bacteria, Bacteriophage and Fungi, p. 447-510. *In* R. C. King (ed.), Handbook of Genetics, 1. Plenum press, New York, NY.

8. **Cove, D. J.** 1966. The induction and repression of nitrate reductase in the fungus *Aspergillus nidulans*. Biochim. Biophys. Acta. **113**:51-56.

9. **de Vries, F. A., J. B. Zonneveld, A. J. de Groot, R. I. Koning, A. A. van Zeeland, and A. Pastink**. 2007. Schizosaccharomyces pombe Rad22A and Rad22B have similar biochemical properties and form multimeric structures. Mutat Res. **615**:143-152.

10. **Di, G. M., M. Barchi, F. Baudat, W. Edelmann, S. Keeney, and M. Jasin**. 2005. Distinct DNA-damage-dependent and -independent responses drive the loss of oocytes in recombination-defective mouse mutants. Proc Natl Acad Sci U. S. A. **102**:737-742.

11. **Fabre, F., A. Chan, W. D. Heyer, and S. Gangloff**. 2002. Alternate pathways involving Sgs1/Top3, Mus81/ Mms4, and Srs2 prevent formation of toxic recombination intermediates from single-stranded gaps created by DNA replication. Proc Natl Acad Sci U. S. A. **99**:16887-16892.

12. **Ferreira, M. G. and J. P. Cooper**. 2004. Two modes of DNA double-strand break repair are reciprocally regulated through the fission yeast cell cycle. Genes Dev. **18**:2249-2254.

13. **Fujimori, A., S. Tachiiri, E. Sonoda, L. H. Thompson, P. K. Dhar, M. Hiraoka, S. Takeda, Y. Zhang, M. Reth, and M. Takata**. 2001. Rad52 partially substitutes for the Rad51 paralog XRCC3 in maintaining chromosomal integrity in vertebrate cells. EMBO J **20**:5513-5520.

14. **Game, J. C. and R. K. Mortimer**. 1974. A genetic study of x-ray sensitive mutants in yeast. Mutat Res **24**:281-292.

15. **Geiser, D. M., C. Gueidan, J. Miadlikowska, F. Lutzoni, F. Kauff, V. Hofstetter, E. Fraker, C. L. Schoch, L. Tibell, W. A. Untereiner, and A. Aptroot**. 2006. Eurotiomycetes: Eurotiomycetidae and Chaetothyriomycetidae. Mycologia. **98**:1053-1064.

16. **Goldman, G. H. and E. Kafer**. 2004. Aspergillus nidulans as a model system to characterize the DNA damage response in eukaryotes. Fungal Genet Biol. **41**:428-442.

17. **Hastings, P. J., C. McGill, B. Shafer, and J. N. Strathern**. 1993. Ends-in vs. ends-out recombination in yeast. Genetics. **135**:973-980.

18. **Hays, S. L., A. A. Firmenich, P. Massey, R. Banerjee, and P. Berg**. 1998. Studies of the interaction between Rad52 protein and the yeast single-stranded DNA binding protein RPA. Mol Cell Biol **18**:4400-4406.

19. **Ishibashi, K., K. Suzuki, Y. Ando, C. Takakura, and H. Inoue**. 2006. Nonhomologous chromosomal integration of foreign DNA is completely dependent on MUS-53 (human Lig4 homolog) in Neurospora. Proc Natl Acad Sci U. S. A. **103**:14871-14876.

20. **Keeney, S., C. N. Giroux, and N. Kleckner**. 1997. Meiosis-specific DNA double-strand breaks are catalyzed by Spo11, a member of a widely conserved protein family. Cell. **88**:375-384.

21. **Keeney, S. and M. J. Neale**. 2006. Initiation of meiotic recombination by formation of DNA double-strand breaks: mechanism and regulation. Biochem Soc Trans **34**:523-525.

22. **Krejci, L., B. Song, W. Bussen, R. Rothstein, U. H. Mortensen, and P. Sung**. 2002. Interaction with Rad51 is indispensable for recombination mediator function of Rad52. J Biol Chem **277**:40132-40141.

23. **Krogh, B. O. and L. S. Symington**. 2004. Recombination proteins in yeast. Annu Rev Genet **38**:233-271.

24. **Lambert, S., B. Froget, and A. M. Carr**. 2007. Arrested replication fork processing: interplay between checkpoints and recombination. DNA Repair (Amst). **6**:1042-1061.

25. **Langston, L. D. and L. S. Symington**. 2004. Gene targeting in yeast is initiated by two independent strand invasions. Proc Natl Acad Sci U. S. A. **101**:15392-15397.

26. **Lewis, L. K. and M. A. Resnick**. 2000. Tying up loose ends: nonhomologous end-joining in Saccharomyces cerevisiae. Mutat Res **451**:71-89.

27. **Lichten, M.** 2001. Meiotic recombination: breaking the genome to save it. Curr Biol **11**:R253-R256.

28. **Lundin, C., K. Erixon, C. Arnaudeau, N. Schultz, D. Jenssen, M. Meuth, and T. Helleday**. 2002. Different roles for nonhomologous end joining and homologous recombination following replication arrest in mammalian cells. Mol Cell Biol **22**:5869-5878.

29. **Lundin, C., M. North, K. Erixon, K. Walters, D. Jenssen, A. S. Goldman, and T. Helleday**. 2005. Methyl methanesulfonate (MMS) produces heat-labile DNA damage but no detectable in vivo DNA double-strand breaks. Nucleic Acids Res. **33**:3799-3811.

30. **Ma, Y., H. Lu, K. Schwarz, and M. R. Lieber**. 2005. Repair of double-strand DNA breaks by the human nonhomologous DNA end joining pathway: the iterative processing model. Cell Cycle **4**:1193-1200.

31. **Meyer, V., M. Arentshorst, A. El-Ghezal, A. C. Drews, R. Kooistra, C. A. van den Hondel, and A. F. Ram**. 2007. Highly efficient gene targeting in the Aspergillus niger kusA mutant. J Biotechnol **128**:770-775.

32. **Milne, G. T. and D. T. Weaver**. 1993. Dominant negative alleles of RAD52 reveal a DNA repair/recombination complex including Rad51 and Rad52. Genes Dev **7**:1755-1765.

33. **Mortensen, U. H., C. Bendixen, I. Sunjevaric, and R. Rothstein**. 1996. DNA strand annealing is promoted by the yeast Rad52 protein. Proc Natl Acad Sci USA **93**:10729-10734.

34. **Mortensen, U. H., N. Erdeniz, Q. Feng, and R. Rothstein**. 2002. A molecular genetic dissection of the evolutionarily conserved N terminus of yeast Rad52. Genetics **161**:549-562.

35. **Muris, D. F., O. Bezzubova, J. M. Buerstedde, K. Vreeken, A. S. Balajee, C. J. Osgood, C. Troelstra, J. H. Hoeijmakers, K. Ostermann, and H. Schmidt**. 1994. Cloning of human and mouse genes homologous to RAD52, a yeast gene involved in DNA repair and recombination. Mutat Res **315**:295-305.

36. **Nielsen, J. B., M. L. Nielsen, and U. H. Mortensen**. 2007. Transient disruption of non-homologous end-joining facilitates targeted genome manipulations in the filamentous fungus Aspergillus nidulans. Fungal Genet Biol. **In press**.

37. **Nielsen, M. L., L. Albertsen, G. Lettier, J. B. Nielsen, and U. H. Mortensen**. 2006. Efficient PCR-based gene targeting with a recyclable marker for *Aspergillus nidulans*. Fungal. Genet. Biol. **43**:54-64.

38. **Ninomiya, Y., K. Suzuki, C. Ishii, and H. Inoue**. 2004. Highly efficient gene replacements in Neurospora strains deficient for nonhomologous end-joining. Proc. Natl. Acad. Sci. U. S. A. **101**:12248-12253.

39. **O'Hara, E. B. and W. E. Timberlake**. 1989. Molecular characterization of the Aspergillus nidulans yA locus. Genetics **121**:249-254.

40. **Ostermann, K., A. Lorentz, and H. Schmidt**. 1993. The fission yeast rad22 gene, having a function in mating-type switching and repair of DNA damages, encodes a protein homolog to Rad52 of Saccharomyces cerevisiae. Nucleic Acids Res **21**:5940-5944.

41. **Paques, F. and J. E. Haber**. 1999. Multiple pathways of recombination induced by double-strand breaks in Saccharomyces cerevisiae. Microbiol Mol Biol Rev. **63**:349-404.

42. **Park, M. S., D. L. Ludwig, E. Stigger, and S. H. Lee**. 1996. Physical interaction between human RAD52 and RPA is required for homologous recombination in mammalian cells. J Biol Chem **271**:18996-19000.

43. **Pellegrini, L. and A. Venkitaraman**. 2004. Emerging functions of BRCA2 in DNA recombination. Trends Biochem Sci **29**:310-316.

44. **Pinson, B., I. Sagot, and B. ignan-Fornier**. 2000. Identification of genes affecting selenite toxicity and resistance in Saccharomyces cerevisiae. Mol Microbiol. **36**:679-687.

45. **Plate, I., L. Albertsen, M. Lisby, S. C. Hallwyl, Q. Feng, C. Seong, R. Rothstein, P. Sung, and U. H. Mortensen**. 2007. Rad52 multimerization is important for its nuclear localization in Saccharomyces cerevisiae. DNA Repair (Amst). **In press**.

46. **Prakash, L.** 1976. The relation between repair of DNA and radiation and chemical mutagenesis in Saccharomyces cerevisiae. Mutat Res. **41**:241-248.

47. **Reddy, G., E. I. Golub, and C. M. Radding**. 1997. Human Rad52 protein promotes single-strand DNA annealing followed by branch migration. Mutat Res. **377**:53-59.

48. **Resnick, M. A.** 1969. Genetic control of radiation sensitivity in Saccharomyces cerevisiae. Genetics **62**:519-531.

49. **Rijkers, T., J. Van Den Ouweland, B. Morolli, A. G. Rolink, W. M. Baarends, P. P. Van Sloun, P. H. Lohman, and A. Pastink**. 1998. Targeted inactivation of mouse RAD52 reduces homologous recombination but not resistance to ionizing radiation. Mol Cell Biol **18**:6423-6429.

50. **Sakuraba, Y., A. L. Schroeder, C. Ishii, and H. Inoue**. 2000. A Neurospora double-strand-break repair gene, mus-11, encodes a RAD52 homologue and is inducible by mutagens. Mol Gen Genet **264**:392-401.

51. **Saleh-Gohari, N. and T. Helleday**. 2004. Conservative homologous recombination preferentially repairs DNA double-strand breaks in the S phase of the cell cycle in human cells. Nucleic Acids Res. **32**:3683-3688.

52. **Schiestl, R. H. and S. Prakash**. 1990. RAD10, an excision repair gene of Saccharomyces cerevisiae, is involved in the RAD1 pathway of mitotic recombination. Mol Cell Biol. **10**:2485-2491.

53. **Schiestl, R. H., J. Zhu, and T. D. Petes**. 1994. Effect of mutations in genes affecting homologous recombination on restriction enzyme-mediated and illegitimate recombination in Saccharomyces cerevisiae. Mol Cell Biol. **14**:4493-4500.

54. **Schroeder, A. L.** 1986. Chromosome instability in mutagen sensitive mutants of Neurospora. Curr Genet. **10**:381-387.

55. **Shen, Z., K. G. Cloud, D. J. Chen, and M. S. Park**. 1996. Specific interactions between the human RAD51 and RAD52 proteins. J Biol Chem **271**:148-152.

56. **Shen, Z., K. Denison, R. Lobb, J. M. Gatewood, and D. J. Chen**. 1995. The human and mouse homologs of the yeast RAD52 gene: cDNA cloning, sequence analysis, assignment to human chromosome 12p12.2-p13, and mRNA expression in mouse tissues. Genomics **25**:199-206.

57. **Shen, Z., S. R. Peterson, J. C. Comeaux, D. Zastrow, R. K. Moyzis, E. M. Bradbury, and D. J. Chen**. 1996. Self-association of human RAD52 protein. Mutat Res **364**:81-89.

58. **Shinohara, A., H. Ogawa, and T. Ogawa**. 1992. Rad51 protein involved in repair and recombination in S. cerevisiae is a RecA-like protein. Cell. **69**:457-470.

59. **Shinohara, A. and T. Ogawa**. 1998. Stimulation by Rad52 of yeast Rad51-mediated recombination. Nature **391**:404-407.

60. **Shinohara, A., M. Shinohara, T. Ohta, S. Matsuda, and T. Ogawa**. 1998. Rad52 forms ring structures and co-operates with RPA in single-strand DNA annealing. Genes Cells. **3**:145-156.

61. **Sinha, R. P. and D. P. Hader**. 2002. UV-induced DNA damage and repair: a review. Photochem. Photobiol. Sci. **1**:225-236.

62. **Sogo, J. M., M. Lopes, and M. Foiani**. 2002. Fork reversal and ssDNA accumulation at stalled replication forks owing to checkpoint defects. Science. **297**:599-602.

63. **Sommers, C. H., E. J. Miller, B. Dujon, S. Prakash, and L. Prakash**. 1995. Conditional lethality of null mutations in RTH1 that encodes the yeast counterpart of a mammalian 5'- to 3'-exonuclease required for lagging strand DNA synthesis in reconstituted systems. J Biol Chem. **270**:4193-4196.

64. **Symington, L. S.** 2002. Role of RAD52 epistasis group genes in homologous recombination and double-strand break repair. Microbiol Mol Biol Rev. **66**:630-70, table.

65. **Takahashi, N. and I. B. Dawid**. 2005. Characterization of zebrafish Rad52 and replication protein A for oligonucleotide-mediated mutagenesis. Nucleic Acids Res **33**:e120.

66. **Tercero, J. A., M. P. Longhese, and J. F. Diffley**. 2003. A central role for DNA replication forks in checkpoint activation and response. Mol Cell. **11**:1323-1336.

67. **Thacker, J.** 2005. The RAD51 gene family, genetic instability and cancer. Cancer Lett. **219**:125-135.

68. **Thijs, H., J. Garde, T. Goosen, B. Tomsett, K. Swart, C. Heyting, and H. W. van den Broek**. 1995. Polarity of meiotic gene conversion is 5' to 3' within the niaD gene of Aspergillus nidulans. Mol Gen Genet. **247**:343-350.

69. **Thomas, B. J. and R. Rothstein**. 1989. Elevated recombination rates in transcriptionally active DNA. Cell. **56**:619-630.

70. **van den, B. M., K. Vreeken, J. B. Zonneveld, J. A. Brandsma, M. Lombaerts, J. M. Murray, P. H. Lohman, and A. Pastink**. 2001. Characterization of RAD52 homologs in the fission yeast Schizosaccharomyces pombe. Mutat Res **461**:311-323.

71. **Villalba, F., J. Collemare, P. Landraud, K. Lambou, V. Brozek, B. Cirer, D. Morin, C. Bruel, R. Beffa, and M. H. Lebrun**. 2008. Improved gene targeting in Magnaporthe grisea by inactivation of MgKU80 required for non-homologous end joining. Fungal Genet Biol. **45**:68-75.

72. **Yamaguchi-Iwai, Y., E. Sonoda, J. M. Buerstedde, O. Bezzubova, C. Morrison, M. Takata, A. Shinohara, and S. Takeda**. 1998. Homologous recombination, but not DNA repair, is reduced in vertebrate cells deficient in RAD52. Mol Cell Biol. **18**:6430-6435.

73. **Zhang, X. and T. T. Paull**. 2005. The Mre11/Rad50/Xrs2 complex and non-homologous end-joining of incompatible ends in S. cerevisiae. DNA Repair (Amst). **4**:1281-1294.

74. **Zou, H. and R. Rothstein**. 1997. Holliday junctions accumulate in replication mutants via a RecA homolog-independent mechanism. Cell. **90**:87-96.

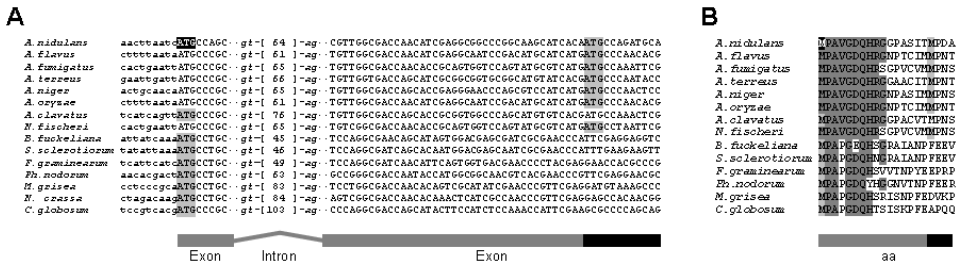

Figure 1

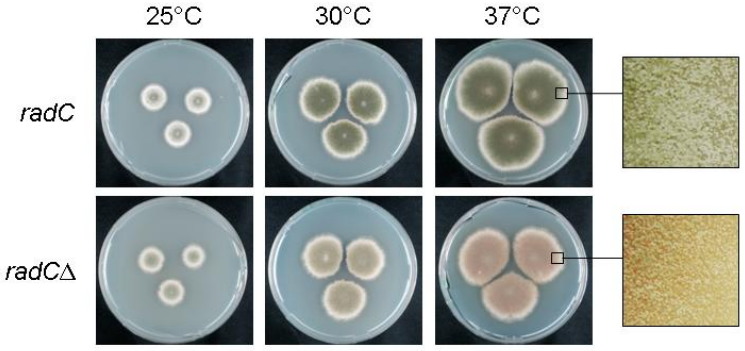

Figure 2

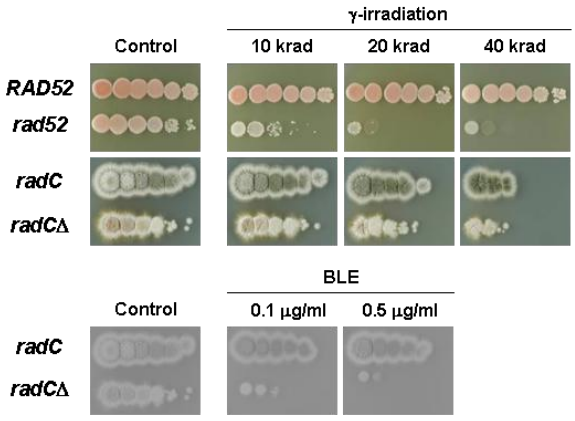

Figure 3

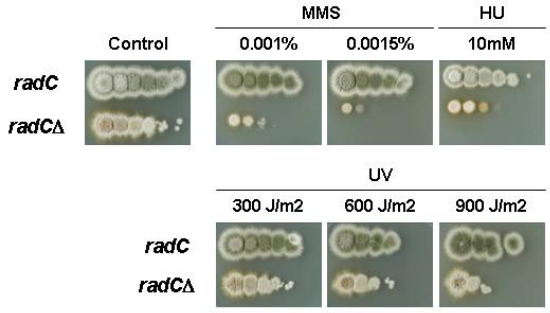

Figure 4

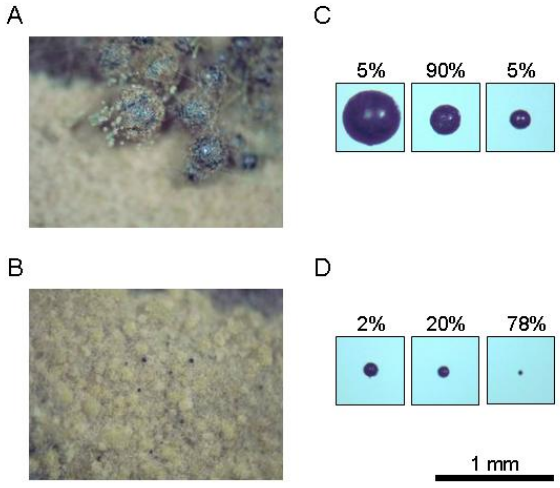

Figure 5

Spore density of colonies resulting from 4 days incubation

Strain	Spore density[a]	
	37°C	30°C
radC	93	57
*radC*Δ	3	11

[a] number of spores x 10^6/cm^2

Table 1

Gene targeting in *radC* and *radC*Δ strains. Yellow colonies are obtained when targeting is succesful.

Trial	*radC*		*radC*Δ	
	green	yellow	green	yellow
1	38	3	57	0
2	68	6	147	0
3	105	13	3	0
5	76	8	12	0
6	343	44	168	2
7	280	37	199	3
	910	111	586	5

Table 2

```
     gggtgactcttcacgtgacttcgcggcatagcagggcatcctgacgcgtttccacgatgggcttcagcctA1AGCCTC2,3AGCG
     ACCCCA4CATGAGTTA5GAACATCAACTCCTTATGATAGCTCTCATAGAGTAACTCATAGAGTAATCTATTCATAAACTTAATC

   1 ATG CCA GC  gtgagtccaccatcacttctcgaccaaactccgacaggctacgtaaactaacgcgtaccgcgtctcag  C
     M   P   A

  78 GTT GGC GAC CAA CAT CGA GGC GGC CCG GCA AGC ATC ACA ATG CCA GAT GCA ACA GGA GTC ATC
...  V   G   D   Q   H   R   G   G   P   A   S   I   T   M   P   D   A   T   G   V   I

...

1006 GAA TTC G  gtaagtaagttgatgcaatgtacagctcattttaccctaggtcgctgatcggatcag  GT GAT GTT TTT
...  E   F   G                                                              D   V   F

...

2082 TCT GCA CAA CAG CAT CAG CAA CAG CAC CAG CAC TAA CACTATCGACCTCGTCTTATGCCAACCCCCGTCCT
     S   A   Q   Q   H   Q   Q   Q   H   Q   H   .

2153 CTCTCACTTTCCACAAAGCATGTACCATATCCGCCTATGCTTCAGTACAACCACCACACCGCAAACTTGCACGACCTTACATT
2236 CGGGGAGTTGGGGAACGGCGTCACGGAGAAACTAGGGCTAATGGAAATAACTGGGCTCATTCGCGTGTTTGTTTCTATGATGA
2319 TTCAAATTTTTCTAAAGGCATTGGACTGGAACCATTTGACTTTCCTTCGGCTTCTGCTATTTGGTGGCTTTTTTTTCCTTTCG
2402 CTATTTTATTCACCGAACAGCAATCTGTGCTTCTTTTTGATGAATAGATCATTCTCGAAA****taaagtgccaaacccatag
```

Supp. Figure 1

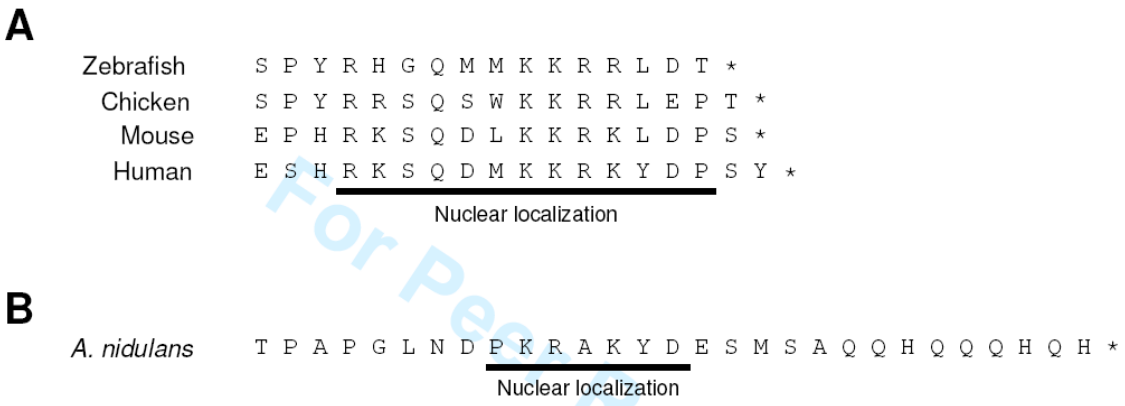

Supp. Figure 2

Chapter 7

Repair of double-strand breaks in recombination and end-joining deficient mutants of *Aspergillus nidulans*

Abstract

Aspergillus nidulans has served as model system for numerous applications with fungal perspectives as well as contributing to issues general for eukaryotes. Within the filamentous fungi, *A. nidulans* can be used as model with the purpose of improving genetic stability in industrial production strains or finding drug targets for pathogenic species. In addition, *A. nidulans* has been a platform for transferable genetic tools. We have studied the effects of deleting key genes in both non-homologous end-joining (NHEJ) and homologous recombination (HR) by genotoxic treatment and gene targeting. The deletion of the DNA ligase IV (*ligD*) and *nkuA*Δ strains were constructed in order to test if LigD in contrast to NkuA is participating in all end-joining activities. We found that exposure to genotoxins revealed no difference in sensitivity between *ligD*Δ and *nkuA*Δ strain. However, the *ligD*Δ improved the targeting rates and end-joining was still performed in the double mutant, albeit at a lower frequency, thus a Ku and LigD-independent pathway end-joining pathway exist in *A. nidulans*. The *radC*Δ and the *nkuA*Δ were both able to perform gene targeting, however the two mutants combined in one strain gave no transformants. Both *nkuA*Δ*radC*Δ and *nkuA*Δ*uvsC*Δ showed additive effects and extreme sensitivity, when they were exposed to γ-rays compared to their single mutants. *nkuA*Δ also was more sensitive to γ-irradiation than *radC*Δ, a situation resembling the one in higher eukaryotes. However, germling cultures of *radC*Δ was very sensitive to γ-irradiation, thus when cells are past G1, HR is applied for the curing of these lesion. The lack of UvsC did not result in more severe defects than with RadC.

Introduction

Cells are constantly exposed to factors that threaten the integrity of DNA. The most severe type of DNA lesion is the double-strand break (DSB). If left unrepaired, DSBs will lead to cell death or chromosomal rearrangements that in mammals can lead to tumorigenesis. DSB repair (DSBR) consists of two relatively conserved pathways; homologous recombination (HR) and non-homologous end-joining (NHEJ). HR uses homologous sequences to fix the breaks and this repair mode is thus error free. However, recombination between different alleles can result in loss of heterozygosity (LOH). NHEJ rejoins the broken ends with little or no processing of ends (Daley *et al*., 2005). This process can be error free, but also error prone due to base loss or insertions. The actions of these two pathways are important for cellular functions other than DSBR. HR is involved in replication fork restart, chromosome segregation in meiosis and is the catalyst in genetic engineering experiments, such as gene targeting (Pâques & Haber, 1999). Some NHEJ proteins regulate the silencing of genes in the vicinity of telomeres and in mammals, NHEJ is essential for the development of antigen display (Boulton & Jackson, 1996; Hefferin & Tomkinson, 2005). Therefore dissecting the function and organization within these pathways contributes to understanding a broad spectrum of cellular functions.

Another motivation for studying DNA repair in filamentous fungi is the relatively low efficiency in gene targeting. Since research in these organisms to a certain extent is fueled by an enormous commercial interest as well as medical interest, much can be gained by increasing targeting efficiency. The popular fungal model *Aspergillus nidulans* has been used by us and other labs to address this issue. (Bird & Bradshaw, 1997; Ichioka et al., 2001; Nayak et al., 2006; Nielsen et al., 2006 - see Chapter 4; Nielsen et al., 2008 - see Chapter 5). The design of the DNA targeting substrate has been one point of research, since the condition of DSBs ends influence the choice of repair pathways and thereby whether substrates are processed by HR or NHEJ (Nielsen *et al*., 2006). However, the main focus has been to eliminate the activity of NHEJ to avoid random

integration. Removal of the Ku heterodimer from numerous filamentous fungi (Ninomiya *et al*., 2004; Krappmann *et al*., 2006; Nayak *et al*., 2006; Takahashi *et al*., 2006; Meyer *et al*., 2007) has in all cases resulted in strains with targeting frequencies close to 100 %, and less stringency in homology requirements for the target sequences. Further, in *N. crassa* it was demonstrated that deletion of NHEJ ligase, *lig-4*, resulted in total abolishment of NHEJ. Despite the significant activity of NHEJ during transformation and gene targeting no apparent phenotypic side-effects could be observed. How is the use of NHEJ and HR balanced in *A. nidulans*?

We attempted to answer this question recently, when the Rad52 homolog in *A. nidulans*, RadC, was deleted to characterize the role of RadC in *A. nidulans* (Nielsen *et al*., 2006; Chapter 6). Rad52 is the protein with the widest influence in the progress of HR in yeast, since it is required for all types of HR events. In addition, gene targeting has not been possible in *rad52*-null strains. Specifically, Rad52 is required for the loading of Rad51 on single-strand DNA and partly on the Rad51-filament formation that leads the strand invasion step. The strong DNA annealing activity makes this protein relevant in all recombination activities. Interestingly, in mammalian cells, the importance of Rad52 is not of the same magnitude and the absence of Rad51 is far more severe. In *A. nidulans*, we observed that in contrast to the absence of Ku, abolishing RadC had significant effects on the morphology with an extensive secretion and binding of a reddish pigment to the mycelium and lack of conidiation under normal growth conditions (Chapter 6). The sensitivity to genotoxins that confer replication stress, e.g. MMS and HU is similar to yeast. However the relative insensitivity to DSB inducing γ-irradiation and the ability to perform gene targeting, albeit at reduced efficiency, resembles the situation reported from mammals and not yeast. This indicates that RadC has a profound role in *A. nidulans* HR and that a RadC-independent recombination pathway exists in *A. nidulans*.

In the present work, we are going further into HR and NHEJ functions by studying a set of single and double mutants. All mutants were subjected to a selection of six genotoxins

to test their ability to repair certain lesions. Two agents were inducing DSBs; γ-rays are one-time exposure and bleomycin was added in the medium for chronic DSB induction. Three mutagens, HU, MMS and UV were chosen for their ability to induce replication stress by creating lesions that block replication or transcription, and by their indirect recruitment of DSBR proteins. The last drug was cisplatin, due to the fact it produces dsDNA cross-link lesions that also utilize DSBR proteins for repair in yeast. Moreover, a gene-targeting assay was applied as a specific test to determine, which of the proteins that are critical for both specific and random integration in *A. nidulans*.

Results

In light of the significant roles for RadC and Ku in *A. nidulans*, the deletions of *nkuA* and *radC* were combined in a single strain, which has not been reported in filamentous fungi before. Hence, analyzing this mutant could reveal if there were any synergistic effects between *nkuA*Δ and *radC*Δ mutations and thus any cross talk between recombination and end-joining pathways in the ability to repair lesions generated by six genotoxic treatments.

*nkuA*Δ*radC*Δ displays synergistic sensitivity to γ-rays

The *radC* was deleted by gene targeting in the *nkuA*Δ strain constructed in a previous study (Nielsen *et al*., 2008) creating a double deletion mutant, which was verified by Southern analysis (data not shown). The *nkuA*Δ*radC*Δ double mutant showed identical morphology to the *radC*Δ strain, which at 37°C displayed reddish mycelium due to excessive pigment production and reduced conidia formation. This effect diminished when the mutants were grown at lower temperatures, 25-30°C. In comparison, such a significant macroscopic phenotype was not observed in *nkuA*Δ that did not deviate from wt in morphology (Nielsen *et al*., 2008). Thus, adding *nkuA*Δ to the *radC*Δ strain did not appear to have any macroscopic effect. Exposing these three strains to the selection of genotoxins revealed more subtle differences in the stress response of the individual strains.

Bleomycin and γ-rays both induce DSBs. Bleomycin is not degraded nor unstable during the growth period, thus the drug provides chronic stress by creating oxygen radicals that cleaves DNA (Tam *et al*., 2007). The *nkuA*Δ strain was as resistant as wild-type (wt), however the *radC*Δ and *nkuA*Δ*radC*Δ were significantly more sensitive to the drug at the two highest concentrations tested, as shown in **Figure 1**. At 5 μg/ml all strains were dead (data not shown). However, exposing the *nkuA*Δ conidia to γ-irradiation, high sensitivity was obtained compared to *radC*Δ and wt with almost a 1000-fold difference in viable spores at the highest doses. The double mutant showed a dramatic decrease in viability already at 20 krad, and was markedly more sensitive than the *nkuA*Δ, indicating a synergistic effect of the double mutation.

Spores in dormancy are in the G1 phase of the cell cycle at least for the first few hours that is dominated by isotropic growth (Harris, 1999). Here NHEJ is the primary choice to fix DSBs, since no homologous template is available for repair (Helleday *et al*., 2005). Hence the effect of γ-irradiating conidia that had begun germination was tested and wt and *radC*Δ spores were inoculated in liquid MM prior to γ-irradiation. By this, a mixed population of swollen spores and germlings that had passed G1 could be monitored. This showed that the mixed population of *radC*Δ conidia and germlings were significantly more sensitive than the dormant *radC*Δ conidia, whereas wt germlings were completely resistant towards γ-irradiation.

The strains were also subjected to treatments that provoke replication stress (**Figure 2**). *nkuA*Δ*radC*Δ and *radC*Δ showed equal sensitivity at all concentrations of MMS, HU and UV and both were more sensitive than the *nkuA*Δ, which was as resistant as wt in all cases. All in all, the results from the genotoxic treatment of *radC*Δ showed a situation resembling yeast, except for the γ-irradiation resistance (Chapter 6). Therefore the homolog was subjected to the same genotoxins to evaluate the relative importance of Rad51p.

*uvsC*Δ strains were not sensitive to replication stress by HU

The *RAD51* homolog (*uvsC*, Seong *et al*., 1997; van heemst *et al*., 1997) was deleted in an *nkuA*Δ background, and the *nkuA*Δ was crossed out from *uvsC*Δ in the parental wt strain. The *uvsC*Δ produced a reddish pigment similar to *radC*Δ but less intense, and had a higher degree of conidiation than *radC*Δ at 37°C. No morphological difference between the *uvsC*Δ and *nkuA*Δ*uvsC*Δ could be observed. *uvsC*Δ and *nkuA*Δ*uvsC*Δ underwent the same treatment as described before for *radC*Δ and the results are shown in **Figure 3** and **Figure 4**. The UvsC deficient strains show the same sensitivity pattern on bleomycin containing plates as the RadC lacking strains. This is also the case after exposure to γ-rays where *radC*Δ and *uvsC*Δ are equally resistant. In combination with *nkuA*Δ, an increase in sensitivity is observed and this double mutant appears to be 10-fold less sensitive than the *nkuA*Δ*radC*Δ. However, this subtle difference cannot be ruled out as simple experimental discrepancies from spore solution preparations. The MMS treatment was as lethal as for the RadC-deficient series. However, HU and UV had almost no effect on *uvsC*Δ and *nkuA*Δ*uvsC*Δ. Cisplatin was slightly less harsh on the *uvsC*Δ strains than on the *radC*Δ strains, though they were more sensitive than the controls and no synergistic effects with the *nkuA*Δ mutation could be observed from five of the six treatments (**Figures 3, 4 and 6**).

*ligD*Δ was as sensitive than *nkuA*Δ to γ-irradiation

The resistance observed in *nkuA*Δ towards the different treatments could be due to residual end-joining activity, hence the effects of deleting the NHEJ specific ligase, LigD, acting downstream of Ku was investigated. *ligD*Δ was generated in a *nkuA*Δ background and the single mutant was obtained from crossing. No difference in phenotypes between the three strains and wild type could be observed at normal growth conditions (data not shown). In **Figure 5**, the γ-irradiation of the mutants is shown, and the *nkuA*Δ, *ligD*Δ and *nkuA*Δ*ligD*Δ all gave equivalent responses. This situation also applied for the five other treatments described (data not shown), and the influence of the *ligD* deletion is the same as seen in the *nkuA*Δ spot series (**Figure 1-4**).

The DNA damaging agents utilized in this study create various lesions, and the lesions can occur throughout the genome. This study was supplied with a gene-targeting assay, where the action of NHEJ and HR could be monitored more precisely and quantitatively.

Random integration can occur without NkuA and LigD

We employed a gene-targeting assay based on a continuous linear piece of DNA with ~2 kb *yA* up- and downstream target sequences flanking the *A. fumigatus pyrG* marker (Chapter 6). This provided a simple screening and evaluation of gene targeting efficiency based on wt green conidia vs. the yellow conidia of the *yA* knock-out mutant. To evaluate the potency of this specific gene-targeting assay, it was tested in the *nkuA*Δ. The gene-targeting frequency of the *nkuA*Δ was 68 % in this assay after five trials, see **Table 1**, though it is considerably higher than in the wild type (~4 %), there is still a substantial end-joining activity left in the cells. Recently, a *lig-4* deletion mutant in *N. crassa* consistently showed no residual end-joining activity after gene targeting (Ishibashi et al., 2006). The *nkuA*Δ*ligD*Δ was included in the assay. However, the number of targeting events did not amount to 100 % in the *nkuA*Δ*ligD*Δ strain as reported from other species, but only 78 %, which was slightly higher than for *nkuA*Δ.

No targeting in the *radC*Δ*nkuA*Δ and *uvsC*Δ strains

The *nkuA*Δ*radC*Δ and *uvsC*Δ mutant strains tested above were also subjected to the gene-targeting test. Firstly, we aimed at revealing whether the residual HR activity observed in a previous study in *radC*Δ with the equivalent substrates could be increased by combining the *radC*Δ mutation with a deletion of one of the main genes in NHEJ. As seen from the control experiments with a replicating plasmid, the *nkuA*Δ*radC*Δ strain did take up DNA and produced colonies, but no colonies appeared after five rounds of gene targeting in the *nkuA*Δ*radC*Δ. Hence, the residual gene-targeting activity observed in the two single mutants is abolished when *nkuA* and *radC* deletions are combined in

one strain. Gene targeting could not be achieved in trials made for the *uvs*CΔ strain. Only random integration were detected.

Discussion

Filamentous fungi have in recent years become the grand players in bioindustrial production and this trend will continue to increase in the future. Moreover, some species are a menace to society, since they can cause serious illness especially in immuno-compromised patients. These are strong arguments for making investments in the research required to tackle the challenges. Regardless of whether the objective is to find drug targets, or to introduce or remove traits from an organism through engineering, an understanding of the genome maintenance is necessary in particular the double-strand break repair pathways, which are relevant for replication fork restart, telomere maintenance, chromosome segregation and genetic diversity, as well as gene targeting. The DSBR pathways are to a large extent conserved, however differences do exist from yeast to human. In the present study, the initial dissection of HR and NHEJ in *A. nidulans* was undertaken, because filamentous fungi are thought to be a valuable model for DNA repair as an evolutionary link in DNA repair between yeast and human (Goldman & Kafer, 2004).

The selection of DNA damaging agents applied in this study represented a pallet of lesions, however they all have one thing in common, which is that certain lesions generated can require a response from the DSBR pathways (Wiseman & Halliwell, 1996; Dolling *et al*., 1999; Hoeijmarkers, 2001). Two of the damaging agents were inducing DSBs directly. Bleomycin delivers chronic exposure and causes oxidative damage resulting in ssDNA breaks and sequence specific blunt ended or single nucleotide overhang DSBs (Wang *et al*., 1997; Tam *et al*., 2007). It is important to note that the conidial suspensions used in the spot assays consist of G1 nuclei (Harris, 1997). Cells that through NHEJ survive the breaks induced in G1 by bleomycin will thus have an opportunity to repair concurrent lesions later in the cell cycle by HR. Firstly, the deletion

of the two NHEJ genes did not cause enhanced sensitivity compared to wt in bleomycin-induced damage. One explanation could be that a Ku- and/or Lig4-independent pathway efficiently repairs the lesions when the cells are in G1. This will carry the cell into the duplication cycle, where HR mediated repair takes over (Fiddy & Trinci, 1976; Pâques & Haber, 1999). The role of HR to repair bleomycin induced damage is more significant than for the main NHEJ pathway. The lack of additive effects for double mutants, *nkuA*Δ*radC*Δ and *nkuA*Δ*uvsC*Δ, certainly leaves out a Ku-mediated pathway-control switch at DSBs, which may instead be dependent on MRX complex. In yeast, it was reported that bleomycin treatment of *yku70*Δ*rad52*Δ rendered cells more sensitive than for *lig4*Δ*rad52*Δ due to role of Ku in telomere maintenance (Tam *et al*., 2007). However, these effects are not seen from the results obtained here, since *nkuA*Δ*radC*Δ and *radC*Δ, as well as the *nkuA*Δ and *ligD*Δ were equally sensitive or resistant to bleomycin, respectively. The general sensitivity of all the strains to bleomycin could reside in the fact that the generated oxygen radicals also attack proteins and fatty acids, therefore high dosage has additional consequences.

As opposed to bleomycin, γ-irradiation is a one-time dosage. Furthermore, the DSB ends created are frayed and heterogeneous and probably require more end-processing to be repaired (Ward, 2000; Tam *et al*., 2007). The spores had less than two hours on the agar before irradiation, meaning that they were still in G1. Correspondingly, the *nkuA*Δ and *ligD*Δ strains were significantly more sensitive than wt and the HR deficient strains. The effect was most prominent in the *nkuA*Δ*radC*Δ and *nkuA*Δ*uvsC*Δ strain. This shows that both pathways examined are required to efficiently repair damage from γ-rays, probably relating to the multiple and complex character of the lesions generated. Moreover, the treatment of pre-cultivated conidia of wt and *radC*Δ that had been allowed to germinate resulted in high mortality in the *radC*Δ, and a practically unaffected wt. This implies that HR, when present, is important for repairing lesions generated by γ-irradiation, whereas NHEJ appears to be sufficient for repairing the lesions, when HR is not present. Consequently, when HR and NHEJ are active as in the

case of the wt germlings, all lesions are readily repaired. In addition, it would reasonable to assume that a pre-cultivated culture of the *nkuA*Δ will be more resistant to γ-rays due to the functional HR. From the results obtained, however it is impossible to infer whether the DSBR occur in a concerted manner between Ku and Rad51 or Rad52.

Three of the genotoxic agents induce replication stress. For restarting replication forks several DNA repair systems are involved depending on the lesion, among these is recombination (Symington, 2005). This was supported by the results obtained in the MMS, HU and UV treatments, where lack of RadC was shown to be most serious. NHEJ did not have any influence on the repair of the lesions occurring after treatment. However, Rad51 is important for alleviating stress from HU in mammals, but in *A. nidulans* UvsC did not seem important for recovery after HU, but instead it appears as if RadC and other HR proteins can relieve the stress from HU. Thus, it is likely that Rad51-mediated strand invasion only takes place in a few cases, and that the DNA annealing activities of RadC somehow could be sufficient for repair. In the UV experiments, one factor that could explain the increased sensitivity of *radC*Δ strains is less of the conidial pigmentation in these strains. The wt green pigment provides some protection against UV-irradiation thus *radC*Δ strains may suffer from this deficiency. All together, the role of RadC in the repair of lesions by the genotoxins applied is not far from the role of Rad52 in yeast. Still, some resistance to γ-ray damage is observed in *radC*Δ and coupled to the gene-targeting performance, the role of RadC in HR of *A. nidulans* appears different from the homologs of human and yeast.

The tremendous improvements in gene-targeting efficiency came after the *ku70* homolog was deleted in *Neurospora crassa* (Ninomiya et al., 2004). Numerous other examples in various fungi including *A. nidulans* have followed up on this trend (Nayak *et al*., 2006; Nielsen *et al*., 2008). Thus, 70-100 % targeting efficiencies are now common success rate with various substrates in various NHEJ-deletion strains (Ninomiya *et al*., 2004; Ishibashi *et al*., 2006; Nayak *et al*., 2006; Nielsen *et al*., 2008). There can be a natural variation

relating to the strain used and the locus for targeting. The gene targeting assay applied in our study only produced 68 % of transformed colonies in *nkuA*Δ, see **Table 1**. This strain has with bipartite substrates shown to target up to 97 % (Nielsen *et al.*, 2008). The difference in targeting efficiency could be related to advantages of the bipartite gene targeting in *A. nidulans*, as well as the short overhangs from cleavage of the vector containing the continuous substrates that favor end joining. The low targeting rate with this substrate was also seen in wt, which only produced 4 % yellow colonies. The residual end-joining activity was in *N. crassa* abolished by deleting the gene encoding the DNA ligase IV.

In order to test whether this situation also applied to *A. nidulans*, an *nkuA*Δ*lig4*Δ double deletion was constructed to test whether DNA ligase IV, acting downstream of NkuA, is involved in all end-joining activities (Daley *et al*., 2005). However, performing targeting in the *nkuA*Δ*lig4*Δ double mutant only improved the gene-targeting frequency with the continuous substrate to a total of 78 %. This implies that a substantial amount of cells still undergo end-joining despite the lack of two central NHEJ genes, and therefore that at least three distinct end-joining pathways exist. One main end-joining pathway involves both Ku and Lig4. Then two minor pathways are Ku-independent and only one these relies on Lig4. A pathway that in yeast has been reported to perform end-joining without requiring Ku and only partially LigD, is the microhomology-mediated end joining pathway, a pathway somewhat similar to single-strand annealing (Ma *et al*., 2003; Daley *et al*., 2005). It requires end processing as it is dependent on the action of Mre11 homolog MreA (Semighini *et al*., 2003), Rad50 and AnRad1. The coupling of *nkuA*Δ*ligD*Δ to *mreA*Δ would reveal whether the residual end-joining was MreA dependent.

The fact that no gene targeting could be performed in *nkuA*Δ*radC*Δ is intriguing since both of the single mutants were able to integrate the substrates. Even though the yellow transformants obtained in the *nkuA*Δ host were generated by RadC action, more

substrates could be expected to be channeled through the RadC-independent HR pathway in the *nkuA*Δ*radC*Δ since a major competing pathway was eliminated. Still, no colonies were obtained, which implies that a sort of indirect communication in repair by Ku and Rad52 cannot be ruled out at this point. Lastly we investigated whether all targeting was dependent on UvsC. In the 18 transformants obtained in this strain, all were ectopic integrants. Ichioka and co-workers reported that the homologous integration of exogenous substrates was abolished in the 50 transformants from gene targeting in the *uvsC*-null strain analyzed (Ichioka *et al*., 2001). However, from our study on RadC, the gene-targeting events in this strain were not observed until the total number of transformants exceeded 150 colonies. Thus, more targeting trials will be performed for this strain and more assays and mutants are underway.

Materials and methods

Experimental procedures

Strains, media and plasmids

The *A. nidulans* strain, IBT27263, (*argB2, pyrG89, veA1*) was used as reference strain and IBT28010 (*argB2, pyrG89, veA1*, *radC*Δ) (Nielsen *et al*., 2006) as *radC*Δ strain in all experiments concerning haploid strains. The *nkuA*Δ (*argB2, pyrG89, veA1*, *nkuA*Δ) was used for all strain construction in this study. In the addition, strains IBT26134 (*pantoA10, veA1*) and IBT28539 (*argB2, pantoA10, veA1, yA-Kpn*I, *radC*Δ) were used for the sexual crosses. All strains are available from the IBT Culture Collection at DTU Biosys, Lyngby, Denmark. *Escherichia coli* strain DH5*α* was used to propagate plasmids.

Minimal medium (MM) and complete medium (CM) were made according to Clutterbuck (Clutterbuck, 1974) except that the salts solution was made according to Cove (Cove, 1966). MM and CM were supplemented with 10 mM uridine, 10 mM uracil, 4 mM L-arginine when necessary. CM containing bleomycin, MMS, HU and cisplatin were made by adding either bleocin (Cat. Nr. 203408, Calbiochem), MMS (M4016, Sigma-Aldrich), HU (H8627, Sigma-Aldrich) or cisplatin (P4394, Sigma-Aldrich),

respectively, to CM containing 2% agar after it had cooled down to 50°C subsequent to autoclavation.

The plasmid pJET-kat1 was constructed as listed in Chapter 6.

Strain construction

The *radC*Δ*nkuA*Δ was constructed using the equivalent bipartite gene targeting strategy as described (Nielsen *et al*., 2006) with the exception that *pyr-4* was replaced with *pyrG* for targeting (Nielsen *et al*., 2008). This marker was also utilized in the construction of *uvsC*Δ (AN1237) and *ligD*Δ (AN0097) in the *nkuA*Δ described (Nielsen et al., 2008). Primers for making the respective deletions are as follows; UvsC-dl-Up-F CACGCTTGTCGCGCTCTC + UvsC-dl-Up-RAd gatccccgggaattgccatg-CCGTATACTCCGTACTAGCAGTCTGATGCGCTGGAGGAAAACGATTGCGG and UvsC-dl-Dw-Fad aattccagctgaccaccatgGAAAGAGCACAATGCTGTTTCCG + UvsC-dl-Dw-R CAGCGTAGTAGCGGTACC. For *ligD*Δ: LigD-dl-up-F TCTCCAACAATGCTGACTGTGG + LigD-dl-up-RA gatccccgggaattgccatgGTTGCAACCTATTCTCGTGC and LigD-dl-dw-FA aattccagctgaccaccatgCAGGGCCCTAGTTCTGAATTAC and LigD-dl-dw-R GCAAACATACCATCGTTCAGG. Transformants were screened by Spore-PCR (Nielsen *et al*., 2008) and true deletions were crossed with IBT26134 for regeneration of *nkuA*. Progeny was screened by spore-PCR and the right clone was plated on 5-FOA for loss of *pyrG*. Spore-PCR verified marker loss.

Sensitivity to DNA damaging agents

Sensitivity to bleomycin, γ-rays, UV, cisplatin, MMS, and HU was tested as described in Chapter 6. Germlings for γ-irradiation were produced by pre-cultivating strains at 30°C for six hours before harvesting cells and dilution. The gene targeting assay is presented in Chapter 6.

Figure legends

Figure 7.1 Sensitivity of wt, *nkuA*Δ, *radC*Δ and *nkuA*Δ*radC*Δ strains to γ-irradiation and bleomycin at the concentrations indicated. Strains were spotted as serial 10-fold dilutions on solid complete medium.

Figure 7.2 Sensitivity of wt, *nkuA*Δ, *radC*Δ and *nkuA*Δ*radC*Δ strains to MMS, HU and UV-irradiation. Strains were spotted as serial 10-fold dilutions on solid medium containing MMS and HU at the concentrations indicated. The same dilutions were spotted on solid medium and subjected to UV-irradiation at the doses shown.

Figure 7.3 Sensitivity of wt, *nkuA*Δ, *uvsC*Δ and *nkuA*Δ*uvsC*Δ strains to γ-irradiation and bleomycin at the concentrations indicated.

Figure 7.4 Sensitivity of wt, *nkuA*Δ, *uvsC*Δ and *nkuA*Δ*uvsC*Δ strains to MMS, HU and UV-irradiation.

Figure 7.5 Sensitivity of wt, *nkuA*Δ, *ligD*Δ and *nkuA*Δ*ligD*Δ strains to γ-irradiation and bleomycin at the concentrations indicated.

Figure 7.6 Sensitivity of wt, *nkuA*Δ, *radC*Δ, *nkuA*Δ *radC*Δ, *uvsC*Δ and *nkuA*Δ*uvsC*Δ strains as indicated on the left of the pictures to cisplatin.

References

Boulton S.J. and Jackson S.P., 1996. Identification of a *Saccharomyces cerevisiae* Ku80 homologue: roles in DNA double strand break rejoining and in telomeric maintenance. *Nucleic Acids Res.* **24(23)**: 4639-4648.

Daley, J.M., Palmbos, P.L., Wu, D., Wilson, T.E., 2005. Nonhomologous end joining in yeast. *Annu. Rev. Genet.* **39**: 431-51.

Dolling, J.A., Boreham, D.R., Brown, D.L., Raaphorst, G.P., and Mitchel, R.E., 1999. Cisplatin-modification of DNA repair and ionizing radiation lethality in yeast, *Saccharomyces cerevisiae*. *Mutat. Res.* **433(2)**: 127-136.

Fiddy, C. and Trinci, A.P., 1976. Mitosis, septation, branching and the duplication cycle in *Aspergillus nidulans*. *J. Gen. Microbiol.* **97(2)**: 169-84.

Goldman, G.H. & Kafer, E., 2004. *Aspergillus nidulans* as a model system to characterize the DNA damage response in eukaryotes. *Fungal. Genet. Biol.* 2004 **41(4)**: 428-442.

Harris, S.D., 1997. The duplication cycle in *Aspergillus nidulans*. *Fungal Genet. Biol*. **22(1)**: 1-12.

Hefferin, M.L. and Tomkinson, A.E., 2005. Mechanism of DNA double-strand break repair by non-homologous end joining. *DNA Repair (Amst)* **4(6)**: 639-648.

Helleday, T., Lo, J., van Gent, D.C., and Engelward, B.P., 2007. DNA double-strand break repair: from mechanistic understanding to cancer treatment. *DNA Repair (Amst)* **6(7)**: 923-935.

Hoeijmakers, J.H., 2001. Genome maintenance mechanisms for preventing cancer. *Nature* **411(6835)**: 366-374.

Ichioka, D., Itoh, T., Itoh, Y., 2001. An *Aspergillus nidulans uvsC* null mutant is deficient in homologous DNA integration. *Mol. Gen. Genet.* **264(5)**: 709-715.

Ishibashi, K., Suzuki, K., Ando, Y., Takakura, C., and Inoue, H., 2006. Nonhomologous chromosomal integration of foreign DNA is completely dependent on MUS-53 (human Lig4 homolog) in *Neurospora*. *PNAS* **103(40)**: 14871-14876.

Krappmann, S., Sasse, C., and Braus, G., 2006. Gene targeting in *Aspergillus fumigatus* by homologous recombination is facilitated in a nonhomologous end-joining-deficient genetic background. *Eukaryot. Cell* **5**: 212-215.

Ma, J.L., Kim, E.M., Haber, J.E., and Lee, S.E., 2003. Yeast Mre11 and Rad1 proteins define a Ku-independent mechanism to repair double-strand breaks lacking overlapping end sequences. *Mol. Cell. Biol*. **23(23)**: 8820-8828.

Meyer, V., Arentshorst, M., El-Ghezal, A., Drews, A.C., Kooistra, R., Van den Hondel, C.A., and Ram, A.F., 2007. Highly efficient gene targeting in the *Aspergillus niger kusA* mutant. *J. Biotechnol*. **128**: 770-775.

Nielsen, J.B., Nielsen, M.L., and Mortensen, U.H., 2008. Transient disruption of non-homologous end-joining facilitates targeted genome manipulations in the filamentous fungus *Aspergillus nidulans*. *Fungal. Genet. Biol.* **45(3)**: 165-170.

Nielsen, M.L., Albertsen, L., Lettier, G., Nielsen, J.B., and Mortensen, U.H., 2006. Efficient PCR-based gene targeting with a recyclable marker for *Aspergillus nidulans*. *Fungal. Genet. Biol*. **43(1)**: 54-64.

Ninomiya, Y., Suzuki, K., Ishii, C., and Inoue, H., 2004. Highly efficient gene replacements in *Neurospora* strains deficient for nonhomologous end-joining. *PNAS* 101: 12248-12253.

Pâques, F. and Haber J.E., 1999. Multiple pathways of recombination induced by double-strand breaks in *Saccharomyces cerevisiae*. *Microbiol. Mol. Biol. Rev.* **63(2)**: 349-404.

Semighini, C.P., von Zeska Kress Fagundes, M.R., Ferreira, J.C., Pascon, R.C., de Souza Goldman, M.H., and Goldman, G.H., 2003. Different roles of the Mre11 complex in the DNA damage response in *Aspergillus nidulans*. *Mol. Microbiol.* **48(6)**: 1693-1709.

Seong KY, Chae SK, Kang HS, 1997. Cloning of an *E. coli* RecA and yeast RAD51 homolog, *radA*, an allele of the *uvsC* in *Aspergillus nidulans* and its mutator effects. *Mol. Cells*. **7(2)**: 284-289.

Symington, L.S., 2005. Focus on recombinational DNA repair. *EMBO Rep*. **6(6)**: 512-517.

Takahashi, T., Masuda, T., and Koyama, Y., 2006. Enhanced gene targeting frequency in *ku70* and *ku80* disruption mutants of *Aspergillus sojae* and *Aspergillus oryzae*. *Mol. Genet. Genomics* **275**: 460-470.

Tam, A.T., Pike, B.L., Hammet, A., and Heierhorst, J., 2007. Telomere-related functions of yeast KU in the repair of bleomycin-induced DNA damage. *Biochem. Biophys. Res. Commun.* **357(3)**: 800-803.

van Heemst, D., Swart, K., Holub, E.F., van Dijk, R., Offenberg, H.H., Goosen, T., van den Broek, and H.W., Heyting, C., 1997. Cloning, sequencing, disruption and phenotypic analysis of *uvsC*, an *Aspergillus nidulans* homologue of yeast RAD51. *Mol. Gen. Genet*. **254(6)**: 654-64.

Wang, P., Zhou, R.H., Zou, Y., Jackson-Cook, C.K., and Povirk, L.F., 1997. Highly conservative reciprocal translocations formed by apparent joining of exchanged DNA double-strand break ends. *PNAS* **94(22)**: 12018-12023.

Ward, J.F., 2000. Complexity of damage produced by ionizing radiation. *Cold. Spring Harb. Symp. Quant. Biol*. **65**: 377-382.

Wiseman, H. and Halliwell, B., 1996. Damage to DNA by reactive oxygen and nitrogen species: role in inflammatory disease and progression to cancer. *Biochem J.* **313(Pt 1)**: 17-29.

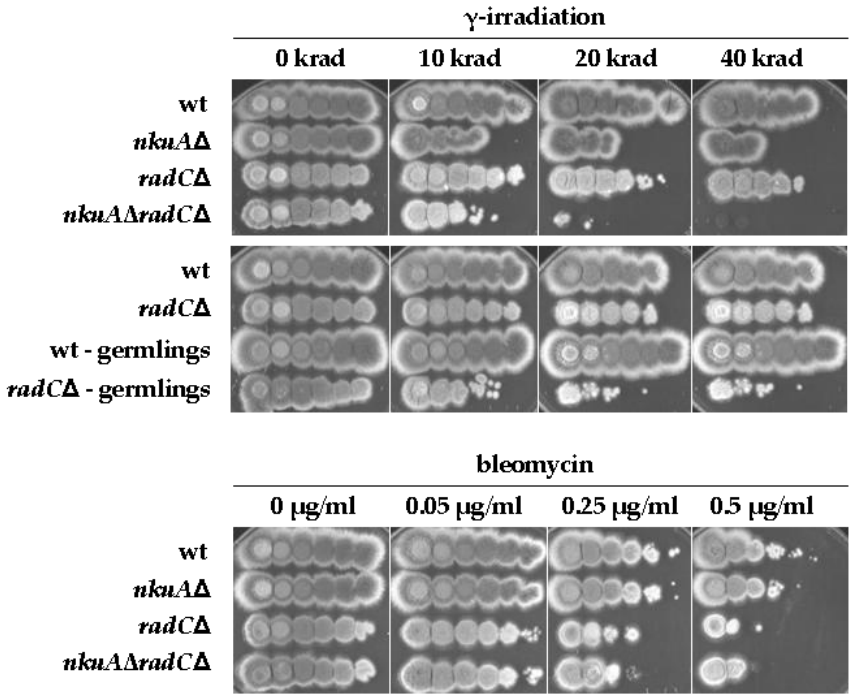

Figure 7.1

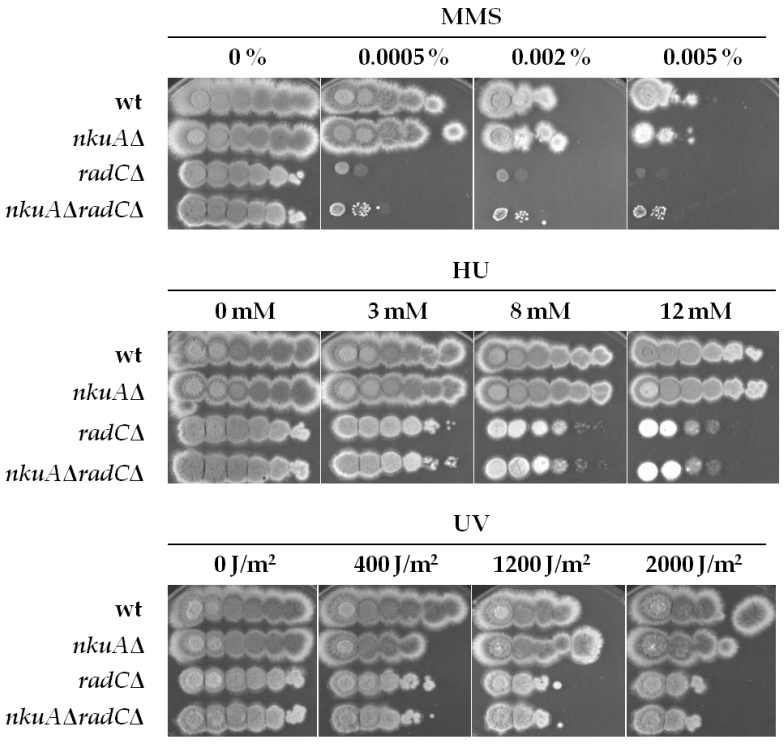

Figure 7.2

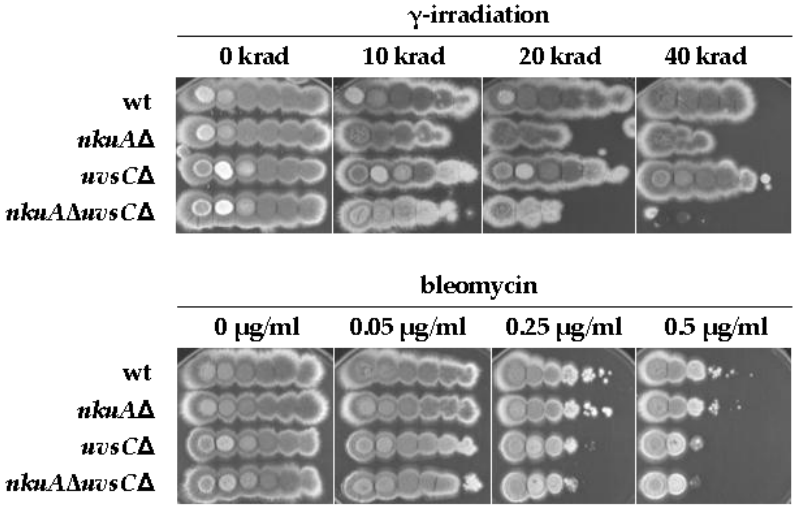

Figure 7.3

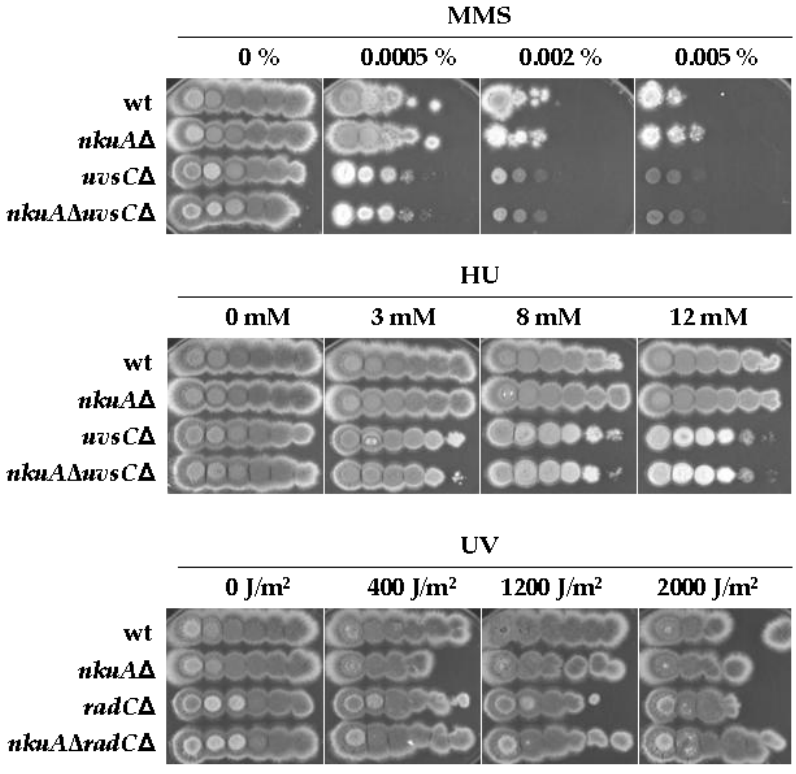

Figure 7.4

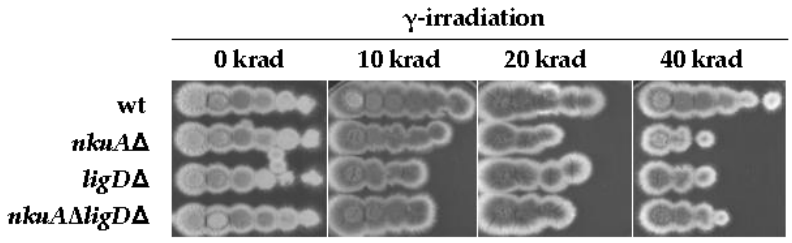

Figure 7.5

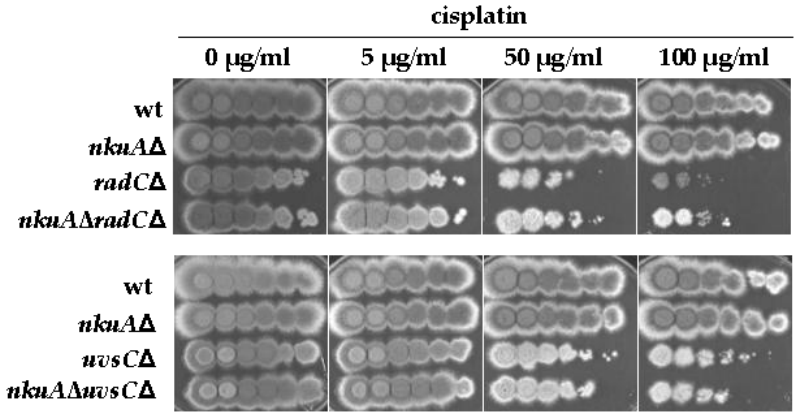

Figure 7.6

Table 1 Gene targeting in DNA repair mutants

Trial	AR1		*nkuA* Δ		*nkuA* Δ*radC* Δ		*nkuA* Δ*lig4* Δ		*uvsC* Δ	
	green	yellow	green	yellow	green	yellow	green	yellow	green	yellow
1	1	0	95	179	0	0	11	52	8	0
2	20	1	34	67	0	0	9	22	10	0
3	145	4	73	145	0	0	47	147	n.d.	n.d.
4	5	1	0	5	0	0	4	17	n.d.	n.d.
5	10	1	2	44	0	0	7	38	n.d.	n.d.
Total	181	7	204	440	0	0	78	276	18	0

Conclusions & perspectives

The first two chapters of the thesis served to introduce the intriguing world and possibilities of filamentous fungi, in particular the ascomycete *A. nidulans* that already has had a substantial role as eukaryotic model organism. One significant problem that have influenced the potential applications of filamentous fungi are the obstacles for conducting precise chromosomal targeting in spite of the wealth of DNA sequence information for numerous filamentous fungi now available. The main concern is the relatively low efficiency of gene targeting in most of these organisms. Different research groups have chosen to tackle this in various ways. Regardless of the path chosen, the mechanisms underlying targeting and random integration reflects the way of the organisms to cope with DNA lesions, thus one chapter served as background for the damage and repair of DNA.

In this era of functional genomics, high-through put generation of mutants is required, and *Aspergillus* is no exception with 8 full sequenced genomes. The strategy chosen to produce the DNA substrates is vital, since this can be one of the bottlenecks. As opposed to the traditional cloning procedure, substrates can rapidly be produced and connected via PCR and this was also the approach followed in the thesis. The selected strategy has its beginning in the swift bipartite gene-targeting technology developed in *S. cerevisiae* as introduced in the end of Chapter 3, due to the advantageous features the design showed to display. These can be summed up to less risk of PCR-derived errors, no misannealing between DRs, reduced false positive background after transformation and that foci formation by repair protein could improve correct integration. However, much higher impact on gene-targeting efficiency is achieved when the pathway behind randomized insertions of DNA, non-homologous end-joining, is impaired. This strategy has been attempted in several organisms where gene targeting is infrequent

with variable success. In mice, the lack of NHEJ enzymes is clearly visible as the mutants suffer from large abnormalities. In filamentous fungi, the loss is more difficult to spot, since no macroscopic effects on morphology were observed. However, more careful studies have shown additional deficiencies for absence of Ku in fungi relating to telomere length and γ-ray sensitivity. In haploid fungi, such as *A. nidulans*, a permanent dysfunctional NHEJ does not seem attractive, as cells use NHEJ to repair in G1 and in early S phase. Further, not all fungi have the possibility to be backcrossed hereby regaining their lost properties. Hence the transient *nkuA* disruption described in Chapter 5 has bypassed this problem, since the regeneration of *nkuA* occurs by a simple selection scheme. However, it still remains to be seen if the regenerated *nkuA* can influence the length of the shortened telomeres positively. Furthermore, the system would benefit from incorporation of another counter-selectable marker in the *nkuA* locus, and instead using *pyrG* for genetic manipulations. This would offer the desired flexibility required in the system. Moreover the implementation of universal marker genes, that is, markers which function in a broad range of species, will definitely increase the potential of the technology.

The improvements for gene targeting in *A. nidulans* described have only been possible due to the knowledge achieved through many decades of research on the mechanisms underlying gene targeting. Therefore the last two chapters are devoted to the initial dissection and characterization of some proteins involved double-strand break-repair to increase the knowledge of recombination and end-joining. Indeed, interesting things came up during the first experiments. For instance RadC, the homolog of Rad52, appear to have an intermediate role compared to yeast and mammals, as RadC, except in G1 cells, is used for curing γ-ray mediated lesions as in yeast, but gene targeting can be performed in the deletion mutant, which is impossible in yeast. Furthermore, in RadC an additional 100 amino acids are present compared to yeast as well as mammals. Correspondingly, Rad51, which is relatively more vital for mammalian HR than yeast HR, has a homolog in *A. nidulans* named UvsC, and it did not prove to be more essential than RadC for HR in the assays applied. However, no targeting was

performed in *uvsC*Δ, but the total number of transformants analyzed has been significantly lower, which makes definite conclusions difficult. When deletion of *radC* was combined with deletion of *nkuA*, a striking additive effect was observed, both in extreme γ-ray sensitivity and not even a single transformant in subsequent gene targeting experiments. When this observation is coupled to a substantial residual end-joining activity of 30 % in *nkuA*Δ*ligD*Δ, which apparently is non-existing in the ascomycete *N. crassa*, it strongly indicates that RadC is required in this process. It could be the annealing activity, which is needed for this end-joining related back-up, however this requires more studies. One candidate for this pathway is microhomology mediated end-joining, therefore a gap repair assay will be used to test how the various DSBR mutants repair the gapped plasmid, since MMEJ tends to give relatively large deletions of several hundred base pairs. If MMEJ is responsible, false positives may efficiently be circumvented by the use of bipartite gene-targeting substrates, since the marker only functions after HR-mediated assembly and repair foci formation could bypass MMEJ.

The work on DNA repair in *A. nidulans* presented here in the thesis has opened many doors, and is thus going to be supported by other immediate and additional experiments. To mention a selection of these; firstly, the remaining targeting data will be collected and more mutants will be included in epistasis analysis and the assays presented. New assays, e.g. DR recombination, inter/intrachromosomal recombination, and gfp-tagging tools are ready or currently under construction, and these will provide a battery of methods, which will take analysis of DNA repair in *A. nidulans* to another level. Transcriptional profiling on our *Aspergillus* DNA array chip of the three mutant strains *nkuA*Δ, *radC*Δ and the respective double mutant, as well as wild type, presented in the thesis will be carried out at normal and DSB induced conditions to reveal which genes are responding to DSBs in *Aspergillus* when important repair pathways are impaired. Ultimately, the molecular tools and the understanding of genome integrity that the work presented and planned experiments will give us, should be applied in strategies regarding a community-wide effort of constructing a *A. nidulans* genome-

wide mutant strain library, which will offer practically all *Aspergillus* researchers a tremendous boost in their projects.